Journal: Ecological Monographs
Manuscript type: Article
Running Head: Carbon cycling in a mid-latitude forest

Carbon budget of the Harvard Forest Long-Term Ecological Research site: pattern, process, and response to global change

Adrien C. Finzi[1], Marc-André Giasson[1], Audrey A. Barker Plotkin[2,*], John D. Aber[3], Emery R. Boose[2], Eric A. Davidson[4], Michael C., Dietze[5], Aaron M. Ellison[2], Serita D. Frey[3], Evan Goldman[6], Trevor F. Keenan[7,8], Jerry M. Melillo[9], J. William Munger[6], Knute J. Nadelhoffer[10], Scott V. Ollinger[3,11], David A. Orwig[2], Neil Pederson[2], Andrew D. Richardson[12,13], Kathleen Savage[14], Jianwu Tang[9], Jonathan R. Thompson[2], Christopher A. Williams[15], Steven C. Wofsy[6], Zaixing Zhou[11], and David R. Foster[2]

[1] Department of Biology, Boston University, Boston, Massachusetts 02215 USA
[2] Harvard Forest, Harvard University, Petersham, Massachusetts 01366 USA
[3] Department of Natural Resources and the Environment, University of New Hampshire, Durham, New Hampshire 03824 USA
[4] University of Maryland Center for Environmental Science, Appalachian Laboratory, Frostburg, Maryland 21532 USA
[5] Department of Earth & Environment, Boston University, Boston, Massachusetts 02215 USA
[6] School of Engineering and Applied Sciences, Harvard University, Cambridge, Massachusetts 02138 USA
[7] Lawrence Berkeley National Laboratory, Berkeley, California 94720 USA
[8] Department of Environmental Science, Policy and Management, UC Berkeley, Berkeley, California 94720 USA
[9] The Ecosystems Center, Marine Biological laboratory, Woods Hole, Massachusetts 02543 USA

[10] Department of Ecology and Evolutionary Biology, University of Michigan, Ann Arbor, Michigan 48109 USA
[11] Earth Systems Research Center, University of New Hampshire, Durham, New Hampshire 03824 USA
[12] School of Informatics, Computing and Cyber Systems, Northern Arizona University, Flagstaff, Arizona 86011 USA
[13] Center for Ecosystem Science and Society, Northern Arizona University, Flagstaff, Arizona 86011 USA
[14] Woods Hole Research Center, 149 Woods Hole Road, Falmouth, MA, 02540 USA
[15] Graduate School of Geography and Department of Biology, Clark University, Worcester, Massachusetts 01610 USA

* **Corresponding Author**: Audrey Barker Plotkin (aabarker@fas.harvard.edu)

Manuscript received 23 January 2020; accepted 22 May 2020; final version received 16 June 2020.

ABSTRACT

How, where, and why carbon (C) moves into and out of an ecosystem through time are long-standing questions in biogeochemistry. Here, we bring together hundreds of thousands of C-cycle observations at the Harvard Forest in central Massachusetts, USA, a mid-latitude landscape dominated by 80–120-year-old closed-canopy forests. These data answered four questions:

(i) where and how much C is presently stored in dominant forest types; (ii) what are current rates of C accrual and loss; (iii) what biotic and abiotic factors contribute to variability in these rates; and (iv) how has climate change affected the forest's C cycle? Harvard Forest is an active C sink resulting from forest regrowth following land abandonment. Soil and tree biomass comprise nearly equal portions of existing C stocks. Net primary production (NPP) averaged 680–750 g C m^{-2} yr^{-1}; belowground NPP contributed 38–47% of the total, but with large uncertainty. Mineral soil C measured in the same inventory plots in 1992 and 2013 were too heterogeneous to detect change in soil-C pools; however, radiocarbon data suggest a small but persistent sink of 10–30 g C m^{-2} yr^{-1}. Net ecosystem production (NEP) in hardwood stands averaged ~300 g C m^{-2} yr^{-1}. NEP in hemlock-dominated forests averaged ~450 g C m^{-2} yr^{-1} until infestation by the hemlock woolly adelgid turned these stands into a net C source. Since 2000, NPP has increased by 26%. For the period 1992–2015, NEP increased 93%. The increase in mean annual temperature and growing season length alone accounted for ~30% of the increase in productivity. Interannual variations in GPP and NEP were also correlated with increases in red oak biomass, forest leaf area, and canopy-scale light-use efficiency. Compared to long-term global change experiments at the Harvard Forest, the C sink in regrowing biomass equaled or exceeded C cycle modifications imposed by soil warming, N saturation, and hemlock removal. Results of this synthesis and comparison to simulation models suggest that forests across the region are likely to accrue C for decades to come but may be disrupted if the frequency or severity of biotic and abiotic disturbances increase.

KEYWORDS

forest ecosystems, ecosystem ecology, carbon cycling, net primary production, gross primary production, belowground production, disturbance, eddy covariance, permanent plots, climate change, long-term ecological research

INTRODUCTION

Understanding how, where, and why C moves through an ecosystem is a long-standing goal in biogeochemistry (e.g., Brown and Escombe 1902, Isaac and Hopkins 1937, Kira and Shidei 1967, Raich and Nadelhoffer 1989, Ryan et al. 1997, Litton et al. 2007). It is an especially important present-day issue because forest C balances both affect and are influenced by climatic and atmospheric changes such as warming and rising concentrations of atmospheric CO_2 (Melillo et al. 1990, Schimel 1995). Understanding feedbacks between forests and the atmosphere is key to understanding whether, how, and for how long the terrestrial biosphere will continue to mitigate anthropogenic CO_2 emissions.

Eastern North American forests have accumulated significant C in recent decades (Urbanski et al. 2007, Pan et al. 2011, Williams et al. 2012, Fahey et al. 2013, Eisen and Barker Plotkin 2015). Recovery from agricultural abandonment and intensive forest harvesting is considered the primary driver of this sink along with episodic disturbance such as the 1938 hurricane (Albani et al. 2006, Thompson et al. 2011, Duveneck et al. 2017). As many forests in this region mature, it is relevant to ask how long they will remain C sinks. Will the sinks disappear as predicted by original theories of forest development because photosynthetic C gain is offset by growing respiratory costs (Kira and Shidei 1967, Odum 1969)? Or, in the absence of large-scale disturbance, will these mature forests remain C sinks long into the future (Carey et al. 2001, Pregitzer and Euskirchen 2004, Zhou et al. 2006, Luyssaert et al. 2008)?

Most research attributes the C sink to the growth of woody biomass. Soil C is lost as a result of row crop agriculture and grazing (Sanderman et al. 2017). In the 18th and 19th centuries, row crop agriculture and livestock grazing were active land uses in New England. There is evidence that regrowth following land abandonment contributes to a persistent C sink (Barford et al. 2001, Urbanski et al. 2007), but to what extent and whether C also accumulates in soils remains uncertain (Compton and Boone 2000, Gaudinski et al. 2000, Sierra et al. 2012).

While forests are regrowing from land abandonment, atmospheric chemistry and climate are changing. In Massachusetts since 1900, atmospheric CO_2 has increased 38% (Sargent et al. 2018). Atmospheric N deposition more than doubled, but is now declining in response to air quality regulations (Bowen and Valiela 2001, Waller et al. 2012). Since 1964, the average annual temperature in central Massachusetts has increased 1.5 °C and total precipitation has increased by 188 mm (SRCC 2019). These factors, alone or together, are likely to affect the C cycle. Indeed, longer growing seasons (Richardson et al. 2010, Yang et al. 2012, Keenan et al. 2014), CO_2 fertilization (Keenan et al. 2016, Williams et al. 2016), enhanced water-use efficiency (Keenan et al. 2013), atmospheric N deposition (Frey et al. 2014), and increasing moisture availability (Schwalm et al. 2011, Pederson et al. 2013) are variously implicated in the increasing rate of C accumulation in New England forests.

The Harvard Forest in central Massachusetts, USA, is one of the most intensively studied forests in the world. Its land-use history of harvesting and agricultural land clearance, reforestation, and subsequent partial harvesting is well-documented and similar to that experienced by much of eastern North America (Foster and Aber 2004). This Long-Term Ecological Research (LTER) site is home to more than a century of study and three decades of intensive measurements of forest compositional and structural change, and C fluxes between the forest, the soil, and the atmosphere (Fig. 1).

A cornerstone of C-cycle research at the Harvard Forest are continuous measurements of forest-atmosphere exchanges of CO_2 that began in 1990 in a mixed hardwood-conifer forest. In a seminal paper, Wofsy et al. (1993) showed that net C uptake in regrowing forests exceeded those assumed for temperate forests at that time. This paper lead, in part, to the hypothesis that global changes such as rising atmospheric CO_2 and N deposition may be enhancing the terrestrial sink for atmospheric CO_2 above that due to land-use change. It also catalyzed interest in developing long-term, whole-ecosystem free-air CO_2 enrichment studies to assess the validity of the CO2 fertilization and N deposition hypotheses (DeLucia et al. 1999, Finzi et al. 2007, Reich et al. 2014). Their paper was followed by an analysis of eight years of C-flux data (Barford et al. 2001) that documented large interannual variations in forest-atmosphere fluxes of C, which they related to growing season length and cloudiness. It also showed comparatively small year-to-year variations in woody biomass

increment and the potential importance of C allocation, particularly to storage compounds, in explaining the difference between the variability in tree growth and that of C exchange. A third study by Urbanski et al. (2007) published 13 years of forest-atmosphere CO_2 exchange at the Harvard Forest (1992–2004). They found that net C uptake by the forest nearly doubled during this 13-year period, which they correlated with increases in leaf-area index, midsummer photosynthetic capacity and the growth of red oak as a canopy dominant. The doubling of C uptake was a surprising result because the changes in the driving variables— e.g., atmospheric CO_2 concentration and N deposition, leaf area index, and growing season length— did not appear to change by a similar magnitude nor could present-day biogeochemical models simulate the observed increase.

A long-term, site-based analysis of these eddy-flux observations has not been published since 2007 and hence a major goal of this synthesis paper is to explore how C fluxes have evolved in this mixed hardwood-conifer site over the period 1992–2015. Two additional eddy-flux towers in an old hemlock and young hardwood forest, and a recent synthesis of soil respiration measurements (Giasson et al. 2013), expand our understanding of ecosystem C flux. A large portfolio of permanent plots provides detailed information on C storage and fluxes in live biomass, dead biomass, and soils, and how storage and uptake have changed over the past quarter-century. A meteorological station on site, ecophysiological studies, and remote sensing data allow investigation of biotic and abiotic factors that potentially control variation in C cycling.

The Harvard Forest hosts several global change experiments designed to simulate soil warming (e.g., Melillo et al. 2017), atmospheric N deposition (e.g., Nadelhoffer et al. 1999a, b, Frey et al. 2014), and invasive insects (Orwig et al. 2013). Each of the experiments pushes the forest in a new direction with consequences for C cycling. Twenty-six years of soil warming at the Harvard Forest resulted in an enhanced rate of soil respiration and a putative loss of soil C of 17% at an average, annualized rate of 60 g C m^{-2} yr^{-1} (Melillo et al. 2017). Interestingly, the increase in soil respiration was marked by four phases. Two phases were characterized by substantial increases with warming, which alternated with two phases when there was no significant effect of warming on soil respiration. Similarly, a 20-year study simulating the effects of N deposition found substantial increases in biomass and soil C storage

in hardwood stands. These stands sequestered C above that in control plots at an average annual rate of 125 g C m^{-2} yr^{-1} with a fertilization rate of 50 kg N ha^{-1} yr^{-1}, and 460 g C m^{-2} yr^{-1} at a fertilization rate of 150 kg N ha^{-1} yr^{-1} (Frey et al. 2014). Most of the additional C was sequestered in biomass, and in the surface soil as a result of reduced rates of organic matter decomposition, but some was also sequestered in deep mineral soil in the N15 treatment (Nadelhoffer et al. 1999a, Frey et al. 2014). In red pine plantations, fertilization with N did not result in soil C accumulation. At the high level of fertilization, red pine trees died, indicating that extreme N deposition has the capacity to fundamentally change the C cycle of forests dominated by red pine. It is unknown, however, how the magnitude of changes in the C cycle elicited by the experimental studies compare to the rate of C sequestration owing to forest regrowth following land-use change. Thus, as a part of this synthesis, we make explicit comparisons of C gains and losses from the experiments to present-day estimates of C sequestration by the forest ecosystem.

Integrating site-based, long-term data sets (e.g., Fahey et al. 2005) provides the opportunity to separate the contributions of C accumulation into internal drivers of ecosystem development (i.e., regrowth and structural and compositional changes following disturbance, nutrient cycling) and global change drivers (e.g., temperature, CO_2, invasive insects, atmospheric deposition, land use). For example, Keenan et al. (2013) suggested that increases in C uptake at the Harvard Forest was in part attributable to increases in water-use efficiency associated with the rise in atmospheric CO_2. Similarly, Keenan et al. (2014) suggested that warming-induced increases in growing season length also contributed to the increase in C uptake. How and whether these patterns persist are a key point for discussion in the present manuscript.

Here, we bring together hundreds of thousands of observations on the C cycle for the Harvard Forest in central Massachusetts, USA, a mid-latitude landscape dominated by closed-canopy forests 80–120 years old. We synthesized these data to answer four key research questions in C-cycle science: (i) where and how much C is presently stored in dominant forest types; (ii) what are rates of C accrual or loss from 1992–2015, the period of intensive measurements; (iii) what biotic and abiotic factors contribute to variability in these rates; and (iv) is there evidence that climate change is affecting the

magnitude and seasonality of the C fluxes? We then placed these results into context. We compared the magnitude of change in the C cycle from forest regrowth and recent climate change to published results from three long-term global change experiments at the Harvard Forest: soil warming, N saturation, and hemlock removal. Finally, we evaluated to what extent the C stocks and accrual rates in the 1500 ha Harvard Forest represent forests in the surrounding ecoregion.

METHODS

Site overview

The ~1500 ha Harvard Forest is in the New England Upland physiographic region of north-central Massachusetts (42.5° N, 72.2° W). Elevation across the Harvard Forest ranges from 220 m to 410 m above sea level. Soils are primarily stony, acidic glacial tills that overlay metamorphic bedrock. The climate is cool and moist; based on data from 1961–1990, July mean temperature is 20.1 °C, January mean temperature is −6.8 °C, and the 1066 mm average annual precipitation is distributed evenly throughout the year (Greenland and Kittel 1997).

Since its establishment in 1907, the Harvard Forest has been a long-term forestry and ecological research site. It is part of several major research networks including the LTER program, the National Ecological Observatory Network (NEON), AmeriFlux, and the Forest Global Earth Observatory (ForestGEO). Research infrastructure includes three eddy-flux towers, a network of phenology observation sites, two gauged headwater streams, a meteorological station, long-term experiments, permanent plots, and extensive records of land-use history and ecological dynamics. The research program integrates historical and reconstructive studies, long-term measurements, large experimental manipulations, and local to regional modeling (Foster and Aber 2004).

Major forest types include oak–maple (*Quercus rubra–Acer rubrum*), eastern hemlock (*Tsuga canadensis*), and red maple (*A. rubrum*), with some oak–pine (*Q. rubra–Pinus strobus*) stands and remnant conifer plantations (Motzkin et al. 1999). Many stands contain multiple age cohorts, but overall forest age as of 2015 was mainly 80–120 years. A few trees exceed 200 years in age. Nearly all the forests in the region are second-growth as a consequence of repeated harvesting and

agricultural clearing that peaked in the mid-1800s, followed by regional reforestation (Foster and Aber 2004). In 1938, a major hurricane damaged 70% of the standing timber of the Harvard Forest. More limited natural disturbances have included a major gypsy moth (*Lymantria dispar*) outbreak in 1981, ice storms, wind damage, and the recent establishment and spread of the hemlock woolly adelgid (*Adelges tsugae*, HWA). Recent timber harvesting (1990–2014) rates at the Harvard Forest averaged 0.4% of the forest land per year, removing an average of approximately 590 m^3 per year (Harvard Forest Archives). This is a lower frequency of harvesting disturbance than the surrounding regions (Worcester Plateau and Lower Worcester Plateau ecoregions), where about 1.4% per year was harvested (mostly at low to moderate intensity) during 1984–2015 (McDonald et al. 2006, Thompson et al. 2017).

Data sources

The Harvard Forest has an extensive portfolio of permanent forest plots and experiments, many with consistent measurements initiated when the LTER program began in 1988 (Fig. 1). Data sets, including those used in this analysis (Appendix S1: Tables S1 and S2) and associated code, are freely available via the Environmental Data Initiative Data Portal (see Data Availability). Unless otherwise noted, we used measurements only from closed-canopy forests. The notable exception is the use of eddy-covariance data from a recently clear-cut site to understand rates of C cycling in a rapidly aggrading stand. For the purposes of C budgeting, we excluded data collected from experimental treatments but retained data from their corresponding control plots. We also compared our C cycle synthesis to published syntheses of global change experiments based at the Harvard Forest (Fig. 1). See Table 1 for abbreviations and acronyms used in the paper.

Climatic and atmospheric data sets

Data for temperature and precipitation from 1964–2015 are available from an on-site meteorological station. When available, we used meteorological data collected at the three eddy-flux towers included in this analysis. For variables that were not measured at the towers themselves (e.g., precipitation), we used the Harvard Forest meteorological station data. We filled gaps in data series by determining the relationship between the variable of interest and the same variable measured at other sites, namely the

Environmental Measurement Site (EMS), hemlock (HEM), and clear-cut (CC) flux towers, and the Harvard Forest meteorological station. We ranked the relationships by quality-of-fit of the regressions and used them to fill gaps in the master data sets. Meteorological variables used in this analysis include air temperature, soil temperature at 10 cm (HEM, CC tower site) or 20 cm depth (EMS), photosynthetic photon flux density, soil water content, vapor pressure deficit, and precipitation.

To examine temporal trends in other global change factors during the study period, we used publicly available atmospheric data, including annual mean CO_2 concentration measured at the Mauna Loa Observatory (Tans and Keeling 2019), ground-level O_3 concentration recorded in Ware Center, MA, 25 km south of the Harvard Forest (EPA 2019), and total N and SO_4^{2-} deposition observed at the Quabbin Reservoir, 17 km southwest of the Harvard Forest (NADP 2019).

Plot-based measurements of carbon pools and fluxes

We used measurements of trees, dead wood, litterfall, soil C, fine root biomass, and root exudates from permanent plot studies and control plots of long-term experiments to estimate current C stocks and temporal trends in C stocks and fluxes. Plot size and number varied by project; since the Harvard Forest is the study site, each plot was considered a replicate sample within the study site, with all units standardized to g C m^{-2} (pools) or g C m^{-2} yr^{-1} (fluxes). Estimates of C flux used varying numbers of plots for each year, depending on the sample frequency of the different studies. Plots were grouped as "hardwood" (mostly oak–maple, along with some maple–birch–ash) or "hemlock" based on a cluster analysis (Fig. 1b; R version 3.3.1, *k*-means function) of the most recent measurement of biomass by species for each plot. We excluded plots in plantation forests from this synthesis; plantations (mainly *Pinus resinosa*, *Picea glauca*, and *Picea abies*) are a small and declining component of the Harvard Forest (< 5% of the land base) and southern New England in general. Pine–oak is another minor forest type at the Harvard Forest, but none of the plots with tagged trees were of this forest type, so these were not included in our analyses.

Trends in live tree biomass (aboveground and coarse roots)

Individual tree measurements from nine studies using repeated measurements from 1988–2015 (115 plots total) were used to characterize live tree C stocks (Appendix S1: Table S3). The studies varied in plot size (from ~120 m^2 to 3 ha), number of plots (1–60), and measurement frequency (mostly annual to decadal). The suite of 34 plots (each 314 m^2) in the EMS tower footprint were first measured in 1993, and tree growth and mortality have been censused annually since 1998. Plots from other studies added data for other forest types and locations in the Harvard Forest. Most of these were censused every 5 or 10 years. One large (2.9 ha) plot has been censused about every decade since 1969. The minimum tree size included varied by study, from 2.5 to 10 cm diameter at breast height (DBH). This is a minor source of variation among studies, because small trees contribute very little to plot-level metrics of C storage and increment. However, estimates of percent mortality used a common minimum DBH of 10 cm, since mortality was more frequent in smaller diameter classes (Appendix S1: Fig. S1). Data from the most recent measure of each plot (varied by project, 2008–2015) were used to calculate current C storage in aboveground and coarse root biomass. We calculated aboveground increment, coarse root increment, and mortality using the subset of nine studies (60 plots) that tracked individual tagged trees and had ≥ 10 years of measurements.

We estimated whole-tree aboveground biomass using species-specific allometric equations (43 species in total, Appendix S1: Table S4). Most of the equations excluded the stump and root crown and included foliage, but there were some exceptions. We developed new allometric equations for 14 of the most common species using a Bayesian data analytic approach that 'fuses' above-stump biomass equations presented in Jenkins et al. (2004; Dietze 2015). These 14 species represented 88% of the individual live tree measurements in the database (>120,000 measurements total). The biomass of the remaining 29 species was estimated using allometric equations chosen from a variety of sources based on: a) availability of data for that species, b) equations developed for the range of diameters represented in our data set, and c) geographic proximity. We estimated C content as 50% of dry woody biomass for all species. Using parameters and equations of Jenkins et al. (2003), we estimated coarse root biomass for each tree based on a proportion of the aboveground biomass that varied based on diameter and species group. Total tree biomass (aboveground + coarse roots) reported here excludes the stump and root crown, so is a slight underestimate of this pool.

Fine litterfall (foliar and non-foliar)

Foliar litterfall was collected in ten different studies (Appendix S1: Table S5). Litterfall of fine, non-foliar material (e.g., twigs, bark, flowers, acorns, etc.) was reported in four of those studies. One study reported only total (foliar + non-foliar) litterfall and no study reported branchfall. Because litterfall was generally collected more than once per year, annual litterfall was calculated as the total mass of fine litter material collected between August and the subsequent July. For plots with multiple litter baskets, the mean litterfall per plot was used as the unit of replication. We measured C content of leaves and it averaged 50% of dry biomass for all species, so litterfall mass was converted to litterfall C content using a C content of 50%.

Woody debris and standing dead wood

Coarse (diameter > 7.5 cm) and fine (0.6–7.5 cm) woody debris and standing dead wood were measured in 4, 4, and 3 studies, respectively (Appendix S1: Table S6), using either the line transect or fixed-radius plot method (Harmon and Sexton 1996). The data sets used contained woody debris mass but no information on C content. Thus, to estimate the C content of the dead wood, we used the percent C content of hemlock coarse woody debris, stumps, and snags measured by Raymer et al. (2013) and of red oak woody debris published by Currie and Nadelhoffer (2002). We calculated the mean percent C content of each decay class for conifers and deciduous trees, and used it to convert dead wood mass into C content for the hardwood and hemlock plots of all studies. For samples in which the decay class was not noted, we used the average percent C content of the five decay classes.

Soil carbon

Soil organic C content was the most widely measured belowground C pool. It was measured in 17 studies over a variety of forest types, topography, and drainage conditions (Appendix S1: Table S7). Organic horizon soil monoliths (of surface area generally 10 × 10, 10 × 20, 15 × 15, or 20 × 20 cm) and mineral soil cores (5 or 10 cm diameter, collected using a hammer corer or power auger, respectively) were brought back to the lab. Samples were sieved to remove rocks and roots,

homogenized, and then dried and ground into a fine powder before dry combustion in an elemental analyzer to determine soil organic C content.

Most of the measurements were of the organic horizon or the top 15 cm of the mineral soil, but in eight studies samples were also collected deeper in the mineral soil (Appendix S1: Table S7). In studies where mineral soil C content was not measured at 15 cm increments (e.g., 10 cm increments), we estimated the C content of a hypothetical 15 cm-thick soil layer by evaluating the distribution of C through the soil profile (regressing C content against depth) and extrapolating the C content of 15 cm-thick soil layers.

Fine root biomass

Fine root (diameter < 2 mm) biomass and C content were measured in eight studies (Appendix S1: Table S8). As with mineral-soil C content, most measurements were from the organic horizon or the top 15 cm of the mineral soil. Only two studies provided deeper measurements in a hemlock stand, and one in a deciduous stand. Samples were collected using the same methodology as for soil C content. Roots were picked manually. Most studies did not separate live and dead roots, so these were pooled together if reported separately. Roots were then washed, dried, and weighed to obtain the dry root biomass content of the samples. In some studies, roots were ground into a fine powder and combusted in an elemental analyzer to determine root percent-C content, which was used to convert root biomass into total root C. For studies where root biomass was known but not root C content, we used root percent C content measured in other studies located in the same or other closely located plots to convert biomass to C stock. When C concentration data were unavailable, we used 43% C content as the conversion factor, the average of the fine root data available.

Dissolved organic carbon export

Dissolved organic carbon (DOC) in stream water was measured during one year in Arthur Brook on the Prospect Hill Tract of the Harvard Forest. Water was sampled (n = 125) and DOC concentration was quantified using a TOC analyzer. The annual export of DOC by the headwater stream was estimated as the product of DOC concentration and streamflow (Wilson et al. 2013).

Root exudates

Two studies reported root C exudation (Brzostek et al. 2013, Abramoff and Finzi 2016). In both cases, exudates were collected using a modified version of the method developed by Phillips et al. (2008). In brief, live roots were carefully excavated, washed, and incubated overnight in a moist soil-sand mixture while remaining attached to the tree. Roots were then placed into glass cuvettes filled with glass beads and a C-free nutrient solution for 24 hours prior to exudate collection. At the time of collection, the now exudate-containing nutrient solution was extracted with two additional flushes of C-free nutrient solution to ensure complete recovery of the exudates. Samples were frozen at −20 °C until analysis for organic carbon content on a TOC analyzer. The daily rate of root exudation was converted to annual fluxes by multiplying the mean daily flux by the mean number of days in the growing season.

Correction for rock content

Because the belowground measurements were based on soil samples containing no large rocks, we corrected the data to account for soil rock volume when not already done for a project. Soil rock fraction was measured in two 0.5 m^3 pits located in a hemlock stand (Raymer et al. 2013) and 70 plots from five different studies in deciduous stands (Borken et al. 2006, Lajtha et al. 2014, Frey et al. 2014).

Aboveground net primary production

Aboveground net primary production (ANPP) was calculated as the sum of aboveground increments, recruitment, and foliar litterfall for each measurement interval. The biomass increment of new recruits was based on the biomass of the tree in the first year it grew above the minimum diameter minus the biomass of the tree at the minimum diameter (Clark et al. 2001). Any growth of trees that died between two consecutive measurements was not included. We used total litterfall from the five studies with > 5 years of total (foliar + non-foliar) annual litterfall measurements. As is true for most studies in forested ecosystems, ANPP is likely underestimated by excluding the following components: branch turnover, woody increment and turnover of shrub and herbaceous vegetation, reductions in litterfall-measured foliar turnover due to herbivory and possibly some decomposition in

the baskets, and changes in non-structural carbohydrates (Clark et al. 2001, Chapin et al. 2006, Ouimette et al. 2018). None of the plots included in the analysis was subject to timber harvest during 1992–2015 (although data from an eddy-flux tower sited in a recently harvested site is part of this overall study), so removal by timber harvest was not a flux considered in the plot-based ANPP calculations.

We examined trends over time for the components of ANPP in the suite of hardwood plots for the period 1998–2014, and in the suite of hemlock plots for the period 2005–2014. In addition to the combined analysis of ANPP across studies, we examined annual woody biomass increment for a longer period, 1960–2011, using tree-ring analysis in two hardwood stands on the Prospect Hill tract. All trees ≥ 10 cm DBH were surveyed and cored in five 13 m radius (531 m^2) plots (two in one stand, and three in the other). We calculated annual biomass increment for each stand and then averaged those results to get annual biomass increment. For detailed methods see Dye et al. (2016). The correlation between growth and climate for *Quercus rubra* and *Acer rubrum*, the two species producing the most biomass in these plots, was calculated using annual radial growth indices and monthly climatic variables from prior June through current August from 1920–2012. The ARSTAN chronology was used for this analysis of tree sensitivity to climate (Cook and Krusic 2005).

Belowground net primary production

Belowground net primary production (BNPP) was calculated as the sum of fine and coarse root production, fine root turnover, and root exudation. There are three published estimates of fine root production plus turnover (i.e., root NPP) for oak-dominated hardwood stands at the Harvard Forest. Gaudinski et al. (2010) used radiocarbon data to estimate fine root NPP at 72 g C m^{-2} yr^{-1}. McClaugherty et al. (1982) used sequential coring to estimate fine root NPP at 270 g C m^{-2} yr^{-1} (assuming 50% C content). Abramoff and Finzi (2016) used minirhizotrons to estimate fine root NPP and turnover time, which we applied to the far broader data set of fine root biomass available in this paper. In particular, fine root turnover time ($FR_{turnover\ time}$, yr) was estimated for the hemlock and hardwood stands by dividing the mean fine root biomass (FR_{mass}, g C m^{-2}) by fine root production ($FR_{production}$, g C m^{-2} yr^{-1}) estimated from minirhizotrons. For the hemlock stand, $FR_{turnover\ time}$ was

calculated using $FR_{production}$ values for 2012, before the hemlock started declining in vigor because of the hemlock woolly adelgid infestation. In the hardwood stand, the installation of 6 out of 10 minirhizotron tubes in the fall of 2012 might have increased root growth rates in subsequent years due to the severing of roots during tube placement. Thus, to minimize the potential for overestimation, $FR_{turnover\ time}$ was calculated using $FR_{production}$ values for 2014, the second year after tube installation and the most recent data available. Abramoff and Finzi (2016) estimated fine root turnover times for oak and hemlock of 1.25 ± 1.40 yr and 2.51 ± 1.88 yr, respectively. Fine root NPP was then estimated as fine root biomass divided by turnover (pool / flux method, Schlesinger and Bernhardt 2013). This results in estimates of 333 ± 385 g C m^{-2} yr^{-1} and 218 ± 174 g C m^{-2} yr^{-1} for oak- and hemlock-dominated forests, respectively.

Unfortunately, there is no simple or straightforward method for determining which of the estimates is closest to the true value (Strand et al. 2008, but see Tierney and Fahey 2002). The minirhizotron study reported here is particularly good at observing the production of fast-turnover fine roots but is sensitive to the amount of time since minirhizotron tubes were installed and technical considerations related to depth of view and root architecture to extrapolate to units of g C m^{-2} yr^{-1}. The sequential coring technique can provide time-resolved estimates of root biomass and root production but is likely to miss the population of roots that were produced and turned over between the time soil cores are collected (c.f., Fahey and Hughes 1994). It also includes substantial spatial variability in its estimate because one cannot sample the same location more than once. Radiocarbon provides very precise estimates of root age and turnover times but may be biased by the assumption of a constant probability of root mortality regardless of age or order (Tierney and Fahey 2002), and stored or recycled carbohydrates (i.e., “older” C) that may contribute to the production of roots years after the C was fixed. No one method works perfectly for estimating fine root production. Therefore, in this study we chose to present the average rate of fine root NPP from three studies.

Soil respiration

Soil respiration (R_s) has been measured at the Harvard Forest using a combination of manual and automated soil respiration chambers for over 20 years. We previously published a synthesis of > 100,000 observations of soil respiration measurements collected through 2010 at the Harvard Forest

(Giasson et al. 2013). For this paper, we extended this data set through 2015 using an empirical function relating R_s to soil temperature (Fig. A4 in Giasson et al. 2013).

Eddy covariance measurements

Ecosystem-scale CO_2 fluxes have been measured continuously since 1992 at the Harvard Forest's EMS tower, since 2004 at the HEM tower, and since 2009 at the CC tower using the eddy covariance (EC) technique. The EMS tower samples from a mosaic of oak–maple stands established between 1900–1945 with small components of eastern hemlock, white pine (*Pinus strobus*), planted red pine (*Pinus resinosa*), and a shrub swamp (Urbanski et al. 2007). Most of the footprint was historically cleared for pasture, with smaller components of permanent woodlot and historically tilled soils (Motzkin et al. 1999). The HEM tower is located at the northeast corner of a stand dominated by eastern hemlock 100–230 years old and large white pine (Hadley and Schedlbauer 2002, Hadley et al. 2008). The sector from 180° to 270° overlaps the hemlock-dominated stand. Most of the forest in the hemlock sector has never been cleared for agriculture but was used as a woodlot during the 1700s and 1800s and was subject to partial harvests into the 20th century (Foster et al. 1992). The sector from 270–180° includes stands of oak and maple, a red pine plantation, and a large forested swamp. Flux data are separated into hemlock and non-hemlock based on wind direction being from the hemlock sector or not. Defoliation of hemlock by HWA was underway by 2012 (Kim et al. 2017). The CC tower is located in an early successional hardwood stand. Formerly a white and Norway spruce (*Picea glauca* and *Picea abies*) plantation where native hardwood trees had grown into gaps (Williams et al. 2013), an area roughly 200 × 400 m, which encompasses most of the flux tower footprint, was harvested in the fall of 2008. All trees were cut except for a few hardwood seed trees.

In this study, we analyzed 24 complete years of data (1992–2015) from the EMS tower, 11 complete years (2005–2015) from the HEM tower, and 6 complete years of data (2010–2015) from the CC tower. EC towers measure net ecosystem exchange (NEE), which is the difference between total ecosystem respiration (R_e) and photosynthesis that we refer to as gross primary production (GPP):

$$NEE = R_e - GPP \quad \text{Eq. 1}$$

NEE is reported with respect to a vertical coordinate defined as positive upward so that negative values of NEE are fluxes of C from the atmosphere to the land surface and as such calculates gains or loss of C from the atmospheric pool. This analysis is interested in gains or losses of C from the forest itself, so we present the eddy-covariance fluxes using the opposite sign convention, which are hereafter referred to as net ecosystem production (NEP):

$$NEP = -NEE = GPP - R_e \quad \text{Eq. 2}$$

Data collections invariably include measurement gaps owing to unfavorable meteorological conditions, instrument calibrations, or malfunctions. Hence, it is standard to gap-fill data sets based on well-established numerical methods (Falge et al. 2001, Reichstein et al. 2005) in order to integrate fluxes to annual sums. All the approaches used here are based on response functions relating respiration to temperature and GPP to light, and excluding data during periods that are too calm (u^* filter) to generate reliable flux measurements. Analysis of component fluxes to environmental variables include only periods when data series were intact and not subject to gap filling.

In this study, we used eddy-covariance data series with the gaps filled by the principal investigator (PI); these data sets are available on the Harvard Forest Data Archive website and are referred herein as "PI-preferred". Gaps in the EMS-tower NEE data set represented 59% of the data and were filled using the algorithm developed by Urbanski et al. (2007). Data from the CC tower contained nearly 72% of gaps which were gap-filled following a marginal distribution sampling method. Briefly, biweekly mean half-hourly estimates were calculated and assigned to missing values or low quality-control values. If gaps were still persistent, biweekly mean half-hourly values averaged from one year prior to one year after a particular gap of concern were used to fill the gap. NEE was then partitioned into R_e and GPP following the approach of Reichstein et al. (2005). The NEE series for the HEM tower contained only data from 180° to 270°, the region of hemlock dominance. The series therefore contained ~70% gaps. Most of the 2004–2007 HEM data, with the main exception of two approximately two-month-long gaps, were gap-filled and partitioned by the PI using non-linear regression (Hadley et al. 2008). We filled the remaining gaps and completed the partitioning for 2008–2015 using the Fluxnet-Canada Research Network (FCRN) gap-filling procedure (Barr et al.

2004, Amiro et al. 2006) with the same *u** threshold estimated by the PI and used to fill gaps in 2004–2007 data. That method gave good agreement with PI-gap-filled data (Giasson et al. 2013). For both the EC and R_s data sets, we used the gap-filled half-hourly or hourly fluxes to calculate daily and monthly fluxes. We also calculated annual sums based on "ecological years" beginning on 1 November, the transition to winter. We estimated aboveground respiration (R_{above}) as the difference between EC-based R_e and chamber-based R_s.

Furthermore, we used two different gap-filling and partitioning algorithms to fill all gaps in the three sites' NEE data series and partition them into NEP, GPP, and R_e. This allowed a common comparison among annual NEP, GPP, and R_e totals of the three sites and to the PI-preferred values. First, we used the REddyProc R package V1.0.0 (Reichstein et al. 2016), which uses a seasonally-varying *u** threshold estimated with the procedure developed by Papale et al. (2006). Second, we filled the same gaps using the FCRN gap-filling procedure (Barr et al. 2004, Amiro et al. 2006) with the same seasonally varying *u** threshold estimated following Papale et al. (2006). The choice of the *u** threshold is the largest source of uncertainty in eddy-covariance data series (Ellison et al. 2006, Papale et al. 2006). Thus, for both the REddyProc and FCRN algorithms, we estimated this uncertainty by repeating the *u** threshold estimation 200 times on a bootstrapped sample. We reported the uncertainty as the 2.5% and 97.5% quantiles of the bootstrapped sample.

Autotrophic and heterotrophic respiration

Autotrophic respiration (R_a), the C respired by vegetation, was calculated as the difference between GPP, NPP and soil C sequestration. Root respiration (R_r) was calculated as the difference between R_a and R_{above}. Heterotrophic respiration, the C emitted by soil microbes and fauna, was calculated as the difference between soil respiration (R_s) and R_r.

GPP response to light

To study interannual variations in whole-canopy photosynthetic rates, we characterized canopy-scale light-use efficiency (LUE) during the height of the growing season. Non-gap-filled GPP was plotted

as a function of PPFD from July 1 to July 31 of a given calendar year. We fitted a rectangular hyperbola function to estimate light-response curve parameters:

$$GPP = \frac{\alpha A_{max} PPFD}{\alpha PPFD + A_{max}} \quad \text{Eq. 3}$$

where $\propto$ is the apparent quantum yield (mol mol^{-1}) and A_{max} is the ecosystem photosynthetic capacity (μmol C m^{-2} s^{-1}).

Plant area index

Plant area index (PAI) was measured within the EMS and HEM flux tower footprints using a LAI-2000 Plant Canopy Analyzer (LI-COR, Inc., Lincoln, NE, USA). The data are reported as PAI rather than leaf area index because they include woody material. Within the EMS tower footprint, PAI was measured in the biometric inventory plots in 1998–1999 and 2005–2015. It was measured at least monthly in mid-summer and more frequently in spring and fall during leaf out and senescence. Within the HEM tower footprint, PAI was measured each August in 2008–2009 and 2012–2016 in 12 plots. At the CC site, leaf area index (LAI, which excludes woody biomass) was measured as described in Khomik et al. (2014). From 2009–2012, LAI at the CC site was measured by destructively sampling all green leaves on representative individuals of dominant species, scanning the area of each leaf with a LI-3000 leaf area meter (LI-COR, Inc., Lincoln, NE, USA), and scaling the total leaf area per square meter of each species by the areal coverage of each species measured with the line-intercept method. In 2013, CC-site LAI was measured with a ceptometer (LI-191, LI-COR, Inc., Lincoln, NE, USA). We converted the CC-site LAI to PAI using a site-specific conversion factor of 1.22 on the tree and shrub portions of total LAI.

Spring and autumn phenology dates

We estimated the duration of the growing season following the approach of Keenan et al. (2014). First, we used singular spectrum analysis to smooth the daily NEP data from the EMS and HEM towers. We then determined the maximum daily NEP for each year from the smoothed time series and calculated the mean maximum daily NEP for each site. We defined the onset of the growing season as the first day of the year when daily NEP exceeded 30% of the mean maximum daily NEP (Richardson

et al. 2010, Keenan et al. 2014). Similarly, the last day of the growing season was defined by the calendar day when NEP fell below this threshold.

We also used a long-term (1990–present) data set of phenological observations recorded at the Harvard Forest (O'Keefe 2015) to estimate the date of bud break (first day when at least 50% of the buds on a tree had leaves), full leaf out (90% of the leaves on a tree reached at least 95% of their final size), and leaf abscission (leaf coloration; the day when at least 20% of the leaves on a tree had changed color). We calculated the average date of occurrence of each phenological event for four red oak trees and five red maples, deemed representative of the EMS-tower footprint, or for five hemlock trees, representing the HEM-tower footprint, and averaged the results across years (1992–2014).

Change over time in aboveground and soil carbon stocks

We examined the C stocks in live tree biomass and deadwood for trends over time. Changes in live tree biomass were estimated as plot-level aboveground growth and recruitment minus mortality. Changes in deadwood were examined in the few studies with repeated measurements of downed and standing dead wood. We also examined the mortality estimates for trends in mortality inputs over time. Finally, we tested for change over time in mineral soil C content in the one study (42 plots) that had repeated measures of soil C over time (1992 and 2013); data for only the 0–15 cm mineral soil layer were available. The soil C stock data included in this analysis was supplemented by published estimates of soil C turnover at the Harvard Forest based on ^{14}C measurements (Gaudinski et al. 2000, Sierra et al. 2012, McFarlane et al. 2013).

Comparison to global change experiments

We compared trends in C fluxes from observational studies to published results from three global change experiments at the Harvard Forest: the Prospect Hill Soil Warming Experiment (established 1990; Melillo et al. 2017), the Chronic Nitrogen Amendment Study (established 1988; Aber et al. 1989, Frey et al. 2014), and the Hemlock Removal Experiment (established 2004; Ellison et al. 2010, Orwig et al. 2013). We updated data from the Hemlock Removal Experiment that were presented in

Orwig et al. (2013) with newer data for litterfall (Barker Plotkin 2017), live biomass (Ellison and Barker Plotkin 2015), and coarse woody debris (Ellison and Barker Plotkin 2018).

Regional comparisons

We evaluated the degree to which forests at the Harvard Forest represent those of the surrounding landscape (Fig. 2) in terms of: 1) GPP, and 2) aboveground biomass stocks. Zhou et al. (2018) estimated GPP for the Harvard Forest and the surrounding 165 km^2 area using the PnET-II ecosystem model. After validation of modeled GPP with estimates from the Harvard Forest EMS tower, the model was run spatially using remotely-sensed estimates of foliar %N for the Harvard Forest and the surrounding 11 × 15 km area. This area was defined by a 2003 aircraft data acquisition from NASA's Airborne Visible / Infrared Imaging Spectrometer (AVIRIS), which was used to generate estimates of foliar %N (Ollinger et al. 2008). Foliar %N is a critical input to PnET-II because it determines photosynthetic capacity (Aber et al. 1996).

We compared field-measured aboveground biomass stocks from the Harvard Forest with estimates obtained from the U.S. Forest Service's Forest Inventory and Analysis (FIA) plot network. There were only 9 FIA plots in the 11 × 15 km area used for the GPP comparison, which showed a mean aboveground C of 7,600 g C m^{-2}. Given the small sample size, we also used FIA data from 184 plots within the two adjoining U.S. EPA Level IV Ecoregions that surround the Harvard Forest (Fig. 2; 58g and 59b; Griffith et al. 2009). Only plots that had not been subject to harvest within the past remeasurement period (ca. 5 years) were included, although the effects of timber harvesting over the past 5–20 years would be apparent in the biomass estimates from these plots.

Statistical analyses

Calculations and statistical analyses were made using R version 3.3.1 and MATLAB R2017b. The standard deviation (SD) of the mean we presented (e.g., Tables 2–4) are the standard variation of the mean across all plots from all studies and all measurement years. When adding different components, each with an error term, we propagated the errors such as $SD = sqrt(SD_1^2 + SD_2^2 + ... + SD_n^2)$. We used a two-sample t-test to determine if C pools and fluxes were significantly different between the

hemlock and hardwood stands (Tables 2, 3) or between the HEM and EMS tower sites (Table 4). We used linear models (lm function, R Core Team 2016) to examine components of NPP and NEP for trends over time. We used nonlinear least square regression in Matlab R2017b to fit light-response curves (Eq. 3).

RESULTS

Climate and atmospheric trends

Climate data indicated trends of increasing temperature and precipitation (Fig. 3a, b) at the Harvard Forest during the study period (1992–2015). The trends included increases in mean annual air temperature (MAT; +0.05 °C yr^{-1}; $p = 0.0134$) as well as in individual seasons. Air temperature increased significantly in April–June (0.07 °C yr^{-1}; $p = 0.0038$), in September–November (0.08 °C yr^{-1}; $p = 0.0014$), and in the April–September periods (0.08 °C yr^{-1}; $p = 0.0009$). Although the 1992–2015 increase in mean annual precipitation through time was not statistically significant (MAP; +7.4 mm yr^{-1}; $p = 0.2500$), there were significant changes in total precipitation during the non-winter months. Precipitation from May to October increased by an average of +7.9 mm yr^{-1} ($p = 0.0435$).

When considering the 52-year record from the Harvard Forest meteorological station (1964–2015), we detected significant trends in mean annual air temperature (+0.02 °C yr^{-1}; $p < 0.001$; Fig. 3a) and precipitation (+6.9 mm yr^{-1}; $p < 0.001$; Fig. 3b). The rates of increase in seasonal mean air temperature and precipitation were smaller over the 1964–2015 record than over the last two decades (1992–2015), with increases in air temperature of 0.02 °C yr^{-1} in April–June ($p = 0.0021$), 0.03 °C yr^{-1} in September–November ($p = 0.0011$), and 0.03 °C yr^{-1} throughout the growing season (April–September, $p < 0.0001$) while May–October precipitation increased an average of +5.4 mm yr^{-1} ($p < 0.0001$). Over the 1964–2015 period, the increase in precipitation at the Harvard Forest was larger than that reported for the entire central Massachusetts region (+3.7 mm yr^{-1}) whereas the increase in temperature was 0.01 °C yr^{-1} smaller (SRCC 2019).

The atmospheric CO_2 concentration measured at the Mauna Loa Observatory has been increasing by 1.52 ± 0.02 ppm yr^{-1} since 1959 ($p < 0.0001$), a trend that rose to 1.96 ± 0.02 ppm yr^{-1} during the

study period ($p < 0.0001$; Fig. 3c). A decreasing trend ($p < 0.0001$) in ground-level ozone concentration has been observed at a U.S. Environmental Protection Agency monitoring site located in a rural setting 25 km south of the Harvard Forest. O_3 concentration decreased by 18% between 1981 and 2015 and by the same percentage between 1992 and 2015 (Fig. 3d). Similarly, measured total N and SO_4^{2-} deposition at the Quabbin Reservoir measurement station of the National Atmospheric Deposition Program, located 17 km southwest of the Harvard Forest, followed decreasing trends over the past several decades ($p < 0.0001$ and $p = 0.0002$, respectively). Total N deposition decreased by 41% between 1982 and 2015 (Fig. 3e) while SO_4^{2-} deposition declined by 75% over the same period (Fig. 3f). Total N and SO_4^{2-} deposition decreased by 45 % and 71% between 1992 and 2015, respectively.

Changes in forest species composition and biomass

The Harvard Forest has accrued woody biomass as the forest recovered from past agricultural land use, timber harvest, and hurricane damage. Measurements in 1937, 1992, and 2013 of 60 plots distributed across the Prospect Hill Tract (Fig. 1b) show that red oak represented only 12% of the forest biomass in 1937 but came to dominate forest-wide woody biomass (Fig. 4a). In 1937, white pine comprised 38% of total biomass at the Harvard Forest (Fig. 4a), but much of this was blown down in a major hurricane in 1938 and salvage-logged. We observed modest shifts in species composition during the focal study period (1992–2013). Red oak increased its share of total biomass from 30% in 1992 to 34% in 2013, whereas red maple decreased from 17% to 14% of total biomass. From 1992 to 2013, white pine and hemlock each maintained about 18% of total biomass. Tree-ring data indicate that red oak biomass increment has dominated total forest growth since at least 1960 (Fig. 4b), and red oak's contribution to total biomass increment increased about 5% from 1992–2012 ($p = 0.003$).

Carbon pools

Ecosystem C stock averaged 34,600 ± 5,400 (mean ± SD) and 29,600 ± 4,700 g C m^{-2} in hemlock and hardwood stands, respectively (Table 2). Of this, 44% was in soil C pools to a depth of 45 cm, 40% was in live aboveground biomass, ~6% was in woody debris, and ~10% was in root biomass in both

stand types. Aboveground live biomass, fine woody debris, coarse and fine roots, and C in the organic horizon and 45 cm deep in the mineral soil were all significantly greater in hemlock than in hardwood stands (Table 2). The only C pool that was significantly larger in hardwood stands was coarse woody debris.

C stocks for individual research projects are summarized for live trees (aboveground plus coarse roots), deadwood, soil, and fine roots in Supplemental Tables S3, S6, S7, and S8, respectively.

Carbon fluxes

NPP

Annual NPP for hemlock- and hardwood-dominated forests averaged 746 ± 239 g C m^{-2} yr^{-1} and 733 ± 197 g C m^{-2} yr^{-1}, respectively (Table 3). ANPP was ~54% of NPP, with foliage production representing 50–60% of ANPP. BNPP was 349 ± 196 g C m^{-2} yr^{-1} and 332 ± 149 g C m^{-2} yr^{-1} in the hemlock- and hardwood-dominated forests, respectively. Root NPP accounted for ≥ 72% of BNPP with the remaining 21–28% accounted for by root exudation (Table 3). For the subset of plots surrounding the HEM and EMS tower sites, NPP and its distribution above- and below-ground were similar to the forest as a whole (Table 4). For brevity, subtle distinctions between tower plots and the entire data set are not described in the text (but compare Table 3 with Table 4).

For the period 1998–2014, mean annual aboveground biomass increment was 200 ± 118 g C m^{-2} yr^{-1} for hardwood-dominated plots (Table 3). Aboveground biomass increment in the hemlock-dominated plots averaged 166 ± 99 g C m^{-2} yr^{-1}. Aboveground biomass increment, based on allometric equations, included both woody and foliar increments, whereas foliage production was measured separately. Nearly all aboveground biomass accrued on existing stems, as recruitment of new trees was < 1% of aboveground biomass increment in all the undisturbed permanent-plot studies.

Total litterfall (a proxy for foliar production) averaged 201 ± 51 g C m^{-2} yr^{-1} for hardwood plots and 231 ± 94 g C m^{-2} yr^{-1} for hemlock plots. Litterfall was the only C flux that was significantly different

between the forest types (Table 3). It was also significantly greater at the HEM than at the EMS site (Table 4).

For the hardwood plots, both biomass increment and annual litterfall increased over the period 1998–2014 (Fig. 5a, b). Biomass increment was 168 g C m^{-2} yr^{-1} in 1998 and increased 7.8 g C m^{-2} yr^{-1} (SE of slope = 1.22; lm, aboveground and coarse root increment~year, $F_{1,506} = 40.7$, $p < 0.05$). Foliar litterfall was 136 g C m^{-2} yr^{-1} in 1998 and increased 2.26 g C m^{-2} yr^{-1} (SE of slope = 0.37; lm, litterfall~year, $F_{1,699} = 37.7$, $p < 0.05$). For the period 2000–2014 (total litterfall data, including foliar and woody components, was not available prior to 2000), NPP (excluding fine roots and root exudates) increased at a rate of ~9.2 g C m^{-2} yr^{-1} from a modeled starting value of 372 g C m^{-2} yr^{-1} in 2000 (Fig. 5c; SE of slope = 3.3; lm NPP~year, $F_{1,13} = 7.7$, $p < 0.05$). Over 14 years, NPP of the hardwood stands increased by nearly 130 g C m^{-2} or ~26%. There were fewer data and years of measurement for hemlock-dominated plots. No trends over time were detected in this forest type (Fig. 6a–c), although decreased foliar production is notable after 2012, as HWA established at the Harvard Forest and hemlock health began to decline.

Annual increment of coarse roots averaged 34 ± 20 and 38 ± 23 g C m^{-2} yr^{-1} for hemlock and hardwood plots, respectively. Fine root production was the largest component of BNPP, averaging 218 ± 174 and 225 ± 136 g C m^{-2} yr^{-1} in hemlock and hardwood plots, respectively (Table 3). Root exudates contributed 97 ± 88 (hemlock) and 69 ± 56 g C m^{-2} yr^{-1} (hardwood). Neither of these fluxes were sampled consistently enough to estimate change over time.

NEP

Eddy-covariance flux estimates of NEP indicated that the EMS and HEM tower sites were net C sinks of 298 ± 153 g C m^{-2} yr^{-1} and 465 ± 83 g C m^{-2} yr^{-1}, respectively, before hemlock trees started declining because of the hemlock woolly adelgid infestation (Table 4, Fig. 7a). At the EMS site, there was an increase in net C uptake for the period 1992–2008 followed by an abrupt decline in 2009–2011 and return to near average conditions thereafter (Fig. 7b). For the full EMS record (1992–2015),

there was a non-significant trend of increasing C uptake with time of 6.9 g C m^{-2} yr^{-1} (p = 0.13). Over 24 years, NEP increased by nearly 168 g C m^{-2} or ~93%.

NEP during the first 8 years of the 11-year record at the HEM site did not suggest a significant trend in net C uptake (Fig. 7b). Beginning in 2013, however, there was a steep decline in NEP following the outbreak of the hemlock woolly adelgid at the site. Cumulative NEP indicated that both tower sites were growing C sinks until 2014 (Fig. 7a), when the HEM tower site turned into a net C source to the atmosphere on an annual basis (Fig. 7b). The CC site was a strong net C source in the years immediately after harvest, but it turned into a net C sink on an annual basis in 2013, the fifth year after the disturbance (Fig. 7b). By the end of 2015, seven years after harvest, the CC site had regained about two thirds of the C it had lost to the atmosphere from on-site decomposition since the harvest (Fig. 7a) and it is expected to become a C sink in the next 3–5 years barring major disturbance.

At the EMS site, GPP ranged from 1,176 to 2,133 g C m^{-2} yr^{-1} (mean = 1,526 g C m^{-2} yr^{-1}) and R_e ranged from 879 to 2,013 g C m^{-2} yr^{-1} (mean = 1,228 g C m^{-2} yr^{-1}; Appendix S1: Table S9). Soil and total ecosystem respiration were significantly larger at the EMS site than at the HEM site (Table 4). Partitioning of the eddy-covariance fluxes suggested that GPP increased more rapidly than R_e for the period 1992–2008 at the EMS site (Fig. 7c, d), leading to the site's growth as a C sink. From 2009 to 2016 the EMS site remained a C sink but the size of the sink declined to the long-term average of ~200–300 g C m^{-2} yr^{-1} (Fig. 7b). At the HEM site, GPP ranged from 1,083 to 1,614 g C m^{-2} yr^{-1} (mean = 1,370 g C m^{-2} yr^{-1}) and R_e from 843 to 1,228 g C m^{-2} yr^{-1} (mean = 1,022 g C m^{-2} yr^{-1}; Appendix S1: Table S9). Initially, there was no clear temporal trend in the partitioned fluxes at the HEM tower site (Fig. 7c, d). Beginning in 2011, however, GPP declined precipitously. At the CC site, GPP ranged from 1,171 to 2,339 g C m^{-2} yr^{-1} and R_e ranged from 1,421 to 2,078 g C m^{-2} yr^{-1} (Appendix S1: Table S9). GPP generally increased from year to year while R_e tended to decrease with time, resulting in a steady increase in NEP (Fig. 7).

There was generally good agreement between annual NEP, GPP, and R_e estimated with the REddyProc, FCRN, or PI-preferred gap-filling and partitioning algorithms (Appendix S1: Fig. S2). At

times, one of the methods gave results very different from the others (e.g., EMS-NEP in 2005 and 2011 [Appendix S1: Fig. S2a], CC-NEP in 2015 [Appendix S1: Fig. S2g]). This was usually in years when one or multiple very large gaps (> 40 days) occurred in the data series during the growing season, or when a larger proportion of data than usual was missing during the growing season. For example, this was the case in 2005 when a storm caused instrument damage.

Interannual variation in mid-summer ecosystem photosynthetic capacity (A_{max}) was > 2-fold at the three tower sites (Fig. 8a–c, Appendix S1: Fig. S3). At saturating light (> 1000 μmol PPFD m^{-2} s^{-1}) GPP varied between 14 and 49 μmol C m^{-2} s^{-1} at the EMS site, 5 and 32 μmol C m^{-2} s^{-1} at the HEM site, and 9 and 45 μmol C m^{-2} s^{-1} at the CC site (Fig. 8a–c). There were significant increases in NEP with LUE (Fig. 9a) and in GPP with A_{max} (Fig. 9b). Plant area index varied by 1 m^2 m^{-2} among years at the EMS site, reflecting variation in summer leaf area, not branch or stem area as indicated by consistent winter PAI minimum (Fig. 8d). GPP increased linearly with PAI at the CC tower site (Fig. 8e) while NEP increased with PAI at the EMS site (Fig. 9c). GPP per unit leaf area was lowest at the HEM tower site (Fig. 8e). Red oak tree-ring increment varied 25% around the 1992–2012 mean, and increment was positively correlated with NEP at the EMS tower (Fig. 9d).

Interannual variation in PAI was not significantly related to interannual variation in A_{max}. Urbanski et al. (2007) found a positive correlation between A_{max} and PAI, but for a limited number of years at the EMS tower site. Data collected since then find high A_{max} for both high and low PAI (Fig. 8, Appendix S1: Fig. S3).

There was pronounced seasonality in the respiratory fluxes of C at the Harvard Forest (Fig. 10). At the EMS tower site, R_e increased with air temperature in the spring following snowmelt and was initially driven by aboveground respiration (Fig. 10a). As the soil warmed, peaking an average of 18 days later than air temperature, belowground respiration came to dominate R_e and aboveground respiration declined. The initial increase in R_e at EMS coincided with increases in tree diameter (measured every one to two weeks by dendrometer bands) and the deployment of leaves (Fig. 11). By mid-August, aboveground growth was largely complete and the preponderance of R_e was from

belowground. A similar phenology was observed at the HEM tower site (Fig. 10b) with the exception that the spring increase in R_e was more equitably distributed between above- and belowground respiration. Interestingly, the autumnal increase of aboveground respiration at the EMS site was not observed at the HEM tower site.

Tree growth was sensitive to interannual and seasonal variation in both temperature and precipitation. Correlations between monthly temperature and precipitation for red oak and red maple (the two dominant hardwood tree species at the Harvard Forest) are presented in Appendix S1: Table S10.

Annual soil respiration (R_s) varied from 628 to 876 g C m^{-2} yr^{-1} (Appendix S1: Table S9). Mean annual R_s was 738 ± 42 g C m^{-2} yr^{-1} and 659 ± 18 g C m^{-2} yr^{-1} in hardwood- and hemlock-dominated forests, respectively. As a percentage of total ecosystem respiration, R_s accounted for 63 ± 9% of the total flux (range: 38–83%, Appendix S1: Table S9).

One year of stream DOC measurements showed an export of 1.72 ± 0.01 g C m^{-2} yr^{-1} over the 24 ha catchment area (Wilson et al. 2013), two orders of magnitude less than NEP.

Spring and autumn phenology

The duration of the growing season, the period between the first and last day of the year when NEP exceeded 30% of the mean maximum daily NEP, increased with time (Fig. 12). At the EMS site, the length of the growing season increased significantly at a rate of 0.85 d yr^{-1} because of both an earlier onset (0.38 d yr^{-1}) and a later end (0.47 d yr^{-1}). At the HEM site the length of the growing season increased, but not statistically significantly so, at a rate of 2.68 d yr^{-1} due to an earlier onset (1.51 d yr^{-1}) and a later end (1.17 d yr^{-1}).

Predictably, there were significant relationships between the timing of the onset and the end of the growing season, and the magnitude of seasonal NEP at the EMS site (Fig. 13a, c). On average, an earlier onset of the growing season by one day resulted in a 3.6 g C m^{-2} increase in March–May NEP. Likewise, a one-day delay in the end of the growing season corresponded to a 5.3 g C m^{-2} increase in

September–November NEP. The relationships between phenology dates and seasonal NEP were statistically significant in the spring but not in the autumn at the HEM site (Fig. 13b, d).

Based on these data, we calculated the contribution of a longer growing season to ANPP and NEP at the EMS site as follows. Assuming a growing season length of 120 days per year (Fig. 12) and an annual rate of ANPP of 390 g C m^{-2} yr^{-1} (Table 4), gives an average daily rate of ANPP of 3.2 g C m^{-2} d^{-1}. Given that the growing season length has increased 0.85 days yr^{-1} (Fig. 12), lengthening of the growing season alone accounts for an additional 2.7 g C m^{-2} yr^{-1} (i.e., 0.85×3.2 g C m^{-2} d^{-1}) in ANPP. Similarly, NEP at the EMS site was 298 ± 153 g C m^{-2} yr^{-1} (Table 4). Given a 120-day growing season, the average daily rate of NEP is 2.5 g C m^{-2} d^{-1}. Lengthening of the growing season therefore accounts for an additional 2.1 g C m^{-2} yr^{-1} in NEP.

Decadal changes in C stocks

We documented a net increase in ecosystem C in the live-tree pool for hardwood and hemlock forests. Based on the nine plot-based studies with multiple tree censuses spanning at least 10 years, net accrual of aboveground C (growth + recruitment − mortality; mean ± SD) averaged 150 ± 125 g C m^{-2} yr^{-1} for hardwood-dominated plots and 19 ± 259 g C m^{-2} yr^{-1} for hemlock-dominated plots (Appendix S1: Table S3). The background annual mortality rate in the permanent plots and experimental controls averaged 1.3 ± 0.7%. Smaller diameter trees had a disproportionately high mortality rate (Appendix S1: Fig. S1). Annual C loss to mortality averaged 57 ± 162 g C m^{-2} yr^{-1} for hardwood plots and 124 ± 224 g C m^{-2} yr^{-1} for hemlock plots and showed no trend over time in either forest type (Appendix S1: Fig. S4). No plot in this analysis experienced timber harvest during the period of study, but averaged across the entire Harvard Forest's ~1500 ha, timber harvest records indicated that removals of C in harvested trees averaged ~11 g C m^{-2} yr^{-1} during the period of 1990–2015.

We detected minor and equivocal changes over time in deadwood C pools (Appendix S1: Fig. S5). For all hardwood plots with deadwood measurements combined, there was no trend over time in standing dead wood stocks. Coarse woody debris (CWD; downed wood > 7.5 cm diameter) pools

began at 1,411 ± 241 g C m^{-2} ($p < 0.001$) and decreased slightly by −31.2 ± 15.7 g C m^{-2} yr^{-1} ($p = 0.049$). Fine woody debris (FWD; downed wood 0.6–7.5 cm diameter) pools began at 112 ± 38 g C m^{-2} and increased slightly by 7.2 ± 2.5 g C m^{-2} yr^{-1}. For the EMS tower plots, CWD had a significantly positive slope (69 ± 30 g C m^{-2} yr^{-1}) in contrast to the overall hardwood trend, and there were no changes over time in standing deadwood or FWD. Although we had many one-time measurements of deadwood C pools in hemlock-dominated sites and a robust estimate of average pools of CWD, FWD, and standing dead wood (Table 2), there were too few repeated measures of deadwood measurements to examine trends over time for the hemlock forests overall or at the HEM tower site.

Nearly all the studies reporting soil C data were from one or two years of study. As a consequence, only data from the PHOREST plots (mineral soil C content sampled in 1992 and 2013 in 42 plots) could provide information on changes in soil C pools through time. In this data set, there was no apparent net accrual of soil C through time (Appendix S1: Table S11). For the period 1992–2013, soil bulk density declined on average 0.05 ± 0.15 g cm^{-3} whereas soil %C increased on average 0.50 ± 2.01% such that the total quantity of C in the soil did not change for the period 1992–2013 (Appendix S1: Table S11).

Regional comparisons

Based on FIA plot data, aboveground C in the two ecoregions surrounding the Harvard Forest ranged from 1,500 to 15,200 g C m^{-2} with a median of 6,500 g C m^{-2} (Fig. 2). This is considerably lower than the median for the Harvard Forest, 11,600 g C m^{-2}.

The PnET-II estimate of GPP for the region ranged from 797 to 1,622 g C m^{-2} yr^{-1} with a mean of 1,324 g C m^{-2} yr^{-1} (Zhou et al. 2018, Fig. 2). Predicted GPP for the Harvard Forest (mean of 1,329 g C m^{-2} yr^{-1}) did not differ from the region-wide mean. The PnET-II estimate of GPP closely matched that estimated from the HEM tower fluxes, for the period 2004–2011. For the EMS tower, mean GPP predicted by the model was 5.6% lower than the tower-based estimate and the model did not capture the observed trend of increasing GPP for the period 1992–2010 (Zhou et al. 2018).

DISCUSSION

This work synthesized hundreds of thousands of observations to quantify the C cycle for the Harvard Forest in central Massachusetts, USA and to place the Harvard Forest within a regional context. These data, collected at a wide range of temporal and spatial scales, consistently described undisturbed forests as active C sinks. The climate of the Harvard Forest has measurably changed with increasing temperature leading to longer growing seasons and higher precipitation during the growing season. There has also been a continuous increase in atmospheric CO_2 concurrent with a decline in ground-level O_3, and sulfate and total N deposition. The results of this study alongside simulation modeling suggest that land-use abandonment at the turn of the last century, a reduction in forest harvesting, and climate and atmospheric changes drive the slow but steady increase in ecosystem C content (Ollinger et al. 2002, Albani et al. 2006, Thompson et al. 2011, Duveneck et al. 2017).

Prior to the outbreak of the hemlock woolly adelgid (HWA), C stocks within hardwood- and hemlock-dominated stands were not significantly different and nearly equally divided between soil and biomass pools. Carbon continued to accumulate, with NEP averaging 298 ± 153 g C m^{-2} yr^{-1} in hardwood stands and 465 ± 83 g C m^{-2} yr^{-1} in hemlock stands prior to the widespread outbreak of HWA in 2013. Since 2013, however, hemlock-dominated stands have become a source of C to the atmosphere. Whereas direct measurements of soil C stocks showed no change between 1992 and 2013 (Appendix S1: Table S11), soil radiocarbon studies suggest a small sink on the order of 10–30 g C m^{-2} yr^{-1} (Gaudinski et al. 2000, Sierra et al. 2012).

Although climate change for the period of intensive measurements reported here (1992–2015) is modest compared to predictions for the future, our findings suggest that it has had a discernible impact on the C cycle. The progressive lengthening and warming of the growing season through time has increased net C uptake in hardwood stands. This is likely reinforced by increasing precipitation, CO_2 fertilization, increases in water-use efficiency (WUE), and changes in atmospheric deposition (Thomas et al. 2010, Keenan et al. 2013). In hemlock stands, a similar phenomenon occurred until 2013 when a growing regional HWA population led to increased hemlock mortality. Invasive insects

alongside other major disturbances (e.g., logging, hurricanes, extreme climate events) are the largest threats to continued atmospheric CO_2 sequestration at this site.

The present-day carbon cycle

There was a near-equal distribution of total ecosystem C between that in live biomass (~50%) and the soil to 45 cm depth (~45%) with the remaining ~5% as woody debris (Table 2). The quantities of C in live aboveground biomass and in soil were similar in hardwood- and hemlock-dominated plots, but the soil organic horizon in hemlock stands contained ~1500 g C m^{-2} more than that found in the hardwood stands. Root biomass was a small C pool at the Harvard Forest, comprising ~20% of total biomass and ~10% of total ecosystem C, consistent with an analysis of global temperate forests in which belowground biomass comprised 20–30% of aboveground biomass (Cairns et al. 1997). It was also consistent with the Hubbard Brook Experimental Forest in central New Hampshire; there, estimated root biomass was ~21% of total biomass (Fahey et al. 2005).

ANPP at the Harvard Forest averaged 390–430 g C m^{-2} yr^{-1} and total NPP averaged 680–750 g C m^{-2} yr^{-1} (Tables 3, 4). Root NPP (BNPP; coarse roots, fine roots, root exudates) averaged 47% and 45% of total NPP in hemlock- and hardwood-dominated stands, respectively (Table 3). Thus, roots represent a major portion of NPP at the site. Unlike aboveground C pools, however, automated measurements and inventories of both root and soil C pools are comparatively scarce for the Harvard Forest, and indeed most forests. There is therefore great uncertainty in this aspect of the C budget. The estimates of root NPP in this study are similar, but by no means identical, to values reported in the literature. For healthy hemlock stands, the only estimate of root NPP is that reported here and it is based on the work of Abramoff and Finzi (2016). For hardwood stands, we report root NPP of 332 ± 149 g C m^{-2} yr^{-1} (Table 3). This is higher than that reported by McClaugherty et al. (1982; 270 g C m^{-2} yr^{-1}) and Gaudinski et al. (2010; 72 g C m^{-2} yr^{-1}).

The substantial variability, particularly the standard deviation of the mean BNPP we report in Tables 3 and 4, argues that more plots, more samples per plot, and more longitudinal studies are needed to constrain these values for the Harvard Forest.

At present, we estimate that soil C pools are neutral to small sinks for atmospheric CO_2. There are, however, only two longitudinal studies of soil C at the Harvard Forest. In the first study (PHOREST), bulk soil C content was surveyed in 1992 (Motzkin et al. 1999) and again in 2013 (Appendix S1: Table S11). This study showed that small and statistically non-significant increases in soil C concentration through time were offset by similarly small and non-significant decreases in soil bulk density such that there was no net change in total soil C in the top 15 cm of mineral soil in hardwood- (n = 31) and hemlock- (n = 11) dominated plots. In the second study, ^{14}C was used to estimate the turnover time of different soil C pools (litter, humified, mineral-associated) in well-drained glacial till, the most prevalent soil type at the Harvard Forest (Gaudinski et al. 2000). Their radiocarbon mass balance estimated a soil-C accrual rate of 10–30 g C m^{-2} yr^{-1}. This rate may have been more rapid immediately following agricultural abandonment in the late 1800s, but nevertheless this approach suggests that a small C sink persists in the soil to this day. Adding confidence to the assessment of Gaudinski et al. (2000), Sierra et al. (2012) resampled the same soil pits and found close agreement with earlier estimates of C pool sizes, fluxes, and turnover times. Although we cannot be sure that these data apply to all forest and soil types at the Harvard Forest, the rate of soil C accrual based on radiocarbon is consistent with data showing generally negligible to small increases in soil organic carbon (SOC) following agricultural abandonment at the Harvard Forest (Compton and Boone 2000), in central New England (Hooker and Compton 2003), the Great Lakes region (Morris et al. 2007), and North American forests more generally (Nave et al. 2013).

Resolving the uncertainty in SOC change a century into forest regrowth is a major challenge. The annual change in SOC, whether positive or negative, is small but the pool of C is large, making it difficult to detect a significant change. As a case in point, we collected 77 soil samples (5 cm diam., from the soil surface to 30 cm depth in the mineral soil) from hemlock forests surrounding the HEM tower to conduct a power analysis for SOC change in the years to come as hemlock declines (Appendix S1: Fig. S6). Using Monte Carlo resampling, we estimated that 2,919 samples would be required to detect a significant change ($p < 0.05$) for a relatively large change in SOC of 150 g C m^{-2}. For a more realistic change on the order of 20 g C m^{-2} the number of samples skyrockets to 164,194. However, the likelihood of detecting small annual changes in SOC increases if samples are collected

many years from one another. For example, to detect a change in SOC of 20 g C m^{-2} yr^{-1} over the 21 years the PHOREST study has been ongoing would require 372 samples for detection at $p < 0.05$. Admittedly, this is a formidable soil processing challenge, but it is possible with sufficient resources and time.

In contrast to an inventory-based approach, the benefit of the radiocarbon approach is that it integrates information on the ages of C in different pools (i.e., SOC, roots). These ages can then be transformed into residence times and fluxes of C in the belowground system (Gaudinski et al. 2000). The radiocarbon approach does, however, require a number of assumptions to calculate C ages, C turnover times, production and consumption of litter inputs, and so on, each of which has its own uncertainty. So, it too must be used in combination with other approaches to build a comprehensive understanding of belowground C cycling. To this end, the recent establishment of a belowground C observatory at the Harvard Forest that uses long-term resampling plots coupled with an array of measurements (i.e., soil respiration, trenching, $\Delta^{14}C$, $\delta^{13}C$) should deepen our understanding of the belowground C cycle at this site.

Seasonal and interannual variations in carbon fluxes

Differences between conifer and hardwood leaf longevity and physiology led to distinct seasonal variations in GPP, R_e, and the DOY the stands became net C sinks (Fig. 10, Appendix S1: Table S12). Atmospheric warming during the transition from winter to spring stimulates ecosystem respiration in advance of the uptick in photosynthesis in both forest types. However, it was not until ~1 July at the EMS tower that carbon uptake balanced the carbon loss from respiration over the non-growing season. By contrast, C uptake at the HEM site balanced C loss from the winter far earlier, on average April 3 (Appendix S1: Table S12). At the CC site, this balance occurred around May 11. The earlier date of net annual C uptake at the HEM site reflects the persistence of a live, overwinter canopy that can actively photosynthesize once temperatures are consistently above 0 °C (Hadley and Schedlbauer 2002). Although photosynthesis can occur at low temperatures, −5 to −11 °C (Burkle and Logan 2003), the data suggest this makes a very minor contribution to overall ecosystem C uptake. At the deciduous-dominated EMS and CC sites, GPP remained very low throughout the winter, but not

necessarily zero because there are some conifers within their footprints. The later DOY for net C uptake at the EMS site is also explained by the comparatively large winter respiration flux, whose source remains as yet unresolved.

At the EMS site, the springtime lag between the increase in air temperature and the later increase in soil temperature resulted in a larger proportion of R_e derived from aboveground biomass and an earlier peak in R_e compared to R_s (Fig. 10). There was strong synchrony between aboveground respiration, leaf area expansion, and diameter growth from spring until peak LAI (Fig. 11). By mid-August, however, aboveground growth was largely complete and the preponderance of R_e was from R_s until the fall when there was an uptick in aboveground respiration that may be related to foliar nutrient retranslocation, foliar senescence, and winter hardening (Fig. 11). The phenology of R_e at the EMS site is consistent with a recent meta-analysis demonstrating that root growth lags behind shoot growth in temperate and boreal forests (Abramoff and Finzi 2015). The phenology of C fluxes at the HEM tower site were similar to those at the EMS site with one notable exception: R_e peaked approximately two weeks later, on average, and declined more rapidly thereafter compared to the EMS site (Fig. 10).

The updated eddy-covariance analysis reported here presents a dynamic picture of forest–atmosphere C exchanges. In particular, among the flux sites analyzed by Keenan et al. (2013), the EMS tower data showed the strongest increase in annual net C uptake. For the 1992 to 2009 period of their analysis, NEP increased an average of 23 g C m^{-2} yr^{-1}, resulting in a gain of 400 g C m^{-2} yr^{-1} in NEP in those 18 years. For the 24-year period (1992–2015) analyzed here, average annual NEP increased 6.9 g C m^{-2} yr^{-1}, or about 168 g C m^{-2} yr^{-1} more uptake in 2015 compared to 1992 (Fig. 7b). This brings the annual increase in NEP at the EMS site in line with the other sites analyzed by Keenan et al. (2013). Importantly, the long-term trend reported here suggests that the rapid increase in NEP between 1998 and 2008 was transient.

Interpretation of the very high NEP from 2004–2008, and very low NEP in 2010–2011 is complex. Advances in flux partitioning, including Wehr et al.'s (2016) work using isotopologues of CO_2 at the

EMS site can help discern the net balance of photosynthesis and R_e. However, Wehr's results apply directly only to the period of that study, which encompasses the 2011–2013 growing seasons. A detailed analysis of the environmental drivers and biotic responses (*sensu* Richardson et al. 2007), and how to apply partitioning studies to the full NEE record, is underway.

There was large inter-annual variation (50–100%) in maximum canopy photosynthetic rate (A_{max}, Fig. 8a–c, Appendix S1: Fig. S3b, Appendix S1: Table S13) and light use efficiency (LUE; α, Appendix S1: Fig. S3a, Appendix S1: Table S13). At the early-successional CC tower site, annual increases in LUE and A_{max} were driven by the accrual of leaf area in this rapidly aggrading stand (Fig. 8c, e). At the closed-canopy EMS tower site, interannual variations in NEP were positively correlated with PAI (Fig. 9c). The slope of this regression line implies that NEP increases by ~280 g C m^{-2} yr^{-1} for every 1 m^2 m^{-2} increase in PAI, which is the maximum variation observed in the data set. We also find that NEP is positively correlated with canopy-scale LUE (Fig. 9a), and that GPP is positively correlated with canopy-scale A_{max} (Fig. 9b). These results suggest that plasticity in canopy-scale attributes like photosynthetic rate and leaf area have a measurable impact on C uptake at this site. However, the causality between interannual variations in C fluxes and those of canopy-scale attributes remains unclear. For example, do increases in A_{max} and PAI drive increases in C uptake or are they the consequence of favorable growing conditions and high C uptake, or both?

Different methods of measuring ecosystem carbon accrual were well correlated, although some differences remained. We compared the difference in net ecosystem production assessed by tower- and ground-based measurements for the two mature forest types (Table 4). Tower-based NEP was higher than plot-based NEP, which corroborates earlier analyses reported by Barford et al. (2001). Twenty-four years of data from the hardwood forest site narrowed the difference between these two measurement approaches to 36%, whereas the difference was 61% after eight years of study of the hemlock forest site. Ecologically, it stands to reason that the difference in NEP estimates narrows through time since biomass is produced from a combination of current-year and stored photosynthate. With many years of data (i.e., a larger sample size), the interannual variations in climate and forest productivity converge towards a mean value whose uncertainty declines.

Stand dynamics and recent global change

At annual to decadal time scales, neither stand biomass nor rates of NPP are at steady state in the mature hardwood-dominated stands at the Harvard Forest. Rather, the stands remain active C sinks as they accrue biomass following land-use abandonment and low rates of forest harvest. This general pattern of land-use history and ecosystem recovery characterizes temperate forests across much of eastern North America (Gough et al. 2016, Nave et al. 2017). At the Harvard Forest, NPP also increased by ~26% from 2000 to 2014 (Fig. 5). Both stand dynamics and global change likely contribute to the observed NPP increase.

Species composition change, particularly increasing red oak dominance, likely contributed to the trend of increasing NPP. Red oak tree-ring increment positively correlated with tower-based NEP (Fig. 9d). Maples and birches initially dominated the mixed-species hardwood forests that developed after agricultural clearing, after old-field white pine harvest, or the 1938 hurricane. Red oak height growth then accelerated and within about 30 years red oak rose to its current dominance in the canopy (Oliver 1975, 1978, Oliver and Stephens 1977). Red oak relative abundance increased from 30% of total biomass in 1992 to 34% in 2013 (Fig. 4a), contributing 45% of the overall increase in live tree biomass during the study period. Its increasing dominance is corroborated by previous, site-specific studies at the Harvard Forest (Fig. 4b; Urbanski et al. 2007, Eisen and Barker Plotkin 2015).

It appears that red oak has an inherently higher growth capacity than the other abundant species at the Harvard Forest. Of the major tree species, it has the highest concentration of N in foliage and the most rapid rate of net photosynthesis (Bassow and Bazzaz 1997). Red oak also has a high water-use efficiency (Turnbull et al. 2002). These ecophysiological traits alongside the fact that red oak trees at Harvard Forest have an average diameter larger than that of the other species present, likely gives rise to red oak's outsized contribution to NPP and NEP (Lutz et al. 2012, Stephenson et al. 2014).

The majority of the NPP at the Harvard Forest is allocated to the production of fast-cycling C pools: leaves (22%), fine roots (29%), and root exudates (8%, Table 4). Leaves and roots have high N

concentration, so the increase in total tree biomass and NPP implies an increase in N uptake through time, or possibly an increase in N-use efficiency (c.f., Finzi et al. 2007). As an ectomycorrhizal (ECM) tree species, red oak can access soil N via fungal symbionts. ECM fungi produce both oxidative and hydrolytic enzymes that are released into soil (Chalot and Brun 1998). These enzymes are often within mucopolysaccharides produced by the fungus that are reabsorbed after the decomposition of organic matter (Lindahl et al. 2005, Hobbie and Hobbie 2008). This strategy confers a competitive advantage for N to the ECM trees relative to free-living microbes and non-ECM trees (Averill et al. 2014). This suggests that ECM fungal association should be added to the list of autecological factors contributing to red oak's dominance and high productivity at the Harvard Forest.

Recent warming trends have altered the rate of C cycling in hardwood- and hemlock-dominated stands. At the EMS site, spring is occurring earlier, the onset of fall is occurring later, and the length of the growing season is increasing with time (Fig. 12). Such changes have decreased springtime net C losses because of earlier onset of C uptake (Fig. 13a), increased fall C uptake (Fig. 13c), and enhanced NEP through time (Fig. 7b).

At the EMS site we found that the length of the growing season increased by just under one day per year. This means ANPP has increased by 2.7 g C m^{-2} yr^{-1}(see *Methods* for details of the calculation). Since the average annual increase in ANPP was 9.2 ± 3.3 g C m^{-2} yr^{-1} (Fig. 5c), lengthening of the growing season alone accounts for up to 30% of the observed annual average increase in ANPP. A similar calculation is possible for NEP. Here we estimate that lengthening of the growing season increases NEP by 2.1 g C m^{-2} yr^{-1}. Because the average annual increase in NEP at the EMS site is 6.9 ± 9.0 g C m^{-2} yr^{-1} (Fig. 7b), lengthening of the growing season alone also accounts for 30% of the annual increase in NEP.

The signature of a changing climate on hemlock forest productivity was also in evidence. The most important of these is the spread of HWA into the footprint of the Harvard Forest and the decline in hemlock (Ellison et al. 2018). The spread of this invasive insect is closely tied to climate, with a northward expansion facilitated by warming temperature. Prior to infestation of the HEM tower site,

however, we observed an earlier onset of springtime, later onset of leaf off of the deciduous component of the forest and lengthening of the growing season (Fig. 12b). None of these trends was statistically significant because there are fewer years of data available at this site (Fig. 12b). Similar to the EMS site, there was a significant relationship of earlier spring resulting in greater C uptake at the HEM site (Fig. 13). By contrast, lengthening of the growing season in the autumn was negatively, albeit not significantly, correlated with NEP. Lengthening of the growing season at the HEM site did not increase net C uptake.

At the same time that the growing season is lengthening, other global change factors are concurrently changing. These include a rise in atmospheric CO_2, a decrease in atmospheric deposition of N and SO_4^{2-}, a decrease in ground-level O_3 concentrations, and the previously discussed increases in temperature and precipitation (Fig. 3). These changes in atmospheric chemistry may be collectively important. For example, the declines in total N and SO_4^{2-} deposition, and the increase in the pH of precipitation (*data not shown*) are leading to a gradual deacidification of soils and soil water in New England and in Europe (Driscoll et al. 1998, Stoddard et al. 1999). It seems reasonable to hypothesize that collectively, the accumulated effect of all these small but significant global changes may also be contributing to the increase in productivity through time (c.f., Fernández-Martínez et al. 2017).

With specific respect to rising atmospheric CO_2, the average annual concentration of CO_2 has increased 13%, from 356 ppm in 1992 to 401 ppm 2015 (+45 ppm, NOAA 2019). Previous research at eddy-covariance sites throughout the northeast correlated increases in NEP over time with increases in WUE owing to rising CO_2 (Keenan et al. 2013). Mechanistically, this occurs because stomatal aperture can decline with rising CO_2 because of the increasing CO_2 concentration gradient between the atmosphere and leaf mesophyll cells. As such, rising CO_2 can allow plants to conserve water, maintain photosynthetic rates, and increase the ratio of C fixed to water transpired (i.e., WUE; Battipaglia et al. 2013).

While there are no whole-system CO_2 exposure studies at the Harvard Forest, greenhouse work with the dominant species at the forest showed that they are responsive to CO_2 under limiting and non-

limiting nutrient conditions (Bazzaz and Miao 1992, Miao 1995, Driscoll et al. 1998). While a formal study of attribution (*sensu* Bindoff et al. 2013) has not been conducted with respect to the CO_2 effect on productivity at the Harvard Forest, Fernández-Martínez et al. (2017) suggest a direct CO_2 enhancement of 1% on NEP across eastern North American and European forests for the period 1995–2011. Regionally, Ollinger et al. (2002) used the simulation model PnET-II to show that rising atmospheric CO_2 and N deposition, alone and in combination, had significant, positive effects on northeastern forest productivity. It therefore seems reasonable to suggest that rising atmospheric CO_2 is having an effect on C exchange at the Harvard Forest. At present, however, we do not have direct, site-specific evidence for a CO_2-fertilization effect on productivity.

Increasing precipitation over the study period (Fig. 3b) also likely contributed to the observed increases in NPP and NEP at the EMS site. Most of the increased precipitation fell during the growing season (May–October). Co-analysis of tree rings and climate variables in red oak indicates that late-summer precipitation can increase growth, suggesting that even mesic forests like the Harvard Forest (Belmecheri et al. 2014), and eastern temperate forests in general, are sensitive to water availability (Martin-Benito and Pederson 2015, D'Orangeville et al. 2018). Regionally, the number of rainless days declined during the past 30 years, suggesting a decline in drought conditions (Bishop and Pederson 2015). Our study period was during one of the wettest eras of not only the last 500 years (Pederson et al. 2013, 2015), but perhaps of the last 5000+ years (Shuman and Marsicek 2016, Marlon et al. 2017). Other drivers of carbon dynamics may be more apparent during this period of measurement because, relative to the past, the occurrence of drought stress has been less frequent.

Comparisons to global change experiments

Forest regrowth following land-use abandonment is likely the largest contributor to the observed C sink at the Harvard Forest during the last century. After that, our findings suggest that climate change and other global change drivers have enhanced the C sink in biomass over the last three decades. Climate and other global change factors may have had an effect further back in time, but prior to 1990 there are fewer systematic measurements of C stocks and fluxes to help us assess earlier changes.

The Harvard Forest hosts long-term global change experiments that simulate aspects of climate change, atmospheric chemistry change, and the spread of invasive insects. Each of these factors affects the C cycle and other ecosystem processes. We compared C-cycle responses from three experimental studies—soil warming, N deposition, and hemlock removal—to the observational data presented here to provide a broad context within which we can interpret the experimental work.

One of the largest uncertainties in the global C cycle is the response of soil C to warming. Globally, soils store more C than is present in the Earth's atmosphere and vegetation combined (Scharlemann et al. 2014, Jackson et al. 2017), so small changes in soil-C cycling may have a large effect on the future climate. Beginning in 1991, soil warming experiments at the Harvard Forest heated the soil +5 °C above ambient (Melillo et al. 2002, 2011, 2017). The IPCC's 5th assessment reported that this level of soil warming would only be achieved under the most extreme scenario for climate change, RCP 8.5, in about the year 2140 (Collins et al. 2013). The initial results from the longest-running soil warming study at this site found that putative soil C losses ranged from 90 to 180 g C m^{-2} yr^{-1} for up to 7 years (Melillo et al. 2002, 2011). This declined to an annual average rate of 60 g C m^{-2} yr^{-1} over 26 years of warming interspersed by periods when there was no effect of +5 °C on soil respiration or C mineralization (Melillo et al. 2017). The average annual rate of C loss with warming is 2–6 fold larger than the estimated soil C sink based on radiocarbon data (10–30 g C m^{-2} yr^{-1}).

Melillo et al. (2017) used a mass-balance approach to estimate that 17% of total soil C was lost from the organic horizon to 60 cm depth in the mineral soil over 26 years of warming. This was not observed directly in the soil samples that were collected from the experimental plots. We can use the soil power analysis to estimate the number of samples required to detect a significant change in soil C content. Melillo et al. (2017) reported an average C loss of 800 g C m^{-2} in the organic horizon of warmed compared to control plots over 26 years. We estimate it would take 73 and 103 samples to detect this change at $p < 0.10$ and $p < 0.05$, respectively. Across the entire profile, they estimate a loss just in excess of 1,500 g C m^{-2} in 26 years. Theoretically, detection would require only 21 and 29 samples at $p < 0.10$ and $p < 0.05$, respectively. In practice, however, the soil C loss was across 60 cm of mineral soil with presumably variable amounts of loss at different increments of depth. Therefore,

it seems that the mass-balance approach they employed is the only means of estimating soil C loss in the absence of terminating the experiment and extracting several hundred soil cores to increase statistical power.

More broadly, ecosystem C gains from forest regrowth overwhelm changes in C uptake and loss rates from observed and simulated climate change. For the 24-year period 1992–2015, coincident with the years of long-term soil warming, hardwood forest NEP averaged 298 ± 153 g C m^{-2} yr^{-1} (Table 4). Since NEP includes C in aboveground biomass and soil, C emissions from the soil in response to extreme warming would need to be 2–7 fold higher to entirely offset C gains from forest regrowth and other potential contributions from climate change, rising CO_2, and atmospheric N deposition. Soil warming may reduce the magnitude of the C sink, but the Harvard Forest will likely remain a net carbon sink because of the large effect of recovery from previous land-use change coupled to longer growing seasons and rising atmospheric CO_2.

Concerns over enhanced N loading from atmospheric deposition motivated a second flagship global change experiment at the Harvard Forest: long-term simulated N deposition in hardwood and red pine plantation forests to assess the N saturation hypotheses of Ågren and Bosatta (1988) and Aber et al. (1989). The Chronic Nitrogen Amendment Study was established in 1988 at two levels of N addition, 5 g N m^{-2} yr^{-1} (N5) and 15 g N m^{-2} yr^{-1} (N15) (Frey et al. 2014). Over 20 years, the hardwood stand sequestered C in biomass and soil above that in control plots at an average annual rate of 125 g C m^{-2} yr^{-1} (N5) and 460 g C m^{-2} yr^{-1} (N15). Most additional C was sequestered in biomass, and in the surface organic horizon via suppressed decomposition, but some was sequestered in deep mineral soil in the N15 treatment (Nadelhoffer et al. 1999a, Frey et al. 2014). In the N5 treatment, 55% of the additional C sink was in the organic horizon and mineral soil, and in the N15 treatment, 63% of the additional C sink was in these same horizons. In the red pine stand, the N5 treatments neither gained nor lost C at a rate different from control plots. In the N15 treatments, however, red pine trees died, indicating that extreme N deposition has the capacity to fundamentally change the C cycle. Widespread tree decline and mortality were observed in parts of Europe and, to a lesser extent, eastern North America, in the 1980s and 1990s (Schulze 1989, Högberg et al. 1996, Emmett et al. 1998). Red

pine, an abandoned plantation species at the Harvard Forest, does not occur in non-plantation areas of the forest and is naturally in decline throughout the research area. Therefore, we do not consider red pine responses further in this study.

Relative to the effects of soil warming and forest regrowth, high (N5) to extreme (N15) fertilization levels stimulate an ecosystem C sink that is 2–7 fold greater than the rate of C loss from soils exposed to extreme warming, and 0.7 to 2 times higher than that of forest regrowth. Nitrogen is thus a potent modifier of ecosystem C capital. Given that the 1990 amendments to the Clean Air Act (U.S., 104 Stat. 2399, Pub.L. 101–549) have decreased atmospheric N deposition across northeastern North America, primarily through reductions in NO_x emissions, the stimulatory effect of N deposition on the C sink may decline in the future (Du et al. 2014, Beachley et al. 2016). We note, however, that NH_3 deposition is presently increasing at a modest rate throughout much of the U.S. including the northeast (Butler et al. 2016). Simultaneous reductions in atmospheric acidity (e.g., SO_4^{2-}, NO_3^-), the primary sink for NH_3, may increase the concentration of NH_4^+ in the soil and contribute to a C sink. At present this remains highly uncertain.

The northeastern U.S. has the greatest number of invasive forest insects in the country (Liebhold et al. 2013), and they have major ecological and economic impacts (Lovett et al. 2016). In central New England, prominent forest invasive insects include the hemlock woolly adelgid (*Adelges tsugae*), gypsy moth (*Lymantria dispar*), emerald ash borer (*Agrilus planipennis*), and localized outbreaks of Asian longhorned beetle (*Anoplophora glabripennis*) (Dodds and Orwig 2011). These insects are poised to selectively impact or in some cases extirpate eastern hemlock, oaks, ash, or various hardwood species, respectively. At the Harvard Forest, gypsy moth outbreaks temporarily reduced oak biomass increment in the early 1980s (Fig. 4b), and now the hemlock woolly adelgid (HWA) is progressively eliminating eastern hemlock. The ecosystem consequences of hemlock loss via HWA has been a research focus at the Harvard Forest since the 1990s (Orwig and Foster 1998, Orwig et al. 2008, 2012) and HWA is now causing decline and mortality at the Harvard Forest (Kim et al. 2017, Orwig et al. 2018).

Prior to HWA's arrival at the Harvard Forest, a third flagship experiment used girdling to kill all hemlock trees in a second-growth forest to simulate the effects of the adelgid on ecosystem processes (Ellison et al. 2010). The transfer of live aboveground biomass to the coarse woody debris (CWD) pool dominated the C cycle consequences of this manipulation. Nine years after girdling, live woody biomass in the girdled plots was about 40% of that in the intact hemlock plots (Orwig et al. 2013). Despite greater productivity in the girdled plots than in control stands (Orwig et al. 2013), C loss from decaying CWD exceeded net uptake for over a decade (Ellison and Barker Plotkin 2018). Using a chronosequence approach, Raymer et al. (2013) estimated that it would take ~20 years for ecosystem C content to recoup losses following hemlock loss in second-growth forests, but nearly 140 years to accumulate as much C as that measured in the primary-growth hemlock stand in which the HEM eddy-covariance tower is located and which is now rapidly declining. Eventually, the predicted loss of C from the thick organic soil horizon in the primary forest would be compensated by greater rates of NPP and C accumulation in biomass by the rapidly aggrading hardwood forest (Finzi et al. 2014).

In and around the HEM tower site, visible signs of hemlock canopy loss began in 2013. The eddy-covariance data show that the HEM site is now a net source of C to the atmosphere on an annual basis (Fig. 7b). For the three-year period 2013–2015, NEP averaged 36 g C m^{-2} yr^{-1} and was lowest in 2015 (−129 g C m^{-2} yr^{-1}). Relative to 2002, peak growing season evapotranspiration decreased > 25% while annual water yield increased 15% in 2013 and 2014 (Kim et al. 2017). Thus, hydrologic and C cycle changes are underway at this site. An intensified effort is now ongoing to quantify changes in C pools and fluxes throughout areas experiencing hemlock decline to test hypotheses generated by both experimental and chronosequence approaches.

Comparison of C cycling at the Harvard Forest to the surrounding region

The continuity and breadth of data, and detailed site history at an intensive ecological research site such as the Harvard Forest LTER offer an unparalleled opportunity to integrate multiple data streams over decades to discern long-term patterns of C cycling and the historical, biotic, and climate factors driving these patterns. Yet by concentrating work at a particular location, questions arise about how representative a site is compared to the broader region (Fahey et al. 2015). We know that the land use

and wind disturbance history at the Harvard Forest are broadly representative of the central New England region. The timing of major land-use changes and percentage of land in agriculture were consistent across Massachusetts (Hall et al. 2002). Hurricane wind damage follows a strong gradient in frequency and intensity from southeastern to northwestern New England, and the most recent major hurricane at the Harvard Forest (1938) affected the surrounding central New England area similarly (Boose et al. 2001). However, nuances in site characteristics and disturbance patterns may lead to differences in C stocks and fluxes between the Harvard Forest, its surrounding ecoregion, and other intensively studied sites.

Based on the remote sensing estimates of GPP, productivity at the Harvard Forest is similar to that of the surrounding ecoregion (Zhou et al. 2018). ANPP at the Harvard Forest averaged 390–430 g C m^{-2} yr^{-1} and total NPP averaged 680–750 g C m^{-2} yr^{-1} (Tables 3, 4), reasonable values compared to estimates of forest NPP in northern New England and New York. Net primary production at the Hubbard Brook Experimental Forest in New Hampshire averaged 585 g C m^{-2} yr^{-1} with ~350–400 g C m^{-2} yr^{-1} in ANPP alone (Fahey et al. 2005). ANPP at the Bartlett Experimental Forest, New Hampshire, ranged from 140 to 376 g C m^{-2} yr^{-1} with a mean of 257 g C m^{-2} yr^{-1} (Ollinger and Smith 2005) and total NPP for the site was estimated to be 615 ± 118 g C m^{-2} yr^{-1} (Ouimette et al. 2018). In the Allegheny Plateau of central New York, Fahey et al. (2013) reported ANPP rates of 386 g C m^{-2} yr^{-1}. In the Catskill Mountains of New York, Lovett et al. (2013) reported ANPP of 160–350 g C m^{-2} yr^{-1}, and in the Adirondack Mountains, Joshi et al. (2003) reported ANPP rates of ~200 g C m^{-2} yr^{-1} for low elevation hardwood stands. The higher overall ranges of NPP and ANPP at the Harvard Forest probably reflect its more southerly location and warmer climate, which likely drive higher rates of net C uptake.

C stocks in biomass are notably higher at the Harvard Forest compared to FIA plots in the surrounding ecoregion. We hypothesize that this reflects a higher intensity of forest management outside of the Harvard Forest during the last half century, as productivity recovers quickly after partial disturbance (Fig. 7d, Amiro et al. 2010, Barker Plotkin et al. 2013), but C stocks can take decades to recover. Recent (1990–2014) timber harvesting rates at the Harvard Forest averaged 0.4% of the land

base per year and did not affect the plots included in this study. This is a lower frequency of harvesting disturbance than the surrounding regions (Worcester Plateau and Lower Worcester Plateau ecoregions), where about 1.4% of the land base per year was harvested during the period of 1984–2015 (McDonald et al. 2006, Thompson et al. 2017). Indeed, timber harvesting is the leading cause of adult tree mortality in northeastern forests (Canham et al. 2013). Partial harvest (20–40% live basal area removed) is most prevalent (Thompson et al. 2017), leading to intermittent removals of live aboveground C that take decades to regrow.

Local site conditions and forest management practices at the Harvard Forest over the past century also lead to differences in forest composition compared to the surrounding region. Oak dominated live biomass C storage and uptake at the Harvard Forest over the study period and increased in relative importance over the past 25 years (Urbanski et al. 2007, Eisen and Barker Plotkin 2015). In contrast, red maple abundance has increased in New England over the past 400 years (Thompson et al. 2013) and surpasses oak biomass in much of the region (McEwan et al. 2011, Butler 2016, 2017, 2018). As discussed above, oaks may have relatively high biomass and production capacity relative to other major tree species at the Harvard Forest, and therefore may partially explain the higher biomass reported in this study compared to the region.

SUMMARY

C accrual persists at the Harvard Forest, consistent with previous studies of long-term forest development (Luyssaert et al. 2008, Urbano and Keeton 2017). Comparative analysis of the observational and experimental data reported here suggests that the largest driver of the C sink at the Harvard Forest is forest regrowth following widespread land-use abandonment. Superimposed on this driver, climate warming and wetting, longer growing seasons, altered phenology, rising CO_2, declines in sulfate and total N deposition, alongside declines in ground-level ozone concentrations are also likely contributing to the forest C sink. In many instances, temporal variations in C cycling were readily interpretable such as the strong seasonal correspondence between R_a, leaf area deployment, and tree diameter growth in hardwood stands. In other instances, the underlying causes were more complicated. These include interannual variations in NEP, PAI and > 2-fold interannual variation in

A_{max}. Developing appropriate statistical methods to parse the contributions of regrowth and climatic and atmospheric changes on the C cycle remains an area of high priority for research.

Estimates of live aboveground C at the Harvard Forest are beginning to approach levels observed in remnant old-growth stands on sites characteristic of the broader region, which range from 17,500 to 25,000 g C m^{-2} (Siccama et al. 2007, Keeton et al. 2011, McGarvey et al. 2015). Estimates of deadwood in old-growth forest are less well studied but a few studies show dead wood stocks that are many times higher than what we observe at the Harvard Forest and other secondary forests in the region (McGee et al. 1999, McGarvey et al. 2015, D'Amato et al. 2017). Simulations using diverse modeling approaches consistently forecast biomass accrual associated with long-term stand development persisting throughout the next century (Albani et al. 2006, Tang et al. 2014, Duveneck et al. 2017, Wang et al. 2017). Simulations also suggest that rising atmospheric CO_2 concentration, higher average temperatures and precipitation, and enhancement of N mineralization rates and possibly N deposition will increase C sequestration despite concomitant increases in respiration (McGuire et al. 1992, Richardson et al. 2010, Savage et al. 2013, Duveneck and Thompson 2017). On this basis, we hypothesize that continued forest regrowth and climate change in the coming century will maintain C sink activity at the Harvard Forest. This hypothesis is predicated on the assumption that major disturbances including invasive insects, logging or other land-use change, hurricanes, and extreme climate events do not increase in frequency or intensity across the forest in the 21st century.

ACKNOWLEDGMENTS

Adrien Finzi, Marc-André Giasson, and Audrey Barker Plotkin are co-first authors of this paper; each contributed equally to the conceptualization of ideas, preparation of data, data analysis and writing. This research was supported in part by the National Science Foundation Harvard Forest Long-Term Ecological Research Program (since 1988; NSF-DEB grant numbers 8811764, 9411975, 0080592, 0620443, and 1237491). Flux tower and associated plot measurements were additionally supported by the AmeriFlux Management Project with funding by the U.S. Department of Energy's Office of Science under Contract No. DE-AC02-05CH11231, and previously through the DOE NIGEC program. Collection of soil carbon data from the soil warming plots was supported by the NSF–

Ecosystem Studies (DEB0447967) and the NSF Long-Term Research in Environmental Biology (DEB1456610) Programs. Additional support for A.C.F. and M.A.G. was provided by the U.S. Department of Energy–Terrestrial Ecosystems Science (DE-SC0006741). T.F.K. acknowledges support by the Director, Office of Science, Office of Biological and Environmental Research of the U.S. Department of Energy under Contract DE-AC02-05CH11231 as part of the RGCM RuBiSCo SFA. S.V.O. and Z.Z. acknowledge support from NSF grant number 1638688, NASA grant numbers NNX08AG14G, NNX14AJ18G, and NNX11AB88G, and USDA-NIFA grant number 1006997. N.P. acknowledges support for the tree-ring work from NSF EF-1241930. C.A.W. acknowledges financial support from NASA's Carbon Monitoring System program (NNH14ZDA001N-CMS) under award NNX14AR39G. We thank Brett Butler for helping to coordinate access to FIA plot locations pursuant to a Memorandum of Understanding 09MU11242305123 between the U.S. Forest Service and Harvard University. Thanks to Elizabeth Nicoll for contributing to data compilation, and to Loïc D'Orangeville for providing the processed Hemlock Tower dendrometer band data. Finally, the authors appreciate the helpful suggestions from anonymous reviewers on a previous version of the manuscript.

LITERATURE CITED

Aber, J. D., K. J. Nadelhoffer, P. Steudler, and J. M. Melillo. 1989. Nitrogen saturation in northern forest ecosystems. Bioscience 39:378–386.

Aber, J. D., P. B. Reich, and M. L. Goulden. 1996. Extrapolating leaf CO_2 exchange to the canopy: a generalized model of forest photosynthesis compared with measurements by eddy correlation. Oecologia 106:257–265.

Abramoff, R. Z., and A. C. Finzi. 2015. Are above- and below-ground phenology in sync? New Phytologist 205:1054–1061.

Abramoff, R. Z., and A. C. Finzi. 2016. Seasonality and partitioning of root allocation to rhizosphere soils in a midlatitude forest. Ecosphere 7:e01547.

Ågren, G. I., and E. Bosatta. 1988. Nitrogen saturation of terrestrial ecosystems. Environmental Pollution 54:185–197.

Albani, M., D. Medvigy, G. C. Hurtt, and P. R. Moorcroft. 2006. The contributions of land-use change, CO_2 fertilization, and climate variability to the Eastern US carbon sink. Global Change Biology 12:2370–2390.

Amiro, B., A. Barr, T. Black, H. Iwashita, N. Kljun, J. Mccaughey, K. Morgenstern, S. Murayama, Z. Nesic, and A. Orchansky. 2006. Carbon, energy and water fluxes at mature and disturbed forest sites, Saskatchewan, Canada. Agricultural and Forest Meteorology 136:237–251.

Amiro, B. D., A. G. Barr, J. G. Barr, T. A. Black, R. Bracho, M. Brown, J. Chen, K. L. Clark, K. J. Davis, A. R. Desai, S. Dore, V. Engel, J. D. Fuentes, A. H. Goldstein, M. L. Goulden, T. E. Kolb, M. B. Lavigne, B. E. Law, H. A. Margolis, T. Martin, J. H. McCaughey, L. Misson, M. Montes-Helu, A. Noormets, J. T. Randerson, G. Starr, and J. Xiao. 2010. Ecosystem carbon dioxide fluxes after disturbance in forests of North America. Journal of Geophysical Research 115:G00K02, doi:10.1029/2010JG001390.

Averill, C., B. L. Turner, and A. C. Finzi. 2014. Mycorrhiza-mediated competition between plants and decomposers drives soil carbon storage. Nature 505:543–545.

Barford, C. C., S. C. Wofsy, M. L. Goulden, J. W. Munger, E. H. Pyle, S. P. Urbanski, L. Hutyra, S. R. Saleska, D. Fitzjarrald, and K. Moore. 2001. Factors controlling long- and short-term sequestration of atmospheric CO_2 in a mid-latitude forest. Science 294:1688–1691.

Barker Plotkin, A. 2017. Litterfall in Hemlock Removal Experiment at Harvard Forest since 2005. Harvard Forest Data Archive. HF161.

Barker Plotkin, A., D. R. Foster, J. Carlson, and A. H. Magill. 2013. Survivors, not invaders, control forest development following simulated hurricane. Ecology 94:414–423.

Barr, A. G., T. A. Black, E. H. Hogg, N. Kljun, K. Morgenstern, and Z. Nesic. 2004. Inter-annual variability in the leaf area index of a boreal aspen-hazelnut forest in relation to net ecosystem production. Agricultural and Forest Meteorology 126:237–255.

Bassow, S. L., and F. A. Bazzaz. 1997. Intra- and inter-specific variation in canopy photosynthesis in a mixed deciduous forest. Oecologia 109:507–515.

Battipaglia, G., M. Saurer, P. Cherubini, C. Calfapietra, H. R. McCarthy, R. J. Norby, and M. Francesca Cotrufo. 2013. Elevated CO_2 increases tree-level intrinsic water use efficiency:

insights from carbon and oxygen isotope analyses in tree rings across three forest FACE sites. New Phytologist 197:544–554.

Bazzaz, F. A., and S. L. Miao. 1993. Successional status, seed size, and responses of tree seedlings to CO_2, light, and nutrients. Ecology 74:104–112.

Beachley, G., M. Puchalski, C. Rogers, and G. Lear. 2016. A summary of long-term trends in sulfur and nitrogen deposition in the United States 1990–2013. JSM Environmental Science and Ecology 4:1030.

Belmecheri, S., R. S. Maxwell, A. H. Taylor, K. J. Davis, K. H. Freeman, and W. J. Munger. 2014. Tree-ring $\delta^{13}C$ tracks flux tower ecosystem productivity estimates in a NE temperate forest. Environmental Research Letters 9:074011.

Bindoff, N. L., P. A. Stott, K. M. AchutaRao, M. R. Allen, N. Gillett, D. Gutzler, K. Hansingo, G. Hegerl, Y. Hu, S. Jain, I. I. Mokhov, J. Overland, J. Perlwitz, R. Sebbari and X. Zhang, 2013: Detection and Attribution of Climate Change: from Global to Regional. In: Climate Change 2013: The Physical Science Basis. Contribution of Working Group I to the Fifth Assessment Report of the Intergovernmental Panel on Climate Change [Stocker, T. F., D. Qin, G.-K. Plattner, M. Tignor, S. K. Allen, J. Boschung, A. Nauels, Y. Xia, V. Bex and P. M. Midgley (eds.)]. Cambridge University Press, Cambridge, United Kingdom and New York, NY, USA.

Bishop, D. A., and N. Pederson. 2015. Regional variation of transient precipitation and rainless-day frequency across a subcontinental hydroclimate gradient. Journal of Extreme Events 02:1550007.

Boose, E. R., K. E. Chamberlin, and D. R. Foster. 2001. Landscape and regional impacts of hurricanes in New England. Ecological Monographs 71:27–48.

Borken, W., E. A. Davidson, K. Savage, E. T. Sundquist, and P. Steudler. 2006. Effect of summer throughfall exclusion, summer drought, and winter snow cover on methane fluxes in a temperate forest soil. Soil Biology & Biochemistry 38:1388–1395.

Bowen, J. L., and I. Valiela. 2001. Historical changes in atmospheric nitrogen deposition to Cape Cod, Massachusetts, USA. Atmospheric Environment 35:1039–1051.

Brown, H. T., and F. Escombe. 1902. The influence of varying amounts of carbon dioxide in the air on the photosynthetic process of leaves and on the mode of growth of plants. Proceedings of the Royal Society of London 70:397–413.

Brzostek, E. R., A. Greco, J. E. Drake, and A. C. Finzi. 2013. Root carbon inputs to the rhizosphere stimulate extracellular enzyme activity and increase nitrogen availability in temperate forest soils. Biogeochemistry 115:65–76.

Burkle, L. A., and B. A. Logan. 2003. Seasonal acclimation of photosynthesis in eastern hemlock and partridgeberry in different light environments. Northeastern Naturalist 10:1–16.

Butler, B. J. 2016. Forests of Massachusetts, 2015. Resource Update FS-89. Newtown Square, PA: U.S. Department of Agriculture, Forest Service, Northern Research Station. 4 p.

Butler, B. J. 2017. Forests of Massachusetts, 2016. Resource Update FS-138. Newtown Square, PA: U.S. Department of Agriculture, Forest Service, Northern Research Station. 4 p.

Butler, B. J. 2018. Forests of Massachusetts, 2017. Resource Update FS-161. Newtown Square, PA: U.S. Department of Agriculture, Forest Service, Northern Research Station. 3 p.

Butler, T., F. Vermeylen, C. M. Lehmann, G. E. Likens, and M. Puchalski. 2016. Increasing ammonia concentration trends in large regions of the USA derived from the NADP/AMoN network. Atmospheric Environment 146:132–140.

Cairns, M. A., S. Brown, E. H. Helmer, and G. A. Baumgardner. 1997. Root biomass allocation in the world's upland forests. Oecologia 111:1–11.

Canham, C. D., N. Rogers, and T. Buchholz. 2013. Regional variation in forest harvest regimes in the northeastern United States. Ecological Applications 23:515–522.

Carey, E. V., A. Sala, R. Keane, and R. M. Callaway. 2001. Are old forests underestimated as global carbon sinks? Global Change Biology 7:339–344.

Chalot, M., and A. Brun. 1998. Physiology of organic nitrogen acquisition by ectomycorrhizal fungi and ectomycorrhizas. FEMS Microbiology Reviews 22:21–44.

Chapin, F. S., G. M. Woodwell, J. T. Randerson, E. B. Rastetter, G. M. Lovett, D. D. Baldocchi, D. A. Clark, M. E. Harmon, D. S. Schimel, R. Valentini, C. Wirth, J. D. Aber, J. J. Cole, M. L. Goulden, J. W. Harden, M. Heimann, R. W. Howarth, P. A. Matson, A. D. McGuire, J. M. Melillo, H. A. Mooney, J. C. Neff, R. A. Houghton, M. L. Pace, M. G. Ryan, S. W. Running, O. E. Sala, W. H. Schlesinger, and E.-D. Schulze. 2006. Reconciling carbon-cycle concepts, terminology, and methods. Ecosystems 9:1041–1050.

Clark, D. A., S. Brown, D. W. Kicklighter, J. Q. Chambers, J. R. Thomlinson, and J. Ni. 2001. Measuring net primary production in forests: concepts and field methods. Ecological Applications 11:356–370.

Collins, M., R. Knutti, J. Arblaster, J.-L. Dufresne, T. Fichefet, P. Friedlingstein, X. Gao, W. J. Gutowski, T. Johns, G. Krinner, M. Shongwe, C. Tebaldi, A. J. Weaver, and M. Wehner. 2013. Long-term climate change: projections, commitments and irreversibility. *in* T. F. Stocker, D. Qin, G.-K. Plattner, M. Tignor, S. K. Allen, J. Boschung, A. Nauels, Y. Xia, V. Bex, and P. M. Midgley, editors. Climate Change 2013: The Physical Science Basis. Contribution of Working Group I to the Fifth Assessment Report of the Intergovernmental Panel on Climate Change. Cambridge University Press, Cambridge, United Kingdom and New York, NY, USA.

Compton, J. E., and R. D. Boone. 2000. Long-term impacts of agriculture on soil carbon and nitrogen in New England forests. Ecology 81:2314–2330.

Cook, E. R., and P. J. Krusic. 2005. Program ARSTAN: a tree-ring standardization program based on detrending and autoregressive time series modeling, with interactive graphics. Lamont-Doherty Earth Observatory, Columbia University, Palisades, NY.

Currie, W. S., and K. J. Nadelhoffer. 2002. The imprint of land-use history: patterns of carbon and nitrogen in downed woody debris at the Harvard Forest. Ecosystems 5:446–460.

D'Amato, A. W., D. A. Orwig, D. R. Foster, A. Barker Plotkin, P. K. Schoonmaker, and M. R. Wagner. 2017. Long-term structural and biomass dynamics of virgin *Tsuga canadensis–Pinus strobus* forests after hurricane disturbance. Ecology 98:721–733.

DeLucia, E. H., J. G. Hamilton, S. L. Naidu, R. B. Thomas, J. A. Andrews, A. Finzi, M. Lavine, R. Matamala, J. E. Mohan, G. R. Hendrey, and W. H. Schlesinger. 1999. Net primary production of a forest ecosystem with experimental CO_2 enrichment. Science 284:1177–1179.

Dietze, M. C. 2015. The PEcAn Project. https://github.com/PecanProject/pecan/blob/develop/modules/allometry/vignettes/AllomVignette.Rmd

Dodds, K. J., and D. A. Orwig. 2011. An invasive urban forest pest invades natural environments — Asian longhorned beetle in northeastern US hardwood forests. Canadian Journal of Forest Research 41:1729–1742.

D'Orangeville, L., J. Maxwell, D. Kneeshaw, N. Pederson, L. Duchesne, T. Logan, D. Houle, D. Arseneault, C. M. Beier, D. A. Bishop, D. Druckenbrod, S. Fraver, F. Girard, J. Halman, C. Hansen, J. L. Hart, H. Hartmann, M. Kaye, D. Leblanc, S. Manzoni, R. Ouimet, S. Rayback, C. R. Rollinson, and R. P. Phillips. 2018. Drought timing and local climate determine the sensitivity of eastern temperate forests to drought. Global Change Biology 24:2339–2351.

Driscoll, C. T., G. E. Likens, and M. R. Church. 1998. Recovery of surface waters in the northeastern U.S. from decreases in atmospheric deposition of sulfur. Water, Air, and Soil Pollution 105:319–329.

Du, E., W. de Vries, J. N. Galloway, X. Hu, and J. Fang. 2014. Changes in wet nitrogen deposition in the United States between 1985 and 2012. Environmental Research Letters 9:095004.

Duveneck, M. J., and J. R. Thompson. 2017. Climate change imposes phenological tradeoffs on forest net primary productivity. Journal of Geophysical Research: Biogeosciences 122, doi:10.1002/2017JG004025.

Duveneck, M. J., J. R. Thompson, E. J. Gustafson, Y. Liang, and A. de Bruijn. 2017. Recovery dynamics and climate change effects to future New England forests. Landscape Ecology 32:1385–1397.

Dye, A., A. Barker Plotkin, D. Bishop, N. Pederson, B. Poulter, and A. Hessl. 2016. Comparing tree-ring and permanent plot estimates of aboveground net primary production in three eastern U.S. forests. Ecosphere 7:e01454.

Eisen, K., and A. Barker Plotkin. 2015. Forty years of forest measurements support steadily increasing aboveground biomass in a maturing, *Quercus*-dominant northeastern forest. Journal of the Torrey Botanical Society 142:97–112.

Ellison, A., and A. Barker Plotkin. 2015. Overstory vegetation in Hemlock Removal Experiment at Harvard Forest since 2003. Harvard Forest Data Archive. HF126.

Ellison, A., and A. Barker Plotkin. 2018. Coarse woody debris in hemlock removal experiment at Harvard Forest since 2005. Harvard Forest Data Archive. HF125.

Ellison, A. M., L. J. Osterweil, J. L. Hadley, A. Wise, E. Boose, L. Clarke, D. R. Foster, A. Hanson, D. Jensen, P. Kuzeja, E. Riseman, and H. Schultz. 2006. Analytic webs support the synthesis of ecological data sets. Ecology 87:1345–1358.

Ellison, A. M., A. A. Barker Plotkin, D. R. Foster, and D. A. Orwig. 2010. Experimentally testing the role of foundation species in forests: the Harvard Forest Hemlock Removal Experiment. Methods in Ecology and Evolution 1:168–179.

Ellison, A. M., Orwig, D. A., Fitzpatrick, M. C., Preisser, E. L. 2018. The Past, Present, and Future of the Hemlock Woolly Adelgid (*Adelges tsugae*) and Its Ecological Interactions with Eastern Hemlock (*Tsuga canadensis*) Forests. Insects 9: 172-189.

Emmett, B. A., D. Boxman, M. Bredemeier, P. Gundersen, O. J. Kjønaas, F. Moldan, P. Schleppi, A. Tietema, and R. F. Wright. 1998. Predicting the effects of atmospheric nitrogen deposition in conifer stands: evidence from the NITREX ecosystem-scale experiments. Ecosystems 1:352–360.

EPA. 2019. Air data: air quality data collected at outdoor monitors across the US. https://www.epa.gov/outdoor-air-quality-data (accessed 27 November 2019).

Fahey, T. J., and J. W. Hughes. 1994. Fine root dynamics in a northern hardwood forest ecosystem, Hubbard Brook Experimental Forest, NH. Journal of Ecology 82:533–548.

Fahey, T. J., T. G. Siccama, C. T. Driscoll, G. E. Likens, J. Campbell, C. E. Johnson, J. J. Battles, J. D. Aber, J. J. Cole, M. C. Fisk, P. M. Groffman, S. P. Hamburg, R. T. Holmes, P. A. Schwarz, and R. D. Yanai. 2005. The biogeochemistry of carbon at Hubbard Brook. Biogeochemistry 75:109–176.

Fahey, T. J., R. E. Sherman, and D. A. Weinstein. 2013. Demography, biomass and productivity of a northern hardwood forest on the Allegheny Plateau. Journal of the Torrey Botanical Society 140:52–64.

Fahey, T. J., P. H. Templer, B. T. Anderson, J. J. Battles, J. L. Campbell, C. T. Driscoll, A. R. Fusco, M. B. Green, K.-A. S. Kassam, N. L. Rodenhouse, L. Rustad, P. G. Schaberg, and M. A. Vadeboncoeur. 2015. The promise and peril of intensive-site-based ecological research: insights from the Hubbard Brook ecosystem study. Ecology 96:885–901.

Falge, E., D. Baldocchi, R. Olson, P. Anthoni, M. Aubinet, C. Bernhofer, G. Burba, R. Ceulemans, R. Clement, H. Dolman, A. Granier, P. Gross, T. Grünwald, D. Hollinger, N.-O. Jensen, G. Katul, P. Keronen, A. Kowalski, C. T. Lai, B. E. Law, T. Meyers, J. Moncrieff, E. Moors, J. W. Munger, K. Pilegaard, Ü. Rannik, C. Rebmann, A. Suyker, J. Tenhunen, K. Tu, S. Verma, T. Vesala, K.

Wilson, and S. Wofsy. 2001. Gap filling strategies for defensible annual sums of net ecosystem exchange. Agricultural and Forest Meteorology 107:43–69.

Fernández-Martínez, M., S. Vicca, I. A. Janssens, P. Ciais, M. Obersteiner, M. Bartrons, J. Sardans, A. Verger, J. G. Canadell, F. Chevallier, X. Wang, C. Bernhofer, P. S. Curtis, D. Gianelle, T. Grünwald, B. Heinesch, A. Ibrom, A. Knohl, T. Laurila, B. E. Law, J. M. Limousin, B. Longdoz, D. Loustau, I. Mammarella, G. Matteucci, R. K. Monson, L. Montagnani, E. J. Moors, J. W. Munger, D. Papale, S. L. Piao, and J. Peñuelas. 2017. Atmospheric deposition, CO_2, and change in the land carbon sink. Scientific Reports 7:9632.

Finzi, A. C., R. J. Norby, C. Calfapietra, A. Gallet-Budynek, B. Gielen, W. E. Holmes, M. R. Hoosbeek, C. M. Iversen, R. B. Jackson, M. E. Kubiske, J. Ledford, M. Liberloo, R. Oren, A. Polle, S. Pritchard, D. R. Zak, W. H. Schlesinger, and R. Ceulemans. 2007. Increases in nitrogen uptake rather than nitrogen-use efficiency support higher rates of temperate forest productivity under elevated CO_2. Proceedings of the National Academy of Sciences 104:14014–14019.

Finzi, A. C., P. C. L. Raymer, M.-A. Giasson, and D. A. Orwig. 2014. Net primary production and soil respiration in New England hemlock forests affected by the hemlock woolly adelgid. Ecosphere 5:art98.

Foster, D. R., and J. D. Aber. 2004. Forests in time: The environmental consequences of 1,000 years of change in New England. Yale University Press, New Haven, CT, USA.

Foster, D. R., T. Zebryk, P. Schoonmaker, and A. Lezberg. 1992. Post-settlement history of human land-use and vegetation dynamics of a *Tsuga canadensis* (hemlock) woodlot in central New England. Journal of Ecology 80:773–786.

Frey, S. D., S. Ollinger, K. Nadelhoffer, R. Bowden, E. Brzostek, A. Burton, B. A. Caldwell, S. Crow, C. L. Goodale, A. S. Grandy, A. Finzi, M. G. Kramer, K. Lajtha, J. LeMoine, M. Martin, W. H. McDowell, R. Minocha, J. J. Sadowsky, P. H. Templer, and K. Wickings. 2014. Chronic nitrogen additions suppress decomposition and sequester soil carbon in temperate forests. Biogeochemistry 121:305–316.

Gaudinski, J. B., S. E. Trumbore, E. A. Davidson, and S. Zheng. 2000. Soil carbon cycling in a temperate forest: radiocarbon-based estimates of residence times, sequestration rates and partitioning of fluxes. Biogeochemistry 51:33–69.

Gaudinski, J. B., M. S. Torn, W. J. Riley, T. E. Dawson, J. D. Joslin, and H. Majdi. 2010. Measuring and modeling the spectrum of fine-root turnover times in three forests using isotopes, minirhizotrons, and the Radix model. Global Biogeochemical Cycles 24, GB3029, doi:10.1029/2009GB003649.

Giasson, M.-A., A. M. Ellison, R. D. Bowden, P. M. Crill, E. A. Davidson, J. E. Drake, S. D. Frey, J. L. Hadley, M. Lavine, J. M. Melillo, J. W. Munger, K. J. Nadelhoffer, L. Nicoll, S. V. Ollinger, K. E. Savage, P. A. Steudler, J. Tang, R. K. Varner, S. C. Wofsy, D. R. Foster, and A. C. Finzi. 2013. Soil respiration in a northeastern US temperate forest: a 22-year synthesis. Ecosphere 4:art140.

Gough, C. M., P. S. Curtis, B. S. Hardiman, C. M. Scheuermann, and B. Bond-Lamberty. 2016. Disturbance, complexity, and succession of net ecosystem production in North America's temperate deciduous forests. Ecosphere 7:art01375.

Greenland, D., and T. Kittel. 1997. A climatic analysis of long-term ecological research sites. https://lternet.edu/wp-content/uploads/2013/12/CLIMDES.pdf (accessed 1 August 2019).

Griffith, G. E., J. M. Omernik, S. A. Bryce, J. Royte, W. D. Hoar, J. W. Homer, D. Keirstead, K. J. Metzler, and G. and Hellyer. 2009. Ecoregions of New England (color poster with map, descriptive text, summary tables, and photographs). U.S. Geological Survey, Reston, Virginia.

Hadley, J. L., and J. L. Schedlbauer. 2002. Carbon exchange of an old-growth eastern hemlock (*Tsuga canadensis*) forest in central New England. Tree Physiology 22:1079–1092.

Hadley, J. L., P. S. Kuzeja, M. J. Daley, N. G. Phillips, T. Mulcahy, and S. Singh. 2008. Water use and carbon exchange of red oak- and eastern hemlock-dominated forests in the northeastern USA: implications for ecosystem-level effects of hemlock woolly adelgid. Tree Physiology 28:615–627.

Hall, B., G. Motzkin, D. R. Foster, M. Syfert, and J. Burk. 2002. Three hundred years of forest and land-use change in Massachusetts, USA. Journal of Biogeography 29:1319–1335.

Harmon, M. E., and J. Sexton. 1996. Guidelines for measurements of woody detritus in forest ecosystems. U.S. LTER Publication No. 20.

Hobbie, E. A., and J. E. Hobbie. 2008. Natural abundance of ^{15}N in nitrogen-limited forests and tundra can estimate nitrogen cycling through mycorrhizal fungi: a review. Ecosystems 11:815–830.

Högberg, P., H. Fan, M. Quist, D. A. N. Binkley, and C. O. Tamm. 2006. Tree growth and soil acidification in response to 30 years of experimental nitrogen loading on boreal forest. Global Change Biology 12:489–499.

Hooker, T. D., and J. E. Compton. 2003. Forest ecosystem carbon and nitrogen accumulation during the first century after agricultural abandonment. Ecological Applications 13:299–313.

Isaac, L. A., and H. G. Hopkins. 1937. The forest soil of the Douglas fir region, and changes wrought upon it by logging and slash burning. Ecology 18:264–279.

Jackson, R. B., K. Lajtha, S. E. Crow, G. Hugelius, M. G. Kramer, and G. Piñeiro. 2017. The ecology of soil carbon: pools, vulnerabilities, and biotic and abiotic controls. Annual Review of Ecology, Evolution, and Systematics 48:419–445.

Jenkins, J. C., D. C. Chojnacky, L. S. Heath, and R. A. Birdsey. 2003. National-scale biomass estimators for United States tree species. Forest Science 49, 12–35.

Jenkins, J. C., D. C. Chojnacky, L. S. Heath, and R. A. Birdsey. 2004. Comprehensive database of diameter-based biomass regressions for North American tree species. Newtown Square, PA: U.S. Department of Agriculture, Forest Service, Northeastern Research Station.

Joshi, A. B., D. R. Vann, A. H. Johnson, and E. K. Miller. 2003. Nitrogen availability and forest productivity along a climosequence on Whiteface Mountain, New York. Canadian Journal of Forest Research 33:1880–1891.

Keenan, T. F., D. Y. Hollinger, G. Bohrer, D. Dragoni, J. W. Munger, H. P. Schmid, and A. D. Richardson. 2013. Increase in forest water-use efficiency as atmospheric carbon dioxide concentrations rise. Nature 499:324–327.

Keenan, T. F., J. Gray, M. A. Friedl, M. Toomey, G. Bohrer, D. Y. Hollinger, J. William Munger, J. O'Keefe, H. P. Schmid, I. S. Wing, B. Yang, and A. D. Richardson. 2014. Net carbon uptake has increased through warming-induced changes in temperate forest phenology. Nature Climate Change 4:598–604.

Keenan, T. F., I. C. Prentice, J. G. Canadell, C. A. Williams, H. Wang, M. Raupach, and G. J. Collatz. 2016. Recent pause in the growth rate of atmospheric CO_2 due to enhanced terrestrial carbon uptake. Nature Communications 7:13428.

Keeton, W. S., A. A. Whitman, G. C. McGee, C. L. Goodale, G. C. Whitman, G. G. McGree, and K. Goodale. 2011. Late-successional biomass development in northern hardwood-conifer forests of the northeastern United States. Forest Science 57:489–505.

Khomik, M., C. A. Williams, M. K. Vanderhoof, R. G. MacLean, and S. Y. Dillen. 2014. On the causes of rising gross ecosystem productivity in a regenerating clearcut environment: leaf area vs. species composition. Tree Physiology 34:686–700.

Kim, J., T. Hwang, C. L. Schaaf, D. A. Orwig, E. Boose, and J. William Munger. 2017. Increased water yield due to the hemlock woolly adelgid infestation in New England. Geophysical Research Letters 44:2327–2335.

Kira, T., and T. Shidei. 1967. Primary production and turnover of organic matter in different forest ecosystems of the western Pacific. Japanese Journal of Ecology 17:70–87.

Lajtha, K., R. D. Bowden, and K. Nadelhoffer. 2014. Litter and root manipulations provide insights into soil organic matter dynamics and stability. Soil Science Society of America Journal 78:S261–S269.

Liebhold, A. M., D. G. McCullough, L. M. Blackburn, S. J. Frankel, B. Von Holle, and J. E. Aukema. 2013. A highly aggregated geographical distribution of forest pest invasions in the USA. Diversity and Distributions 19:1208–1216.

Lindahl, B. D., R. D. Finlay, and J. W. G. Cairney. 2005. Enzymatic activities of mycelia in mycorrhizal fungal communities. Pages 331–348 *in* J. Dighton, J. F. White, and P. Oudemans, editors. The fungal community: its organization and role in the ecosystem, 3rd edition. CRC Press, Boca Raton, FL, USA.

Litton, C. M., J. W. Raich, and M. G. Ryan. 2007. Carbon allocation in forest ecosystems. Global Change Biology 13:2089–2109.

Lovett, G. M., M. A. Arthur, K. C. Weathers, R. D. Fitzhugh, and P. H. Templer. 2013. Nitrogen addition increases carbon storage in soils, but not in trees, in an eastern US deciduous forest. Ecosystems 16:980–1001.

Lovett, G. M., M. Weiss, A. M. Liebhold, T. P. Holmes, B. Leung, K. F. Lambert, D. A. Orwig, F. T. Campbell, J. Rosenthal, D. G. McCullough, R. Wildova, M. P. Ayres, C. D. Canham, D. R. Foster, S. L. LaDeau, and T. Weldy. 2016. Nonnative forest insects and pathogens in the United States: Impacts and policy options. Ecological Applications 26:1437–1455.

Lutz, J. A., A. J. Larson, M. E. Swanson, and J. A. Freund. 2012. Ecological importance of large-diameter trees in a temperate mixed-conifer forest. PLoS ONE 7:e36131.

Luyssaert, S., E. -Detlef Schulze, A. Börner, A. Knohl, D. Hessenmöller, B. E. Law, P. Ciais, and J. Grace. 2008. Old-growth forests as global carbon sinks. Nature 455:213–215.

Marlon, J. R., N. Pederson, C. Nolan, S. Goring, B. Shuman, A. Robertson, R. Booth, P. J. Bartlein, M. A. Berke, M. Clifford, E. Cook, A. Dieffenbacher-Krall, M. C. Dietze, A. Hessl, J. B. Hubeny, S. T. Jackson, J. Marsicek, J., McLachlan, C. J., Mock, D. J. P. Moore, J. Nichols, D. Peteet, K. Schaefer, V. Trouet, C. Umbanhowar, J. W. Williams, and Z. Yu. 2017. Climatic history of the northeastern United States during the past 3000 years. Climate of the Past 13:1355–1379.

Martin-Benito, D., and N. Pederson. 2015. Convergence in drought stress, but a divergence of climatic drivers across a latitudinal gradient in a temperate broadleaf forest. Journal of Biogeography 42:925–937.

McClaugherty, C. A., J. D. Aber, and J. M. Melillo. 1982. The role of fine roots in the organic matter and nitrogen budgets of two forested ecosystems. Ecology 63:1481–1490.

McDonald, R. I., G. Motzkin, M. S. Bank, D. B. Kittredge, J. Burk, and D. R. Foster. 2006. Forest harvesting and land-use conversion over two decades in Massachusetts. Forest Ecology and Management 227:31–41.

McEwan, R. W., J. M. Dyer, and N. Pederson. 2011. Multiple interacting ecosystem drivers: toward an encompassing hypothesis of oak forest dynamics across eastern North America. Ecography 34:244–256.

McFarlane, K. J., M. S. Torn, P. J. Hanson, R. C. Porras, C. W. Swanston, M. A. Callaham Jr., and T. P. Guilderson. 2013. Comparison of soil organic matter dynamics at five temperate deciduous forests with physical fractionation and radiocarbon measurements. Biogeochemistry 112:457–476.

McGarvey, J. C., J. R. Thompson, H. E. Epstein, and H. H. Shugart Jr. 2015. Carbon storage in old-growth forests of the Mid-Atlantic: toward better understanding the eastern forest carbon sink. Ecology 96:311–317.

McGee, G. G., D. J. Leopold, and R. D. Nyland. 1999. Structural characteristics of old-growth, maturing, and partially cut northern hardwood forests. Ecological Applications 9:1316–1329.

McGuire, A.D., J. M. Melillo, L. A. Joyce, D. W. Kicklighter, A. L. Grace, B. Moore III, and C. J. Vorosmarty. 1992. Interactions between carbon and nitrogen dynamics in estimating net primary productivity for potential vegetation in North America. Global Biogeochemical Cycles 6:101–124.

Melillo, J. M., T. V. Callaghan, F. I. Woodward, E. Salati, and S. K. Sinha. 1990. Climate change-effects on ecosystems. in J. T. Houghton, G. J. Jenkins, and J. J. Ephraums, editors. Climate Change - The IPCC Scientific Assessment. Cambridge University Press, Cambridge, Great Britain, New York, NY, USA, and Melbourne, Australia.

Melillo, J. M., P. A. Steudler, J. D. Aber, K. Newkirk, H. Lux, F. P. Bowles, C. Catricala, A. Magill, T. Ahrens, and S. Morrisseau. 2002. Soil warming and carbon-cycle feedbacks to the climate system. Science 298:2173–2176.

Melillo, J. M., S. Butler, J. Johnson, J. Mohan, P. Steudler, H. Lux, E. Burrows, F. Bowles, R. Smith, L. Scott, C. Vario, T. Hill, A. Burton, Y.-M. Zhou, and J. Tang. 2011. Soil warming, carbon-nitrogen interactions, and forest carbon budgets. Proceedings of the National Academy of Sciences of the United States of America 108:9508–9512.

Melillo, J. M., S. D. Frey, K. M. DeAngelis, W. J. Werner, M. J. Bernard, F. P. Bowles, G. Pold, M. A. Knorr, and A. S. Grandy. 2017. Long-term pattern and magnitude of soil carbon feedback to the climate system in a warming world. Science 358:101–105.

Miao, S. 1995. Acorn mass and seedling growth in *Quercus rubra* in response to elevated CO_2. Journal of Vegetation Science 6:697–700.

Morris, S. J., S. Bohm, S. Haile-Mariam, and E. A. Paul. 2007. Evaluation of carbon accrual in afforested agricultural soils. Global Change Biology 13:1145–1156.

Motzkin, G., P. Wilson, D. R. Foster, and A. Allen. 1999. Vegetation patterns in heterogeneous landscapes: The importance of history and environment. Journal of Vegetation Science 10:903–920.

Nadelhoffer, K. J., M. R. Downs, and B. Fry. 1999a. Sinks for ^{15}N additions to an oak forest and a red pine plantation. Ecological Applications 9:72–86.

Nadelhoffer, K. J., B. A. Emmett, P. Gundersen, O. J. Kjønaas, C. J. Koopmans, P. Schleppi, A. Tietema, and R. F. Wright. 1999b. Nitrogen deposition makes a minor contribution to carbon sequestration in temperate forests. Nature 398:145–148.

NADP. 2019. National Atmospheric Deposition Program data and maps. http://nadp.slh.wisc.edu/data (accessed 27 November 2019).

Nave, L. E., C. W. Swanston, U. Mishra, and K. J. Nadelhoffer. 2013. Afforestation effects on soil carbon storage in the United States: a synthesis. Soil Science Society of America Journal 77:1035–1047.

Nave, L. E., C. M. Gough, C. H. Perry, K. L. Hofmeister, J. M. Le Moine, G. M. Domke, C. W. Swanston, and K. J. Nadelhoffer. 2017. Physiographic factors underlie rates of biomass production during succession in Great Lakes forest landscapes. Forest Ecology and Management 397:157–173.

NOAA. 2019. Average annual atmospheric CO_2 concentration at the Mauna Loa Observatory. ftp://aftp.cmdl.noaa.gov/products/trends/co2/co2_annmean_mlo.txt. (accessed 27 November 2019)

Odum, E. P. 1969. The strategy of ecosystem development. Science 164:262–270.

O'Keefe, J. 2015. Phenology of woody species. Harvard Forest Data Archive. HF003.

Oliver, C. D. 1975. The development of northern red oak (*Quercus rubra* L.) in mixed species, even-age stands in central New England. Yale University.

Oliver, C. D. 1978. The development of northern red oak in mixed stands in central New England. Yale School of Forestry and Environmental Studies Bulletin No. 91.

Oliver, C. D., and E. P. Stephens. 1977. Reconstruction of a mixed-species forest in central New England. Ecology 58:562–572.

Ollinger, S. V., and M.-L. Smith. 2005. Net primary production and canopy nitrogen in a temperate forest landscape: an analysis using imaging spectroscopy, modeling and field data. Ecosystems 8:760–778.

Ollinger, S. V., J. D. Aber, P. B. Reich, and R. J. Freuder. 2002. Interactive effects of nitrogen deposition, tropospheric ozone, elevated CO_2 and land use history on the carbon dynamics of northern hardwood forests. Global Change Biology 8:545–562.

Ollinger, S. V., A. D. Richardson, M. E. Martin, D. Y. Hollinger, S. E. Frolking, P. B. Reich, L. C. Plourde, G. G. Katul, J. W. Munger, R. Oren, M.-L. Smith, K. T. Paw U, P. V. Bolstad, B. D. Cook, M. C. Day, T. A. Martin, R. K. Monson, and H. P. Schmid. 2008. Canopy nitrogen, carbon assimilation, and albedo in temperate and boreal forests: Functional relations and potential climate feedbacks. Proceedings of the National Academy of Sciences of the United States of America 105:19336–19341.

Orwig, D. A., and D. R. Foster. 1998. Forest response to the introduced hemlock woolly adelgid in southern New England, USA. The journal of the Torrey Botanical Society 125:60–73.

Orwig, D. A., R. C. Cobb, A. W. D'Amato, M. L. Kizlinski, and D. R. Foster. 2008. Multi-year ecosystem response to hemlock woolly adelgid infestation in southern New England forests. Canadian Journal of Forest Research 38:834–843.

Orwig, D. A., J. R. Thompson, N. A. Povak, M. Manner, D. Niebyl, and D. R. Foster. 2012. A foundation tree at the precipice: *Tsuga canadensis* health after the arrival of *Adelges tsugae* in central New England. Ecosphere 3:art10.

Orwig, D. A., A. A. Barker Plotkin, E. A. Davidson, H. Lux, K. E. Savage, and A. M. Ellison. 2013. Foundation species loss affects vegetation structure more than ecosystem function in a northeastern USA forest. PeerJ 1:e41.

Orwig, D.A., P. Boucher, I. Paynter, E. Saenz, Z. Li, and C. Schaaf. 2018. The potential to characterize ecological data with terrestrial laser scanning in Harvard Forest, MA. Interface Focus 8:20170044.

Ouimette, A. P., S. V. Ollinger, A. D. Richardson, D. Y. Hollinger, T. Keenan, L. C. Lepine, and M. Vadeboncoeur. 2018. Carbon fluxes and interannual drivers in a temperate forest ecosystem

assessed through comparison of top-down and bottom up approaches. Agricultural and Forest Meteorology 256–257:420–430.

Pan, Y., R. A. Birdsey, J. Fang, R. Houghton, P. E. Kauppi, W. A. Kurz, O. L. Phillips, A. Shvidenko, S. L. Lewis, J. G. Canadell, P. Ciais, R. B. Jackson, S. W. Pacala, A. D. McGuire, S. Piao, A. Rautiainen, S. Sitch, and D. Hayes. 2011. A large and persistent carbon sink in the world's forests. Science 333:988–993.

Papale, D., M. Reichstein, M. Aubinet, E. Canfora, C. Bernhofer, W. Kutsch, B. Longdoz, S. Rambal, R. Valentini, T. Vesala, and D. Yakir. 2006. Towards a standardized processing of Net Ecosystem Exchange measured with eddy covariance technique: algorithms and uncertainty estimation. Biogeosciences 3:571–583.

Pederson, N., A. R. Bell, E. R. Cook, U. Lall, N. Devineni, R. Seager, K. Eggleston, and K. P. Vranes. 2013. Is an epic pluvial masking the water insecurity of the greater New York City region? Journal of Climate 26:1339–1354.

Pederson, N., A. W. D'Amato, J. M. Dyer, D. R. Foster, D. Goldblum, J. L. Hart, A. E. Hessl, L. R. Iverson, S. T. Jackson, D. Martin-Benito, B. C. McCarthy, R. W. McEwan, D. J. Mladenoff, A. J. Parker, B. Shuman, and J. W. Williams. 2015. Climate remains an important driver of post-European vegetation change in the eastern United States. Global Change Biology 21:2105–2110.

Phillips, R. P., Y. Erlitz, R. Bier, and E. S. Bernhardt. 2008. New approach for capturing soluble root exudates in forest soils. Functional Ecology 22:990–999.

Pregitzer, K. S., and E. S. Euskirchen. 2004. Carbon cycling and storage in world forests: biome patterns related to forest age. Global Change Biology 10:2052–2077.

Raich, J. W., and K. J. Nadelhoffer. 1989. Belowground carbon allocation in forest ecosystems: global trends. Ecology 70:1346–1354.

Raymer, P. C. L., D. A. Orwig, and A. C. Finzi. 2013. Hemlock loss due to the hemlock woolly adelgid does not affect ecosystem C storage but alters its distribution. Ecosphere 4:art63.

R Core Team. 2016. R: A language and environment for statistical computing. R Foundation for Statistical Computing, Vienna, Austria. https://www.R-project.org.

Reich, P.B., Hobbie, S.E. and Lee, T.D., 2014. Plant growth enhancement by elevated CO 2 eliminated by joint water and nitrogen limitation. *Nature Geoscience*, *7*(12), p.920.

Reichstein, M., E. Falge, D. Baldocchi, D. Papale, M. Aubinet, P. Berbigier, C. Bernhofer, N. Buchmann, T. Gilmanov, A. Granier, T. Grunwald, K. Havrankova, H. Ilvesniemi, D. Janous, A. Knohl, T. Laurila, A. Lohila, D. Loustau, G. Matteucci, T. Meyers, F. Miglietta, J.-M. Ourcival, J. Pumpanen, S. Rambal, E. Rotenberg, M. Sanz, J. Tenhunen, G. Seufert, F. Vaccari, T. Vesala, D. Yakir, and R. Valentini. 2005. On the separation of net ecosystem exchange into assimilation and ecosystem respiration: review and improved algorithm. Global Change Biology 11:1424–1439.

Reichstein, M., A. M. Moffat, T. Wutzler, K. Sickel, O. Menzer, and M. Migliavacca. 2016. REddyProc: Data processing and plotting utilities of (half-) hourly eddy-covariance measurements. R package version 1.0.0. http://cran.r-project.org/package=REddyProc.

Richardson, A. D., D. Y. Hollinger, J. D. Aber, S. V. Ollinger, and B. H. Braswell. 2007. Environmental variation is directly responsible for short-but not long-term variation in forest-atmosphere carbon exchange. Global Change Biology 13:788–803.

Richardson, A. D., T. A. Black, P. Ciais, N. Delbart, M. A. Friedl, N. Gobron, D. Y. Hollinger, W. L. Kutsch, B. Longdoz, S. Luyssaert, M. Migliavacca, L. Montagnani, J. W. Munger, E. Moors, S. Piao, C. Rebmann, M. Reichstein, N. Saigusa, E. Tomelleri, R. Vargas, and A. Varlagin. 2010. Influence of spring and autumn phenological transitions on forest ecosystem productivity. Philosophical Transactions of the Royal Society of London. Series B, Biological Sciences 365:3227–3246.

Ryan, M. G., D. Binkley, and J. H. Fownes. 1997. Age-related decline in forest productivity: pattern and process. Advances in Ecological Research 27:213–262.

Sanderman, J., T. Hengl, and G. J. Fiske. 2017. Soil carbon debt of 12,000 years of human land use. Proceedings of the National Academy of Sciences of the United States of America 114:9575–9580.

Sargent, M., S. C. Wofsy, and T. Nehrkorn. 2018. CO_2 observations, modeled emissions, and NAM-HYSPLIT footprints, Boston MA, 2013–2014. ORNL DAAC, Oak Ridge, Tennessee, USA. https://doi.org/10.3334/ORNLDAAC/1586

Savage, K. E., W. J. Parton, E. A. Davidson, S. E. Trumbore, and S. D. Frey. 2013. Long-term changes in forest carbon under temperature and nitrogen amendments in a temperate northern hardwood forest. Global Change Biology 19:2389–2400.

Scharlemann, J. P. W., E. V. J. Tanner, R. Hiederer, and V. Kapos. 2014. Global soil carbon: understanding and managing the largest terrestrial carbon pool. Carbon Management 5:81–91.

Schimel, D. S. 1995. Terrestrial ecosystems and the carbon cycle. Global Change Biology 1:77–91.

Schlesinger, W. H., and E. S. Bernhardt. 2013. Biogeochemistry: an analysis of global change, 3rd ed. Academic press.

Schulze, E. D. 1989. Air pollution and forest decline in a spruce (*Picea abies*) forest. Science 244:776–783.

Schwalm, C. R., C. A. Williams, and K. Schaefer. 2011. Carbon consequences of global hydrologic change, 1948–2009. Journal of Geophysical Research 116, G03042, doi:10.1029/2011JG001674.

Shuman, B. N., and J. Marsicek. 2016. The structure of Holocene climate change in mid-latitude North America. Quaternary Science Reviews 141:38–51.

Siccama, T. G., T. J. Fahey, C. E. Johnson, T. W. Sherry, E. G. Denny, E. Binney Girdler, G. E. Likens, and P. A. Schwarz. 2007. Population and biomass dynamics of trees in a northern hardwood forest at Hubbard Brook. Canadian Journal of Forest Research 37:737–749.

Sierra, C. A., S. E. Trumbore, E. A. Davidson, S. D. Frey, K. E. Savage, and F. M. Hopkins. 2012. Predicting decadal trends and transient responses of radiocarbon storage and fluxes in a temperate forest soil. Biogeosciences 9:3013–3028.

SRCC. 2019. Southern Regional Climate Center – Climate Trends. Available from: http://charts.srcc.lsu.edu/trends/ (accessed 11 January 2019).

Stephenson, N. L., A. J. Das, R. Condit, S. E. Russo, P. J. Baker, N. G. Beckman, D. A. Coomes, E. R. Lines, W. K. Morris, N. Rüger, E. Álvarez, C. Blundo, S. Bunyavejchewin, G. Chuyong, S. J. Davies, Á. Duque, C. N. Ewango, O. Flores, J. F. Franklin, H. R. Grau, Z. Hao, M. E. Harmon, S. P. Hubbell, D. Kenfack, Y. Lin, J.-R. Makana, A. Malizia, L. R. Malizia, R. J. Pabst, N. Pongpattananurak, S.-H. Su, I-F. Sun, S. Tan, D. Thomas, P. J. van Mantgem, X. Wang, S. K. Wiser, and M. A. Zavala. 2014. Rate of tree carbon accumulation increases continuously with tree size. Nature 507:90–93.

Stoddard, J. L., D. S. Jeffries, A. Lükewille, T. A. Clair, P. J. Dillon, C. T. Driscoll, M. Forsius, M. Johannessen. J. S. Kahl, J. H. Kellogg, A. Kemp, J. Mannio, D. T. Monteith, P. S. Murdoch, S. Patrick, A. Rebsdorf, B. L. Skjelkvåle, M. P. Stainton, T. Traaen, H. van Dam, K. E. Webster, J. Wieting, and A. Wilander. 1999. Regional trends in aquatic recovery from acidification in North America and Europe. Nature 401:575–578.

Strand, A. E., S. G. Pritchard, M. L. McCormack, M. A. Davis, and R. Oren. 2008. Irreconcilable differences: fine-root life spans and soil carbon persistence. Science 319:456–458.

Tang, G., B. Beckage, and B. Smith. 2014. Potential future dynamics of carbon fluxes and pools in New England forests and their climatic sensitivities: A model-based study. Global Biogeochemical Cycles 28:286–299.

Tans, P., and R. Keeling. 2019. Trends in atmospheric carbon dioxide. https://www.esrl.noaa.gov/gmd/ccgg/trends/data.html (accessed 27 November 2019).

Teets, A., S. Fraver, D. Y. Hollinger, A. R. Weiskittel, R. S. Seymour, and A. D. Richardson. 2018. Linking annual tree growth with eddy-flux measurements of net ecosystem productivity across twenty years of observation in a mixed conifer forest. Agricultural and Forest Meteorology 249:479–487.

Thomas, R. Q., C. D. Canham, K. C. Weathers, and C. L. Goodale. 2010. Increased tree carbon storage in response to nitrogen deposition in the US. Nature Geoscience 3:13–17.

Thompson, J. R., D. R. Foster, R. Scheller, and D. Kittredge. 2011. The influence of land use and climate change on forest biomass and composition in Massachusetts, USA. Ecological Applications 21:2425–2444.

Thompson, J. R., D. N. Carpenter, C. V. Cogbill, and D. R. Foster. 2013. Four centuries of change in northeastern United States forests. PLoS ONE 8:e72540.

Thompson, J. R., C. D. Canham, L. Morreale, D. B. Kittredge, and B. Butler. 2017. Social and biophysical variation in regional timber harvest regimes. Ecological Applications 27:942–955.

Tierney, G. L., and T. J. Fahey. 2002. Fine root turnover in a northern hardwood forest: a direct comparison of the radiocarbon and minirhizotron methods. Canadian Journal of Forest Research 32:1692–1697.

Turnbull, M. H., D. Whitehead, D. T. Tissue, W. S. Schuster, K. J. Brown, V. C. Engel, and K. L. Griffin. 2002. Photosynthetic characteristics in canopies of *Quercus rubra*, *Quercus prinus* and *Acer rubrum* differ in response to soil water availability. Oecologia 130:515–524.

Urbano, A. R., and W. S. Keeton. 2017. Carbon dynamics and structural development in recovering secondary forests of the northeastern U.S. Forest Ecology and Management 392:21–35.

Urbanski, S., C. Barford, S. Wofsy, C. Kucharik, E. Pyle, J. Budney, K. McKain, D. Fitzjarrald, M. Czikowsky, and J. W. Munger. 2007. Factors controlling CO_2 exchange on timescales from hourly to decadal at Harvard Forest. Journal of Geophysical Research 112, G02020, doi:10.1029/2006JG000293.

Waller, K., C. Driscoll, J. Lynch, D. Newcomb, and K. Roy. 2012. Long-term recovery of lakes in the Adirondack region of New York to decreases in acidic deposition. Atmospheric Environment 46:56–64.

Wang, W. J., H. S. He, F. R. Thompson, J. S. Fraser, and W. D. Dijak. 2017. Changes in forest biomass and tree species distribution under climate change in the northeastern United States. Landscape Ecology 32:1399–1413.

Wehr, R., J. W. Munger, J. B. McManus, D. D. Nelson, M. S. Zahniser, E. A. Davidson, S. C. Wofsy, and S. R. Saleska. 2016. Seasonality of temperate forest photosynthesis and daytime respiration. Nature 534:680–683.

Williams, C. A., G. James Collatz, J. Masek, and S. N. Goward. 2012. Carbon consequences of forest disturbance and recovery across the conterminous United States. Global Biogeochemical Cycles 26, GB1005, doi:10.1029/2010GB003947.

Williams, C. A., M. K. Vanderhoof, M. Khomik, and B. Ghimire. 2013. Post-clearcut dynamics of carbon, water and energy exchanges in a midlatitude temperate, deciduous broadleaf forest environment. Global Change Biology 20:992–1007.

Williams, C. A., H. Gu, R. MacLean, J. G. Masek, and G. James Collatz. 2016. Disturbance and the carbon balance of US forests: A quantitative review of impacts from harvests, fires, insects, and droughts. Global and Planetary Change 143:66–80.

Wilson, H. F., J. E. Saiers, P. A. Raymond, and W. V. Sobczak. 2013. Hydrologic drivers and seasonality of dissolved organic carbon concentration, nitrogen content, bioavailability, and export in a forested New England stream. Ecosystems 16:604–616.

Wofsy, S. C., M. L. Goulden, J. W. Munger, S.-M. Fan, P. S. Bakwin, B. C. Daube, S. L. Bassow, and F. A. Bazzaz. 1993. Net exchange of CO_2 in a mid-latitude forest. Science 260:1314–1317.

Yang, X., J. F. Mustard, J. Tang, and H. Xu. 2012. Regional-scale phenology modeling based on meteorological records and remote sensing observations. Journal of Geophysical Research: Biogeosciences 117, G03029, doi:10.1029/2012JG001977.

Zhou, G., S., Z. Li, D. Zhang, X. Tang, C. Zhou, J. Yan, and J. Mo. 2006. Old-growth forests can accumulate carbon in soils. Science 314:1417.

Zhou, Z., S. V. Ollinger, and L. C. Lepine. 2018. Landscape variation in canopy nitrogen and carbon assimilation in a temperate mixed forest. Oecologia 188:595–606.

Data Availability

Data are publicly available from the Environmental Data Initiative:
https://doi.org/10.6073/pasta/e7113c9ea3ec7f99e400f2f0bc662c02

Table 1. List of abbreviations used.

Abbreviation	Definition	Units
A_{max}	Ecosystem photosynthetic capacity	μmol C m^{-2} s^{-1}
ANPP	Aboveground net primary production	g C m^{-2} yr^{-1}
BNPP	Belowground net primary production	g C m^{-2} yr^{-1}
C	Carbon	-
CC	Clear-cut (flux tower site)	-
CWD	Coarse woody debris	-
DBH	Diameter at breast height	cm
DOC	Dissolved organic carbon	g C m^{-2}
DOY	Day of year	-
EC	Eddy covariance	-
ECM	Ectomycorrhizal	-
EMS	Environmental Measurement Site (flux tower site)	-
FCRN	Fluxnet-Canada Research Network	-
FIA	Forest Inventory and Analysis	-
FR_{mass}	Fine root biomass	g C m^{-2}
$FR_{production}$	Fine root production	g C m^{-2} yr^{-1}
$FR_{turnover\ time}$	Fine root turnover time	yr
FWD	Fine woody debris	-
GPP	Gross primary production	g C m^{-2} yr^{-1}
GSL	Growing season length	d
HEM	Hemlock (flux tower site)	-
LAI	Leaf area index	m^2 leaves m^{-2} ground
LTER	Long-Term Ecological Research	-
LUE	Light use efficiency	μmol C μmol^{-1} PPFD
MAP	Mean annual precipitation	mm

MAT	Mean annual temperature	°C
N	Nitrogen	-
NEE	Net ecosystem exchange	g C m^{-2} yr^{-1}
NEP	Net ecosystem production	g C m^{-2} yr^{-1}
NPP	Net primary production	g C m^{-2} yr^{-1}
PAI	Plant area index	m^2 plant tissue m^{-2} ground
PI	Principal investigator	-
PPFD	Photosynthetic photon flux density	μmol photon m^{-2} s^{-1}
R_a	Autotrophic respiration	g C m^{-2} yr^{-1}
R_{above}	Aboveground respiration	g C m^{-2} yr^{-1}
R_e	Ecosystem respiration	g C m^{-2} yr^{-1}
R_h	Heterotrophic respiration	g C m^{-2} yr^{-1}
R_r	Root respiration	g C m^{-2} yr^{-1}
R_s	Soil respiration	g C m^{-2} yr^{-1}
SD	Standard deviation	-
SE	Standard error	-
SOC	Soil organic carbon	-
WUE	Water use efficiency	-

Table 2. Contemporary C stocks for mature hemlock- and hardwood-dominated stands at the Harvard Forest. Units are g C m^{-2} ± SD (*n*). Carbon stocks for aboveground live biomass and coarse roots are based on the most recent plot measurements (2008–2015, depending on the study), since these C pools have increased over the study period. All other C pools are based on means across all plots and years of measurement. The hemlock and hardwood means are significantly different at $p < 0.05$ (*), $p < 0.01$ (**), $p < 0.001$ (***), or not tested (†).

Component	Hemlock	Hardwood
Aboveground live biomass		
Wood + Foliage[1] *	14,007 ± 3,838 (34)	11,952 ± 3,730 (81)
Woody debris total†	2,047 ± 986	2,076 ± 1,248
Coarse woody debris (>7.5 cm diameter)*	643 ± 562 (38)	987 ± 955 (160)
Fine woody debris (0.6–7.5 cm diameter)***	344 ± 182 (35)	203 ± 135 (170)
Standing dead wood	1,060 ± 790 (38)	886 ± 792 (154)
Fine roots total†	547 ± 149	416 ± 118
Fine roots organic horizon***	148 ± 85 (73)	100 ± 45 (134)
Fine roots mineral horizon 0–15 cm	177 ± 80 (102)	191 ± 109 (200)
Fine roots mineral horizon 15–30 cm	117 ± 84 (23)	70 ± 8 (4)
Fine roots mineral horizon 30–45 cm*	105 ± 40 (8)	55 ± 6 (4)
Coarse roots total[1] ***	2,913 ± 811 (34)	2,285 ± 707 (81)
Soil total†	15,059 ± 3,548	12,851 ± 2,560
Soil organic horizon***	4,305 ± 2,624 (54)	2,700 ± 1,322 (145)
Soil mineral horizon 0–15 cm	5,170 ± 1,931 (98)	5,324 ± 1,649 (291)
Soil mineral horizon 15–30 cm	3,052 ± 1,326 (22)	2,907 ± 1,032 (30)
Soil mineral horizon 30–45 cm*	2,532 ± 464 (8)	1,920 ± 1,010 (21)
Total C content†	34,573 ± 5,382	29,580 ± 4,747
Distribution (% of total)		
Live aboveground	40%	40%

Woody debris	6%	7%
Roots	10%	9%
Soils	44%	44%

[1]Based on allometric equations.

Table 3. Average rates of net primary production for mature hemlock- and hardwood-dominated stands throughout the Harvard Forest. Units are g C m^{-2} yr^{-1} ± 1 SD (*n*, plot × year). The hemlock and hardwood means are significantly different at $p < 0.05$ (*), $p < 0.01$ (**), $p < 0.001$ (***), or not tested (†).

Flux	Hemlock	Hardwood
Aboveground biomass increment [wood + foliar increment] (1998 – 2014)†	166 ± 99 (191)	200 ± 118 (508)
Foliar litterfall	157 ± 49 (204)	160 ± 36 (681)
Non-foliar litterfall***	74 ± 68 (204)	41 ± 29 (681)
Litterfall total (1989 – 2015)[1] ***	231 ± 94 (204)	201 ± 51 (681)
Aboveground net primary production (ANPP)†	**397 ± 137**	**401 ± 129**
Fine root net primary production (<2mm)[2]†	218 ± 174	225 ± 136
Coarse root biomass increment (1998 – 2014)	34 ± 20 (191)	38 ± 23 (508)
Root exudates (2010 – 2013)	97 ± 88 (8)	69 ± 56 (14)
Belowground net primary production (BNPP)†	**349 ± 196**	**332 ± 149**
Total net primary production (NPP)†	**746 ± 239**	**733 ± 197**

[1] Before calculating the mean foliar, non-foliar, and total litterfall of all studies listed in Appendix S1: Table S5, we estimated the fractions of foliar and non-foliar litterfall for the studies where both components were reported and applied them to the studies where only foliar or total litterfall was reported.

[2] Fine root net primary production in hardwood forests is the average of estimates from McClaugherty et al. (1982), Gaudinski et al. (2010), and Abramoff and Finzi (2016). Fine root net primary production in hemlock forests is based on data from Abramoff and Finzi (2016); no other data were available for this type of forest.

Table 4. C fluxes within the EMS and HEM tower footprints only. NEP, GPP, R_e, and R_s are the average of 1992–2015 (EMS) and 2005–2012 (HEM). Units are g C m^{-2} yr^{-1} ± 1 SD (*n*; plot × year). The hemlock and hardwood means are significantly different at $p < 0.05$ (*), $p < 0.01$ (**), $p < 0.001$ (***), or not tested (†). The uncertainty for the eddy-flux data includes interannual variability, but not gap-filling uncertainty. As discussed in the text, there is more gap-filling in the HEM tower data than the EMS tower data.

		HEM	EMS
Input flux	Gross primary production (GPP; tower-calculated)	1,441 ± 97 (8)	1,526 ± 227 (24)
Net primary production	Total net primary production (NPP)†	688 ± 197	678 ± 182
	Aboveground		
	Wood + foliage (plot-measured, allometries)	158 ± 84 (124)	199 ± 119 (575)
	Foliar litterfall*** (plot-measured)	182 ± 58 (84)	149 ± 34 (416)
	Non-foliar litterfall*** (plot-measured)	89 ± 72 (84)	41 ± 28 (416)
	Litterfall total[1]***	271 ± 109 (84)	191 ± 44 (416)
	Aboveground net primary production (ANPP)†	429 ± 138	390 ± 127
	Belowground		
	Fine root net primary production[2]†	129 ± 107	199 ± 110
	Coarse root biomass increment (estimated from allometries)	33 ± 18 (124)	38 ± 23 (575)
	Root exudates	97 ± 88 (8)	51 ± 65 (6)

	Belowground net primary production (BNPP)†	259 ± 140	288 ± 130
Soil sequestration	OH to 50 cm depth (isotope-estimated)[3]	20 ± 10	20 ± 10
Output flux	Tower-based ecosystem respiration ($R_{e,\ tower}$)*	976 ± 82 (8)	1,228 ± 255 (24)
Component fluxes	Soil respiration (R_s)* (chamber measurement)	682 ± 27 (8)	727 ± 54 (24)
	Aboveground respiration (R_{above}): $R_e - R_s$	294 ± 86 (8)	501 ± 261 (24)
	Autotrophic respiration (R_a): GPP − NPP − soil sequestration	733 ± 220	828 ± 291
	Root respiration (R_r): $R_a - R_{above}$	439 ± 236	327 ± 391
	Heterotrophic respiration (R_h): $R_s - R_r$	243 ± 238	400 ± 395
Net ecosystem production (NEP)	Tower-based [NEP_{tower}]	465 ± 83 (8)	298 ± 153 (24)
	Inventory-based [NEP_{inv}]: Net change in live biomass + net change in soil C	183 ± 109	190 ± 82
	Comparison of NEP calculations: $NEP_{tower} - NEP_{inv}$	282 ± 137	108 ± 174
	Percentage NEP difference (relative to tower)	61	36

[1] Before calculating the mean foliar, non-foliar, and total litterfall of all studies listed in Appendix S1: Table S5, we estimated the fractions of foliar and non-foliar litterfall for the studies where both components were reported and applied them to the studies where only foliar or total litterfall was reported.

[2] Between the top of the organic horizon and 15 cm depth in the mineral soil. Fine root net primary production in the EMS tower footprint is the average of estimates from McClaugherty et al. (1982), Gaudinski et al. (2010), and Abramoff and Finzi (2016). Fine root net

primary production in the HEM tower footprint is based on data from Abramoff and Finzi (2016); no other data were available for this location.

[3] We assume a standard deviation equal to 50% of the mean value of the range reported by Gaudinski et al. (2000).

Figure legends

Figure 1. a) A timeline of ecosystem C measurements at the Harvard Forest. The timeline is divided into biomass components, soil components, fluxes, and global change experiments. Lines indicate measurements across all studies. Asterisks on the mineral SOC line indicate the years in which mineral soil C sampling was repeated in the same set of plots. b) Map of the Harvard Forest tracts, eddy-flux towers, and plots. The types of measurements collected varied across plots and studies; for plots with aboveground biomass measurements, forest type was determined using *k*-means cluster analysis.

Figure 2. Regional comparison of production and C stocks in biomass. Distribution of C in biomass in FIA plots (black dots) within EPA ecoregions 58g and 59b (green polygon) is lower than that at the Harvard Forest (red outline). GPP estimated from AVIRIS (blue box) does not differ between the Harvard Forest and full AVIRIS footprint.

Figure 3. Long-term (1964–2015) annual mean air temperature (a) and total precipitation (b) at the Harvard Forest. Also presented are trends in annual mean CO_2 concentration (c) at the Mauna Loa Observatory (1959–2015), ground-level O_3 concentration (d) in Ware Center, MA, 25 km south of the Harvard Forest (1981–2015), and total N deposition (e) and SO_4^{2-} deposition (f) at the Quabbin Reservoir, 17 km southwest of the Harvard Forest (1982–2015). Statistically significant ($p < 0.05$) linear relationships in (a), (b), (d), (e), and (f) are shown for the full record (solid lines) and for the period of interest for this study (1992–2015; dashed lines).

Figure 4. (a) Changes in aboveground carbon stocks (mean ± SD) of the four major tree species at the Harvard Forest, based on 60 plots distributed across the Prospect Hill Tract (the PHOREST study). The plots were originally sampled in 1937, the year prior to a major hurricane that resulted in 70% loss of timber volume at the Harvard Forest. Through time stand biomass has steadily increased with red oak emerging as the dominant species. (b) Tree-ring analysis shows annual aboveground carbon increment of trees in the oak–maple-dominated Lyford Plot and EMS plots. Red oak dominated biomass increment at this site for the past >50 years, with minor contributions from red maple and

other species. There was a drought in the mid-1960s, and a severe gypsy moth defoliation in 1981.

Figure 5. Components of NPP at the Harvard Forest over time for hardwood-dominated plots: a) biomass increment (aboveground and coarse roots), SE of slope = 1.22, $p < 0.001$, Adj-r^2= 0.07; b) foliar litter production, SE of slope = 0.37, $p < 0.001$, Adj-r^2= 0.05; c) NPP combining woody increment aboveground, coarse root increment, and total litter production, SE of slope = 3.3, p = 0.016, Adj-r^2= 0.32. Data for total litterfall began in 1999 for the hardwood plots, which is why panel (c) shows data only from 2000–2014.

Figure 6. Components of NPP at the Harvard Forest over time for hemlock-dominated plots: a) biomass increment (aboveground and coarse roots); b) foliar litter production; c) NPP combining woody increment aboveground, coarse root increment, and total litter production. None of these showed a significant trend over time. Data for total litterfall began in 2005 for the hemlock plots, which is why panel (c) shows data only from 2006–2014.

Figure 7. Cumulative (a) and annual (b) net ecosystem production and its component fluxes R_e (c) and GPP (d). Star symbols represent years during which hemlocks were in decline. The black lines in (b–d) represent the significant (solid) or non-significant (dashed) trends in increasing NEP, R_e, and GPP with time at the EMS site (NEP: Adj-r^2 = 0.06, p = 0.127; R_e: Adj-r^2 = 0.17, p = 0.026; GPP: Adj-r^2 = 0.51, $p < 0.001$).

Figure 8. Notable features of the eddy-covariance and plant-area index data sets. July GPP as a function of photosynthetic photon flux density for the (a) HEM, (b) EMS, and (c) CC tower sites. The fitted lines model light-use-efficiency using Eq. 3. Data were averaged within 50 μmol photon m^{-2} s^{-1} bins of PPFD. (d) The seasonal time course of LAI at the EMS site, and (e) median July mid-day GPP as a function of plant area index. Data from the HEM site are restricted to the time before clear sign of HWA-associated decline (2005–2012). The black line in (e) is the regression between CC-tower PAI and GPP.

Figure 9. Relationship between (a) NEP and LUE (Adj-r^2 = 0.13, p = 0.045), (b) GPP and A_{max} (Adj-r^2 = 0.20, p = 0.018), (c) NEP and PAI (Adj-r^2 = 0.23, p = 0.035), and (d) NEP and red oak tree-ring-based biomass increment (Adj-r^2 = 0.35, p = 0.003) at the EMS site.

Figure 10. Median daily fluxes of C at the (a) EMS and (b) HEM sites. The data in this figure were first published in Giasson et al. (2013) but were updated through the end of 2015. Ecosystem respiration is based on new data from the two eddy-covariance tower sites. No additional soil respiration data have been collected since Giasson et al. (2013) and the time series is extended based on an empirical model fit between flux and soil temperature data collected between 1992 and 2010 (see Figure A4 in Giasson et al. 2013). For the HEM site, data from the period during which hemlocks were declining (2013–2015) were not used. The shaded regions above and below the points reflect 1 SD of the average daily flux across the 24- and 8-year records, respectively. Soil temperature was measured 20 cm below the soil surface at the EMS site and 10 cm below the surface at the HEM site. (c) The ratio of soil and total ecosystem respiration at the two sites. The median daily (d) ecosystem respiration, (e) soil respiration, and (f) aboveground respiration at the EMS and HEM sites. Open symbols represent the HEM site and closed symbols the EMS site. In (c), star symbols indicate years during which hemlocks were in decline.

Figure 11. Mean daily DBH increment (mm d^{-1}), mean daily aboveground respiration (R_{above}, g C m^{-2} d^{-1}), and plant area index (PAI, m^2 m^{-2}) at the EMS site for 1998–2003 and 2006. A total of 1320 trees (>5 cm DBH) of 16 species were measured 6–19 times per year.

Figure 12. Climate metrics at the Harvard Forest. Start and end dates of the growing season and the length of the growing season at the (a) EMS and (b) HEM eddy-covariance sites. All regressions for the EMS site are statistically significant (Adj-r^2 = 0.15, p = 0.0351; Adj-r^2 = 0.13, p = 0.0459; Adj-r^2 = 0.27, p = 0.0052 for the start, end, and length of the growing season, respectively). No regression was statistically significant at the HEM site (Adj-r^2 = 0.03, p = 0.310; Adj-r^2 = −0.09, p = 0.531; Adj-r^2 = −0.01, p = 0.368 for the start, end, and length of the growing season, respectively). The 95% confidence interval of the slopes are indicated. Solid lines show statistically significant relationships

and dashed lines insignificant ones.

Figure 13. Relationship between the date of the onset of the growing season and springtime NEP for the EMS (a) and HEM (b) sites. Also, relationship between the date of the end of the growing season and autumn NEP for the EMS (c) and HEM (d) sites. The onset of the growing season is defined as the first day of the year when daily NEP was above a threshold of 30% of the mean maximum daily NEP. Similarly, the last day when NEP was above the threshold was considered the end of the growing season. Spring is defined as March–May and autumn is September–November. Regressions are statistically significant (EMS-spring: Adj-r^2 = 0.27, p = 0.006; EMS-autumn: Adj-r^2 = 0.61, p < 0.001; HEM-spring: Adj-r^2 = 0.42, p = 0.049) except in the autumn at the HEM site (Adj-r^2 = 0.02, p = 0.333). The 95% confidence interval of the slopes are indicated. Solid and dashed lines represent significant and insignificant relationships, respectively.

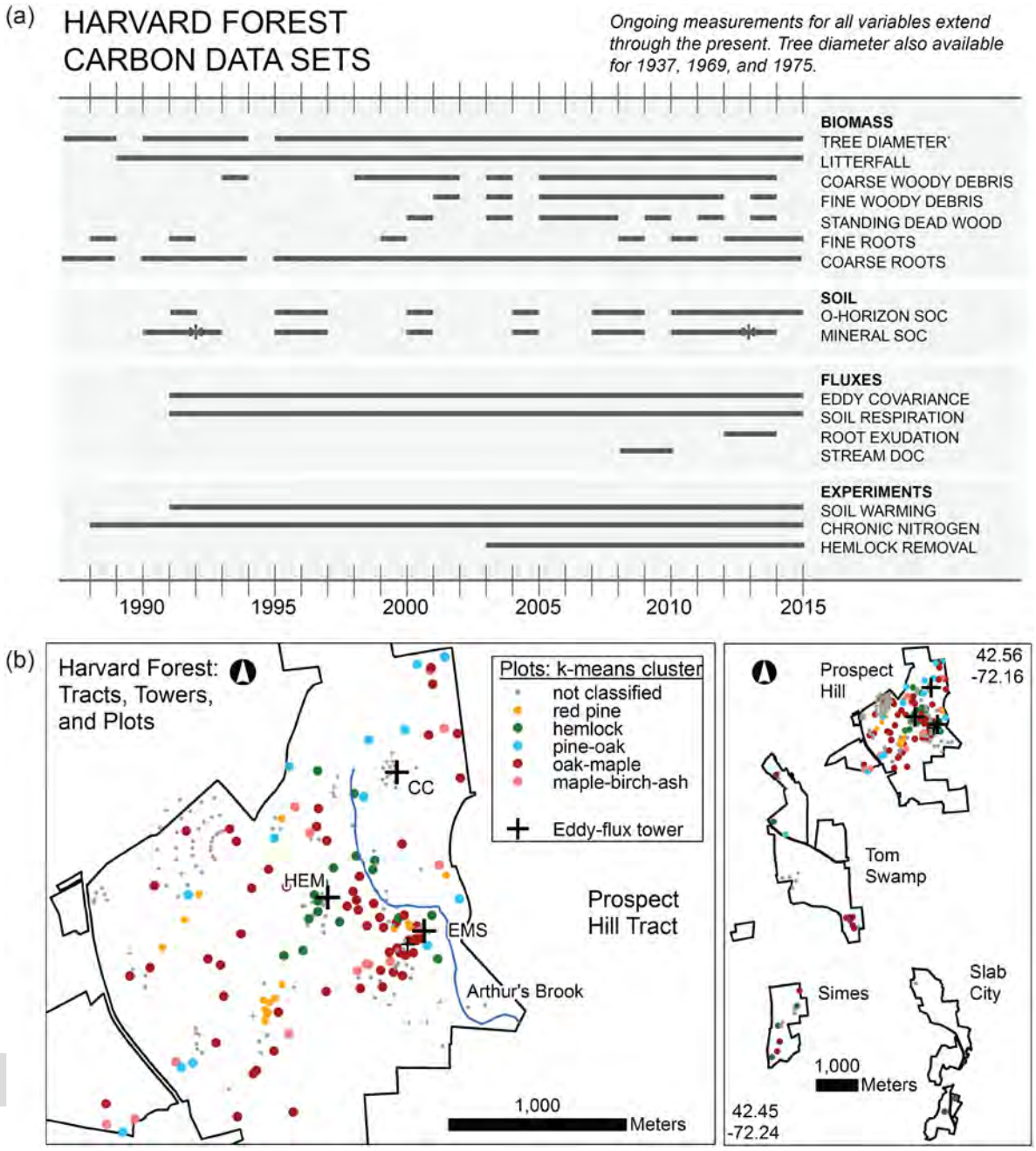

ecm_1423_f1.tif

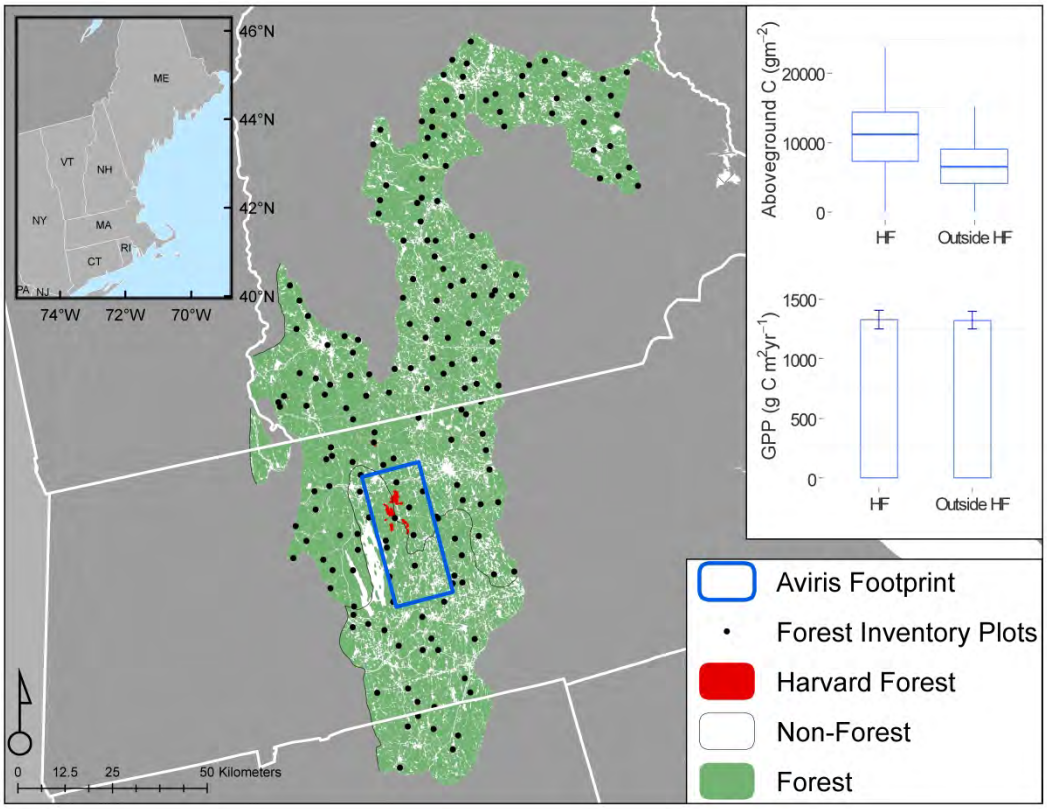

ecm_1423_f2.jpg

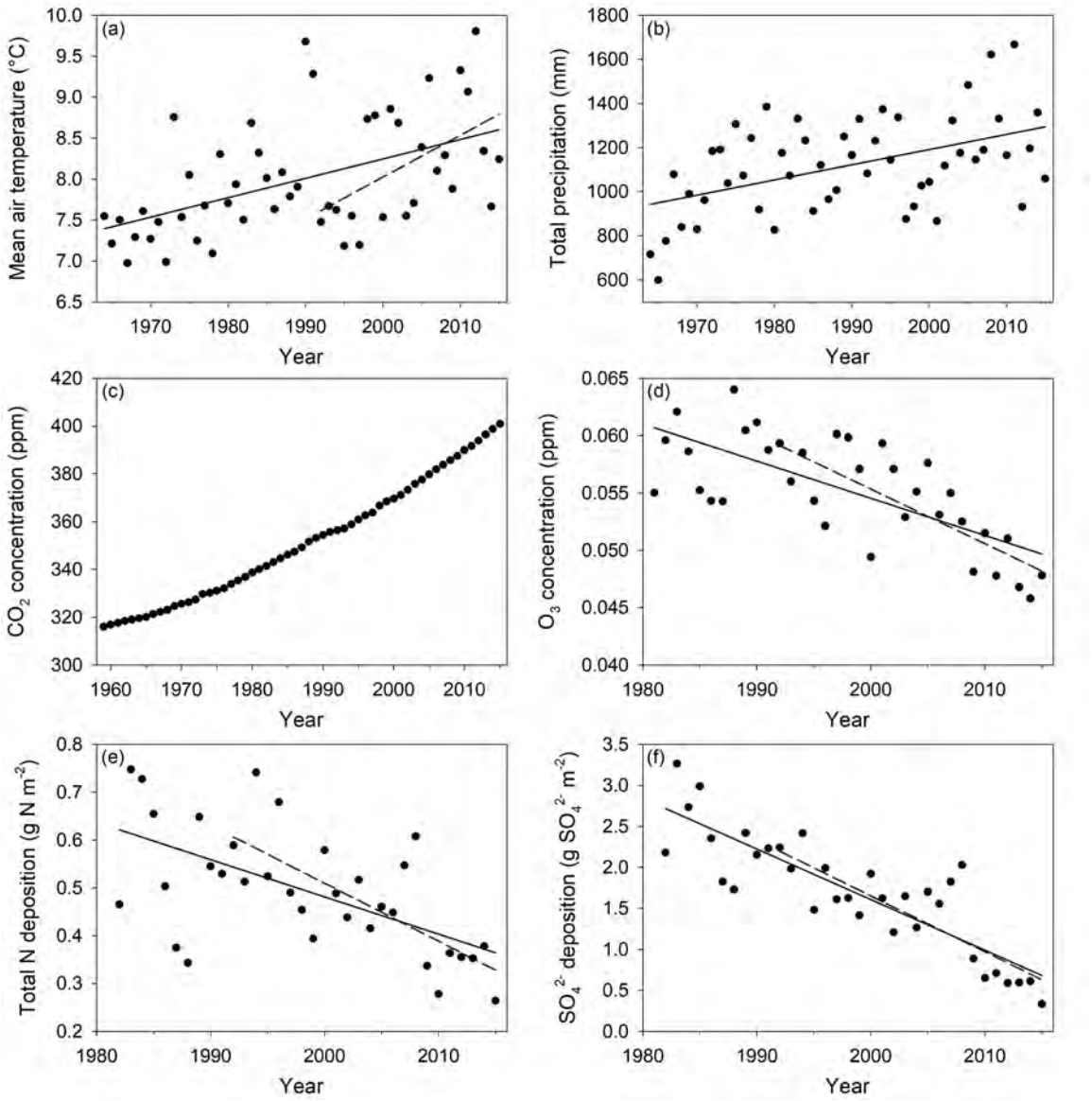

ecm_1423_f3.jpg

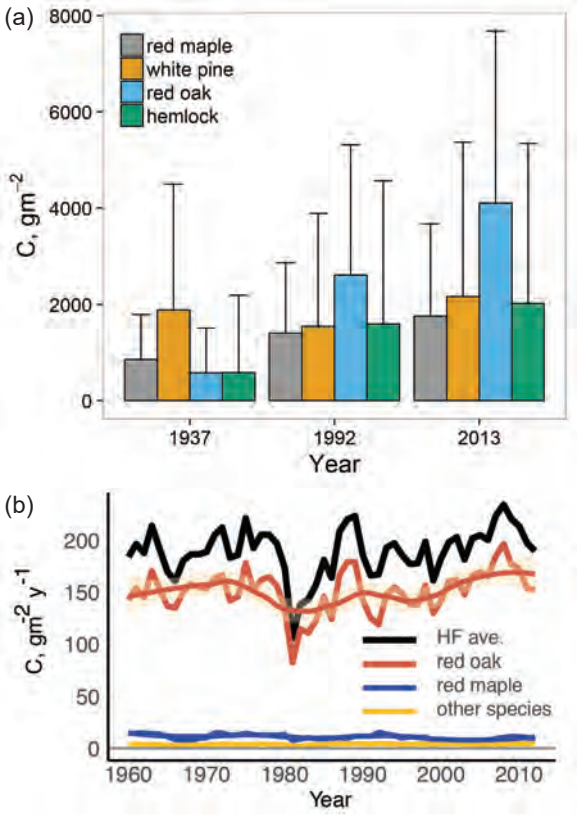

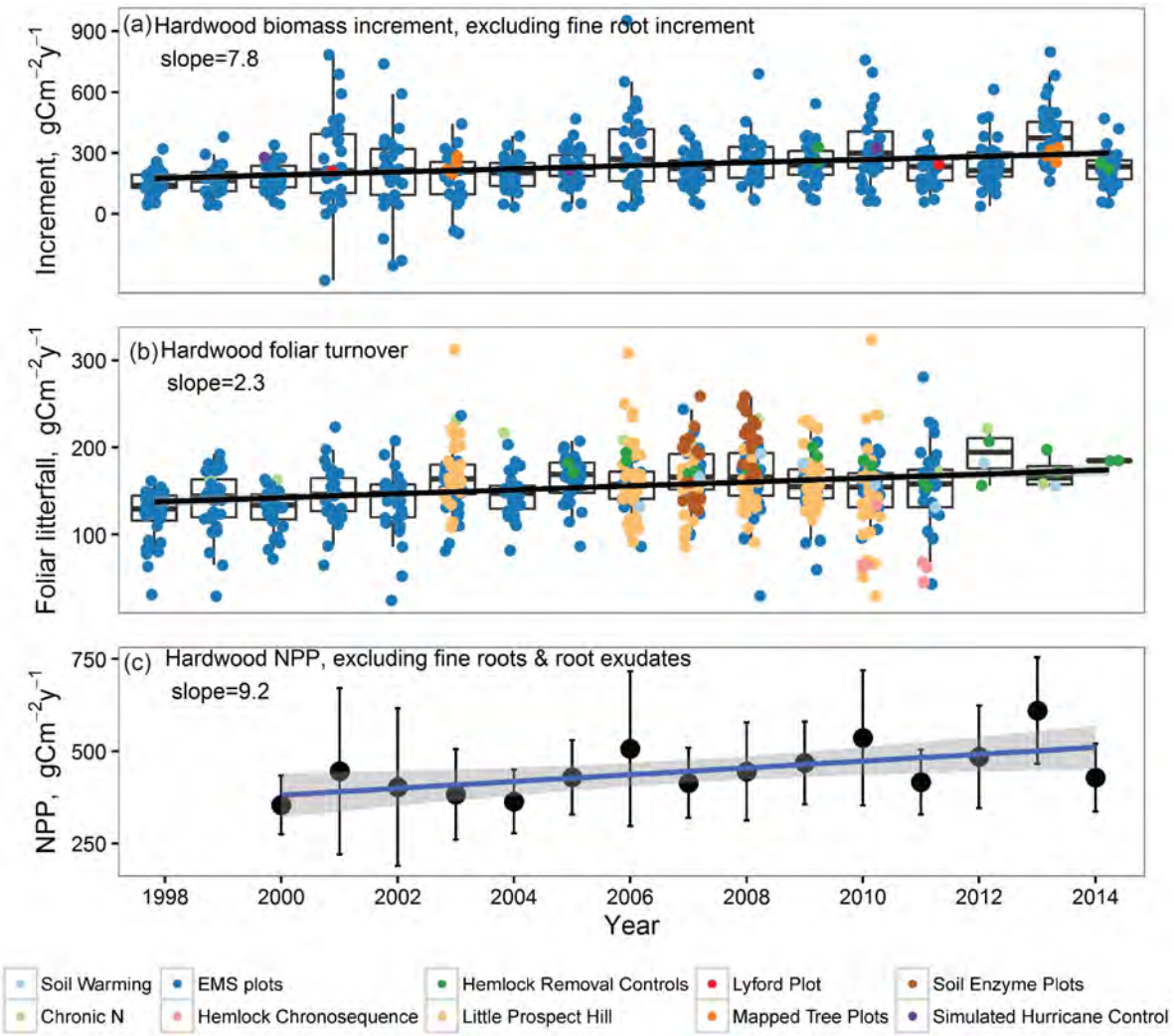

ecm_1423_f5.tif

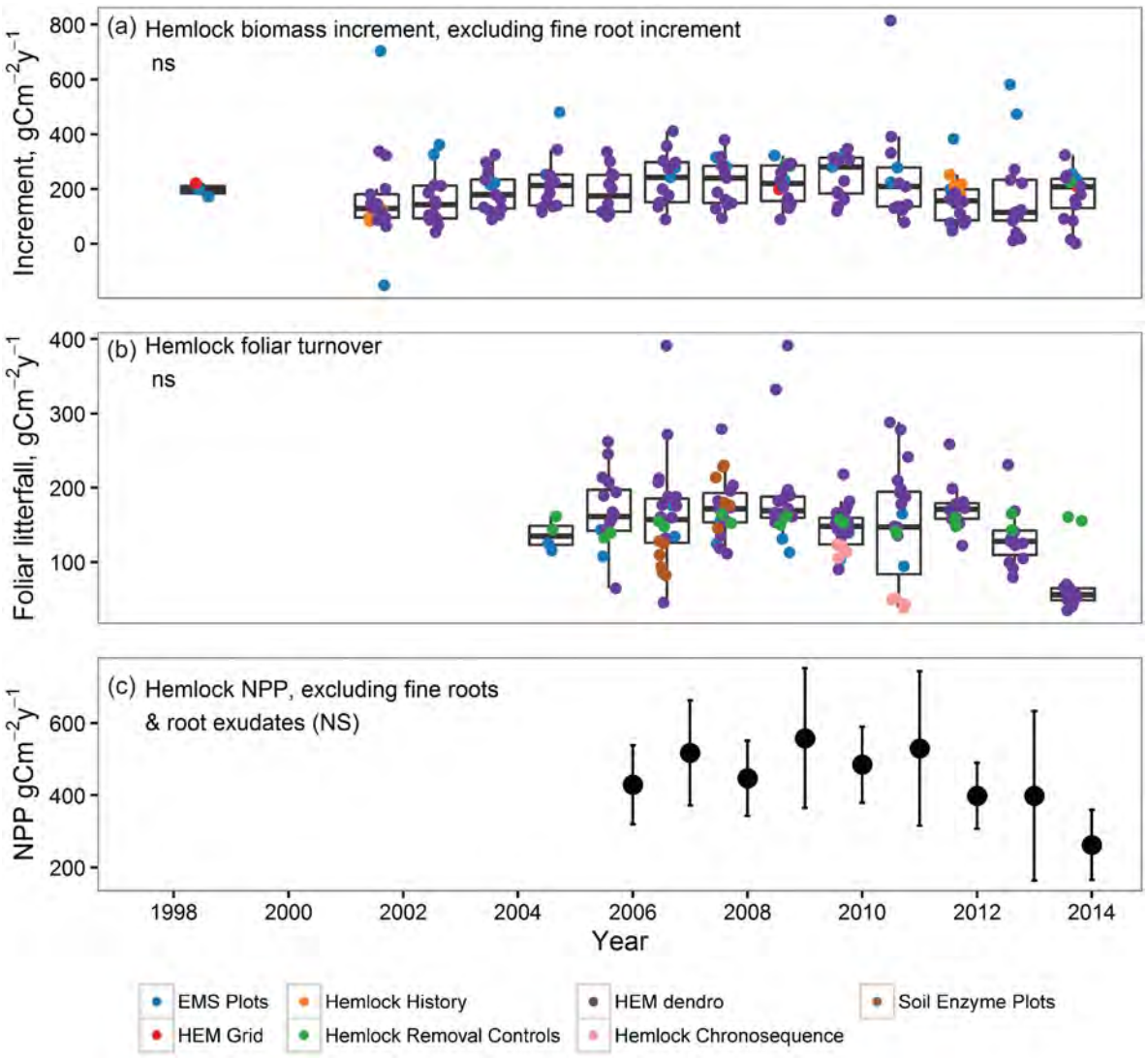

ecm_1423_f6.tif

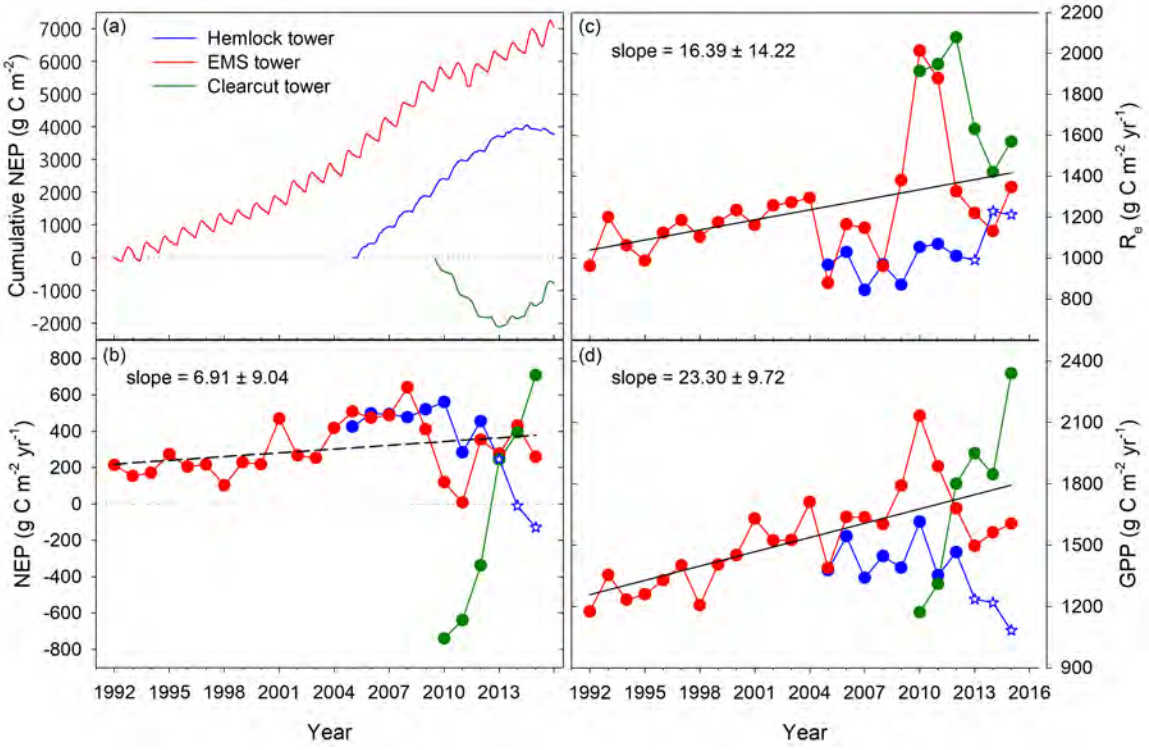

ecm_1423_f7.jpg

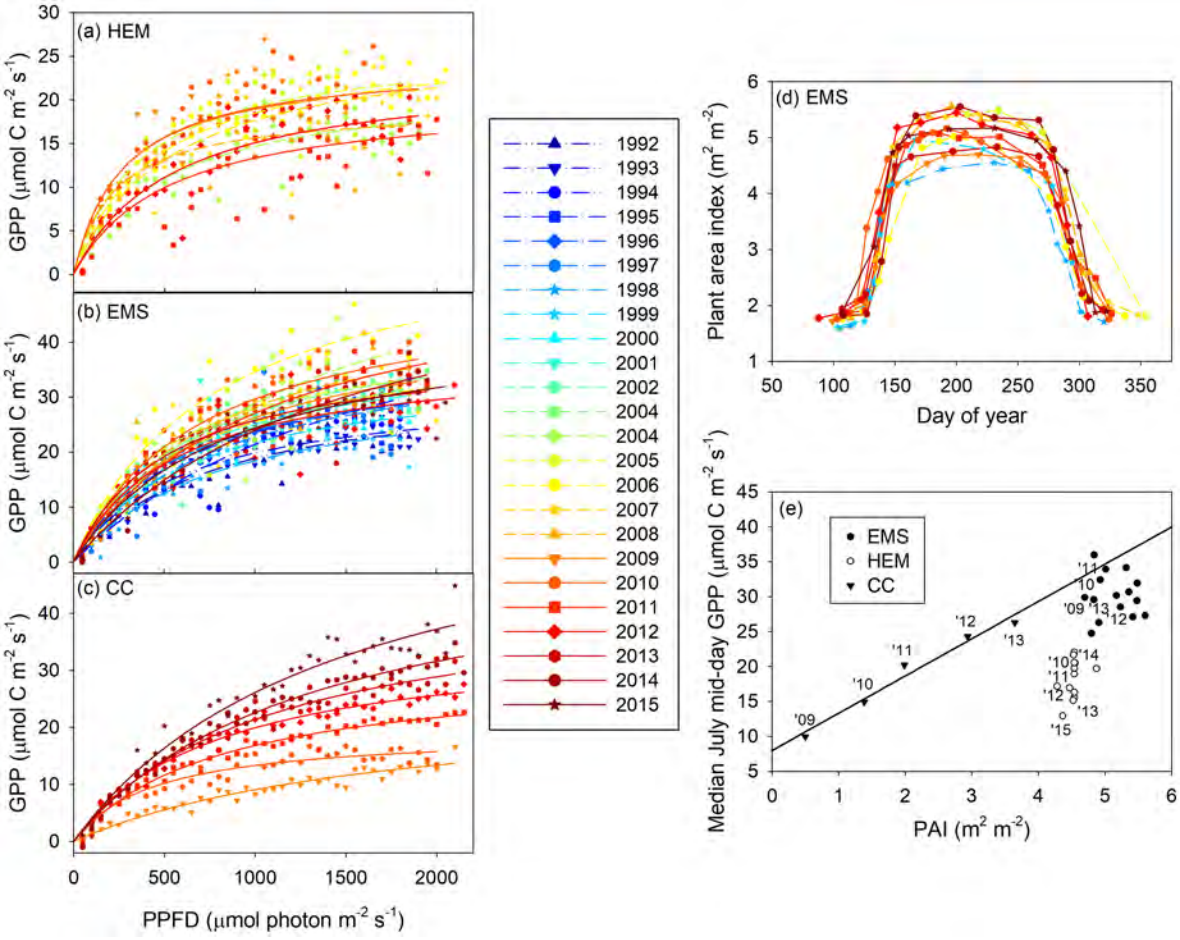

ecm_1423_f8.jpg

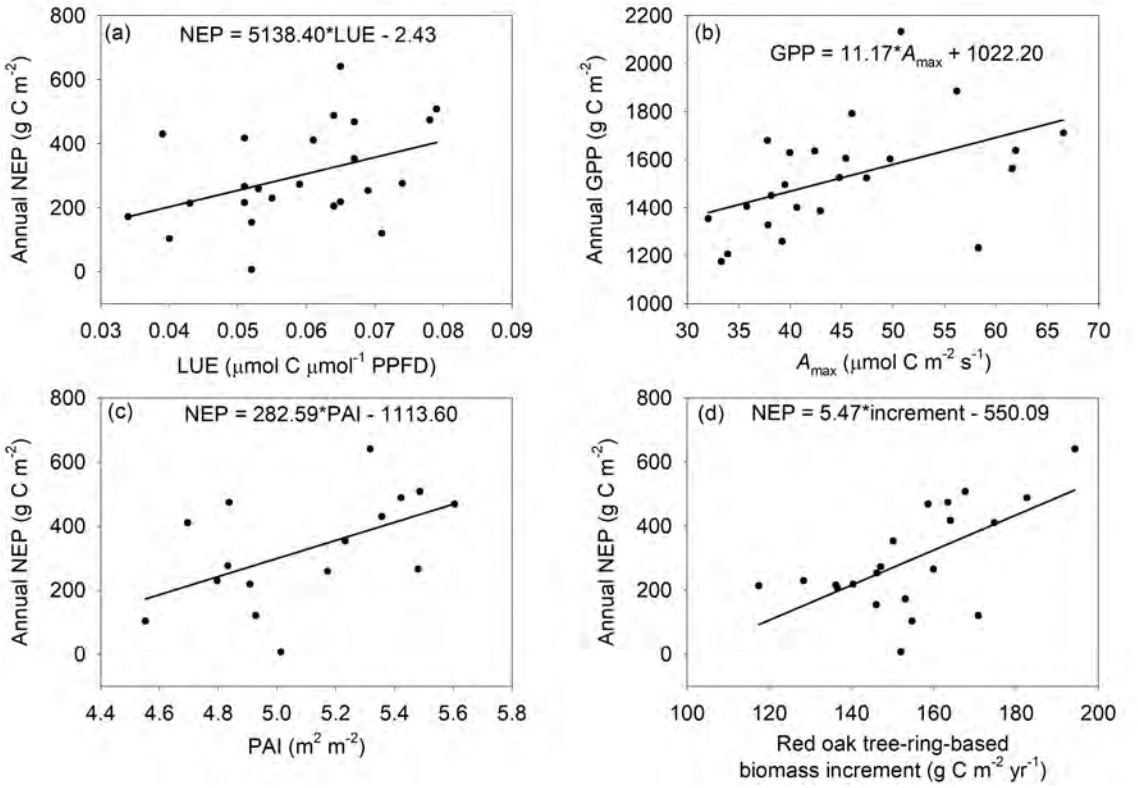

ecm_1423_f9.jpg

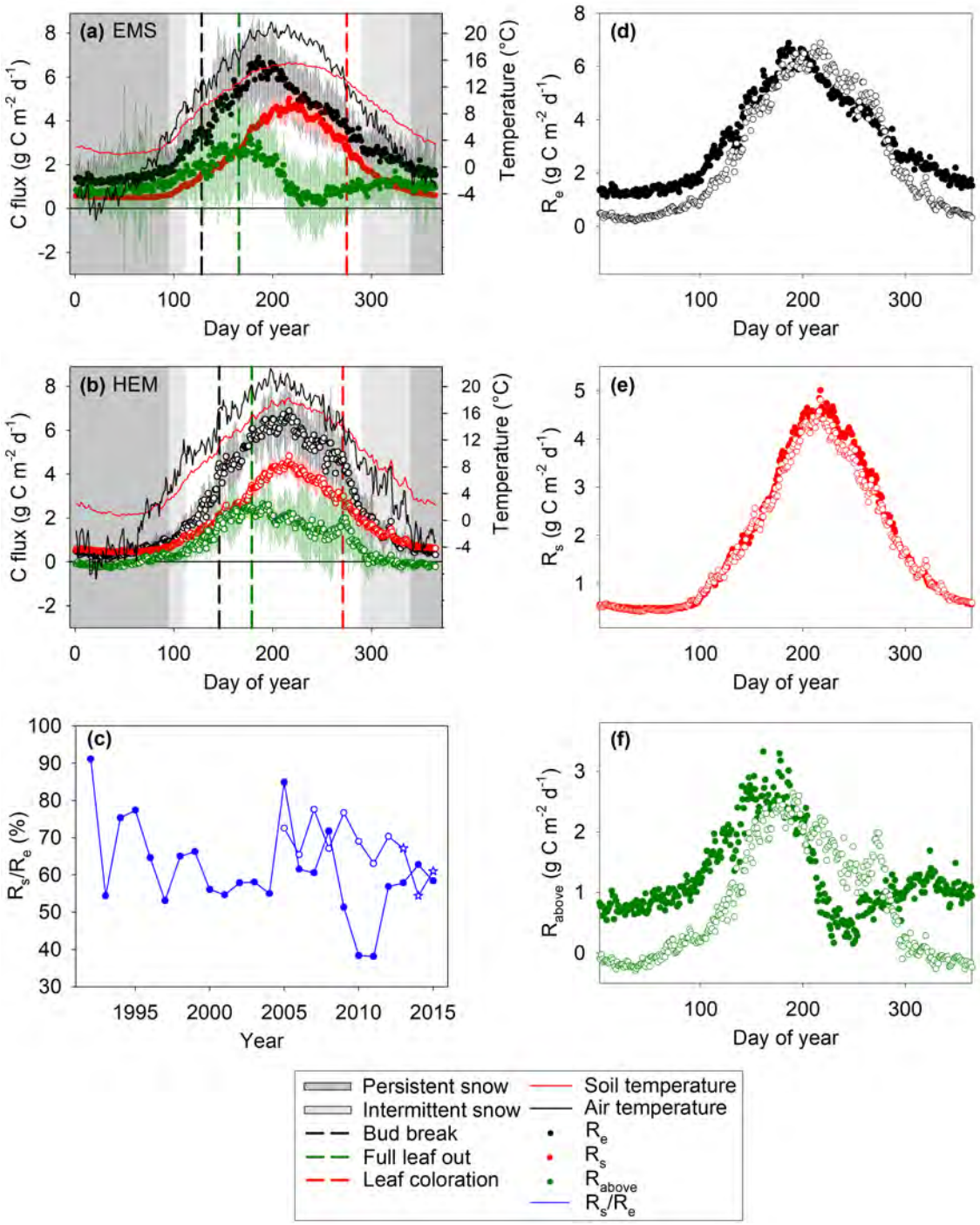

ecm_1423_f10.jpg

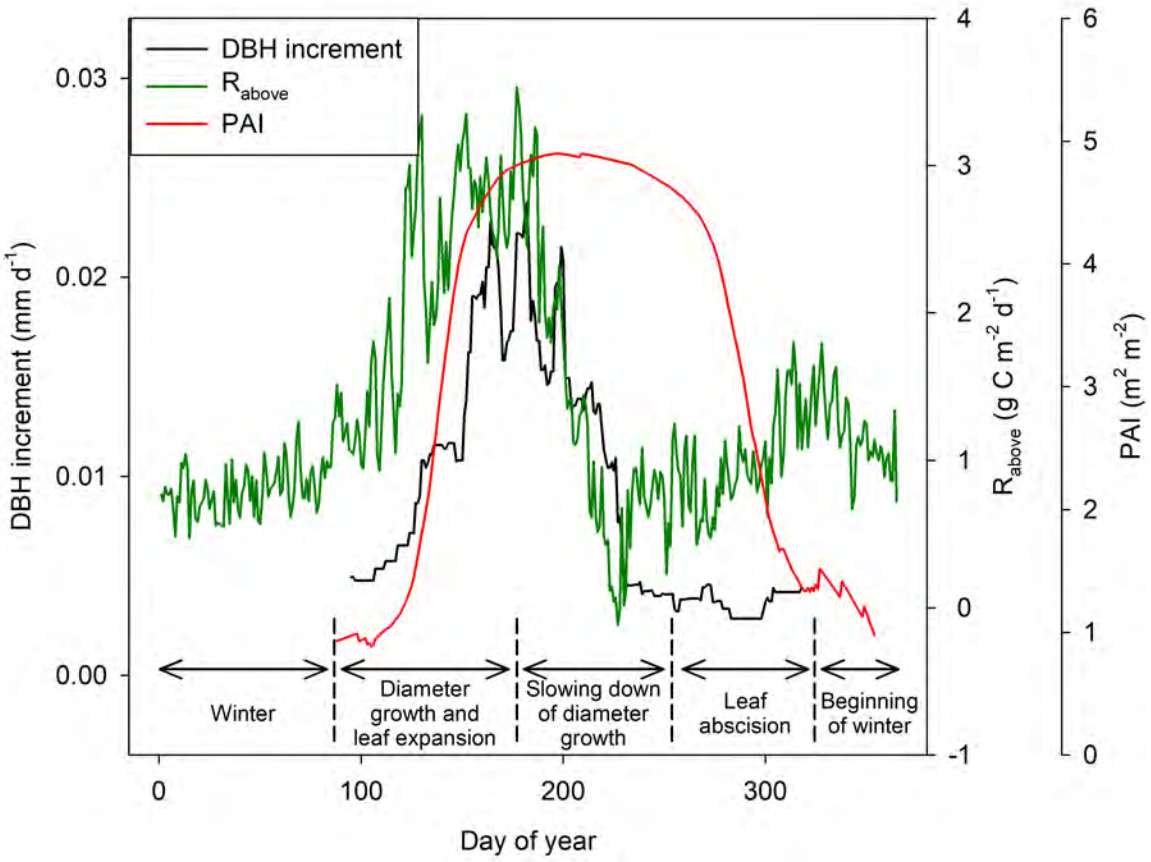

ecm_1423_f11.jpg

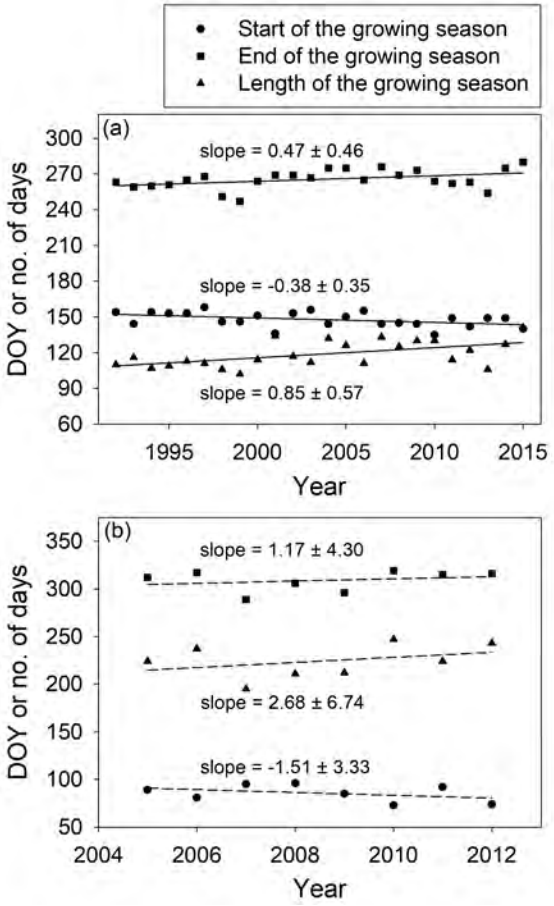

ecm_1423_f12.jpg

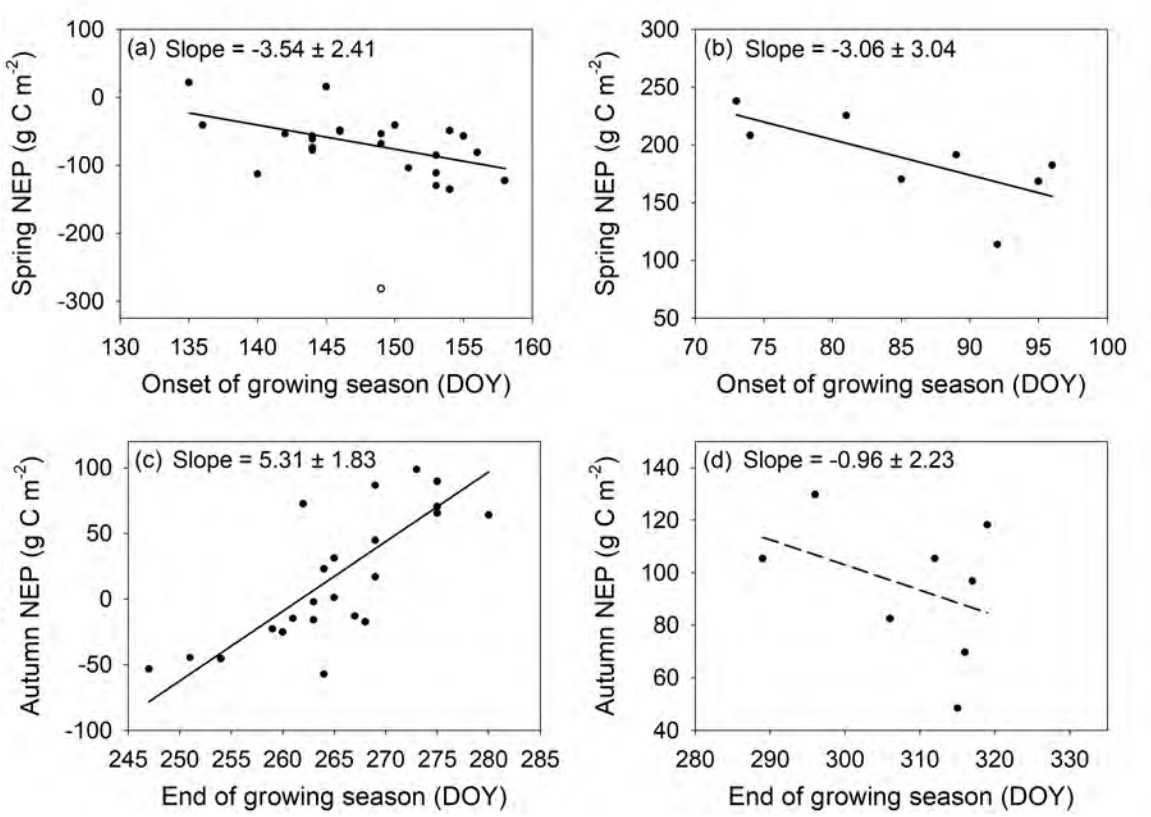

ecm_1423_f13.jpg